Geological sampling in the Great Australian Bight: Scientific post-cruise report - R/V *Rig Seismic* Cruise 102

by

D A Feary et al

RECORD 1993/18

AGSO
AUSTRALIAN GEOLOGICAL SURVEY ORGANISATION

AUSTRALIAN GEOLOGICAL SURVEY ORGANISATION

Division of Marine Geoscience and Petroleum Geology

AGSO Record 1993/18

SCIENTIFIC POST-CRUISE REPORT -
R/V *RIG SEISMIC* Cruise 102

GEOLOGICAL SAMPLING IN THE GREAT AUSTRALIAN BIGHT

AGSO Project 121.27

Cruise Leader:
D.A. Feary

Shipboard Scientific Staff:
G. Birch, T. Boreen, E. Chudyk, R. Lanyon, P. Petkovic, S. Shafik

Shore-based Scientific Contributions:
N.F. Alley, D. Almond, Y. Bone, A.J. Crawford, D.T. Heggie, N.P. James, J. Lane, B. McGowran

Technical Staff:
C. Buchanan, P. Butler, C. Dyke, L. Hatch, S. Milnes, U. Reike, J. Roberts, C. Saroch, D. Sewter, G. Sparksman, J. Stratton, P. Vujovic, V. Wierzbicki, S. Wiggins

DEPARTMENT OF PRIMARY INDUSTRIES AND ENERGY

Minister for Resources: Hon. Michael Lee
Secretary: Greg Taylor

AUSTRALIAN GEOLOGICAL SURVEY ORGANISATION

Executive Director: Roye Rutland

ISSN: 1039-0073

ISBN: 0 642 19250 2

TABLE OF CONTENTS

APPENDICES

FIGURES

TABLES

EXECUTIVE SUMMARY

RIG SEISMIC Cruise 102 sailed from Fremantle at 1600 hrs on the 12th June 1991, with the intention of carrying out geological sampling operations at a range of sites across Australia's Southern Margin. At the conclusion of the survey, the ship docked in Fremantle at 0915 hrs on the 10th July 1991. The Southern Margin Sampling Program (121.27) was proposed as a multi-objective survey, designed to address a range of geological problems. The primary objectives of the survey emphasised (i) the further evaluation of the hydrocarbon prospectivity of the deep Ceduna Sub-basin segment of the Great Australian Bight Basin, to complement and expand on earlier *RIG SEISMIC* surveys; and (ii) the development of a high energy, cool-water, carbonate hydrocarbon reservoir model based on the sedimentary characteristics of Cenozoic carbonate deposits on the Eucla Shelf-Eyre Terrace. Additional objectives involved seafloor sampling for Quaternary paleochemistry and mantle magmatism projects, and the collection of bathymetric data for AGSO's Offshore Resource Map Series (Fig. 1).

Prior to departure it was recognised that weather conditions at this time of year were far from optimum for any type of marine work, and accordingly that some time was likely to be lost through bad weather. In addition, logistic and ship maintenance requirements determined that the ship must both depart from, and return to Fremantle, involving considerable transit time. Nevertheless, despite a full and seemingly optimistic program, virtually all objectives were satisfactorily fulfilled. A total of 10 dredge sites, 28 gravity core sites, and 8 grab and vibrocore sites were successfully occupied. In addition, 4600 line km of magnetometer data and 6560 line km of bathymetric data were collected.

Sampling results, with respect to the objectives for each area, are as follows:
AREA A - to determine the biostratigraphy and sedimentary facies of the deep Ceduna Sub-basin sequence. During this segment of the survey, particularly poor weather conditions resulted in considerable difficulty in precise core and dredge operations. A total of 6 dredges (3 successful) and 17 gravity cores (12 successful) were attempted at 11 sites. The successful dredge hauls recovered an extensive suite of terrigenous siliciclastic rocks and, in one dredge, a range of calcareous (calcarenite, calcilutite, and semi-lithified foraminifer ooze) and dolomitic rocks. Nannofossil data show that the calcareous rocks are of Middle Eocene to mid-late Oligocene age; palynological study shows that the terrigenous siliciclastic rocks are of Late Cretaceous (Campanian to latest Maastrichtian) age. Attempts to use a short-barrelled gravity corer to sample older sediments was only marginally successful; Quaternary cover prevented penetration through to Mesozoic targets in all but two cores, which recovered late Maastrichtian mudstones. The recovery of Late Cretaceous mudstones and Eocene-Oligocene limestones indicates that the known distributions of the Potoroo Formation and Wilson Bluff Limestone may be extended. These samples provide important new data concerning Late Cretaceous and Early Tertiary depositional environments in the Ceduna Sub-basin.
AREA B - to determine the sedimentary characteristics and develop an appropriate facies model for high energy, cool-water Cenozoic carbonate deposition on the Eucla Shelf-Eyre Terrace. A small program of high-resolution, single watergun seismic required to provide facies geometry data on which to base the sampling

transect had to be abandoned as a result of failure of the seismic acquisition system. Nevertheless, a total of 10 successful gravity cores recovered some 32 m of core at the seaward end of the transect, while 7 successful vibrocores recovered between 0.30 and 1.37 m of sediment at the nearshore end of the transect. Vibrocores reveal that the surface of the Eyre Shelf consists of Tertiary or ?Pleistocene carbonates mantled with a thin Holocene mollusc and lithoclast lag on the inner shelf, and by a 9,000-13,000 year old rhodolith pavement on the deeper outer shelf. Quaternary sedimentation on the upper slope and Eyre Terrace is represented by foraminifer nannofossil oozes. The ubiquitous bioturbation present in shallower cores is progressively less intense at deeper sites, resulting in the appearance of poorly-defined colour banding. This banding is more pronounced in the deeper Ceduna Terrace (Area C) cores.

AREA C - to document the Late Quaternary paleochemistry of the southern margin, in order to evaluate the nature and extent of glacial/interglacial cyclicity as the control on sea-level variation, organic carbon fluxes, seafloor mineral accumulation, and continental weathering. A total of 6 successful gravity cores on a transect across the western end of the Ceduna Terrace recovered more than 18 m of Quaternary foraminifer nannofossil ooze in water depths between 1000 and 3500 m. A further gravity core attempt, into a coarser-grained sandy substrate at the nearshore end of the transect, was unsuccessful. The applicability of these cores to the Australian margin paleochemistry project must await further shore-based work; nevertheless the sedimentology of these cores provides valuable Quaternary environmental data. Increasingly well-preserved colour banding in the deeper cores, coinciding with decreased bioturbation, probably reflects climate-controlled cyclic oxygenation variations caused either by Antarctic bottom water fluctuations or by distal Leeuwin Current effects.

AREA D - to determine the geochemical characteristics of Southern Ocean magmatism between the continent-ocean boundary and magnetic anomaly 13 (approximately 38 Ma), in order to determine the changing composition, organisation, and longevity of mantle reservoirs supplying ridge basalts during the breakup of Gondwana and the rifting of Australia and Antarctica. Outstandingly successful dredging at four widely-spaced sites produced an extensive and varied assemblage of tholeiitic basalt and gabbroic rocks. Although seafloor and possible hydrothermal alteration is present in most rocks recovered, initial indications are that sufficient less-altered rock is available for detailed geochemical and isotopic analyses. In addition, two further dredges with oceanic crust targets recovered large quantities of manganese nodules and crusts. Although unsuccessful in their primary aim, these dredge hauls nevertheless provide valuable data on the nature and extent of Southern Ocean seafloor mineralisation.

AREA E - a request for bathymetric data to fill critical data gaps in AGSO's Offshore Resource Map Series EYRE and ESPERANCE sheets, presently in the final stages of preparation, was received shortly before the cruise departed. More than 900 line km of apparently high quality bathymetric data were collected to fulfil this objective.

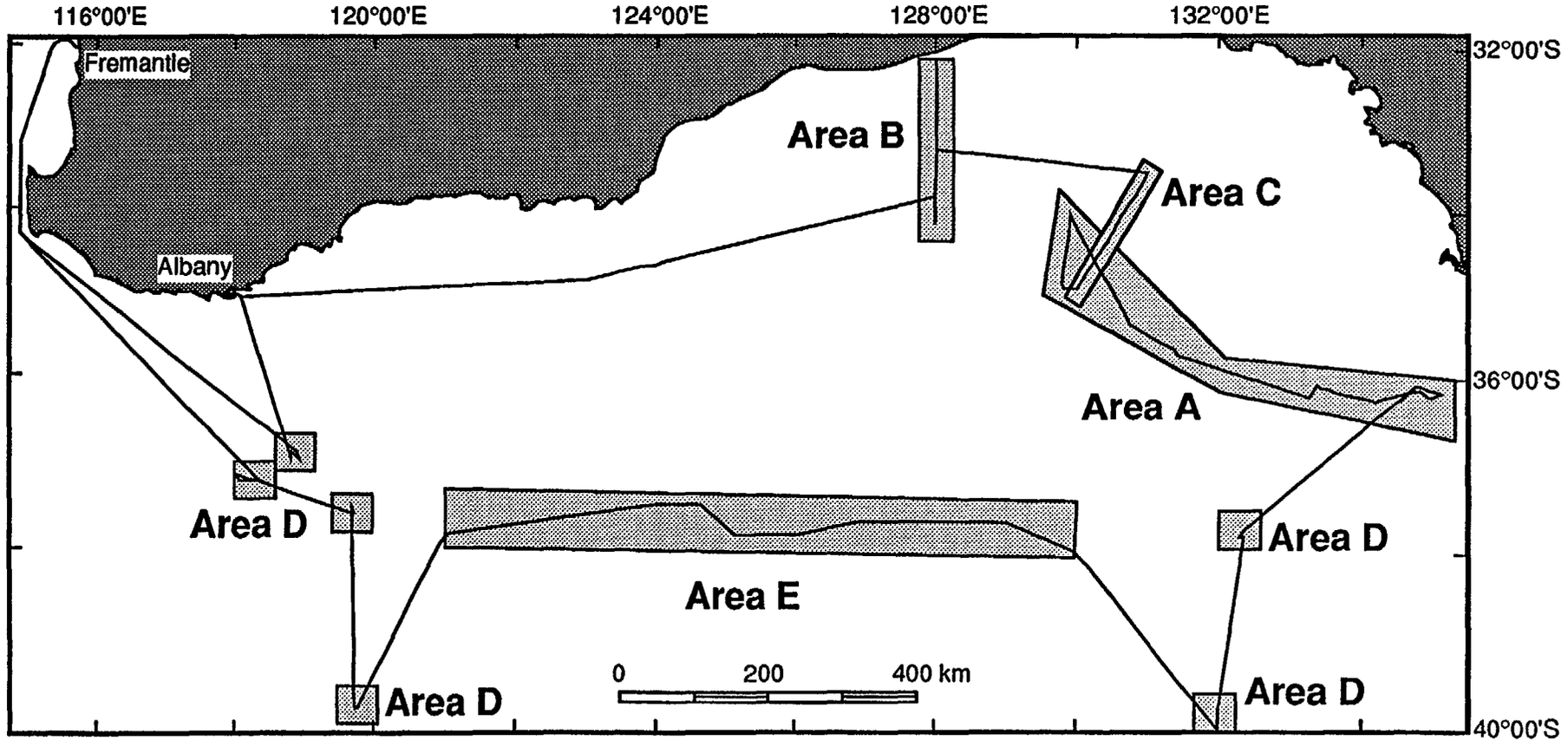

FIGURE 1. Cruise 102 ship's track and location of sampling areas.

1. INTRODUCTION

The Great Australian Bight region (Fig. 2) has been one of the primary areas of investigation for AGSO's Continental Margins Program. This reflects the reconnaissance nature of most earlier basin studies along the 1300 km of margin between the Duntroon Embayment and Cape Leeuwin, which, despite the identification of up to 12 km of sediment thickness and the drilling of 5 wells, remains very poorly understood. The AGSO southern margin work program has been designed both to undertake broad framework studies with a view to evaluating petroleum prospectivity, as well as to refine models of mantle magmatism, cool-water depositional systems, passive margin tectonic evolution, and basin development.

The geology and petroleum prospectivity of Australia's southern margin has primarily been discussed as part of regional reviews, based on patchy distribution of high quality seismic and other geophysical data, a notable paucity of geological data, and 5 exploration wells. More focussed reviews of specific geographic areas have described the Ceduna Terrace (Whyte, 1978; Fraser and Tilbury, 1979; Tilbury and Fraser, 1981) and Eyre Terrace (Bein and Taylor, 1981) sequences.

Earlier cruises of the *R/V RIG SEISMIC* in 1986 (surveys 65 and 66) further refined the geological and geophysical framework of the Eyre and Ceduna Terrace sequences. Analysis of data collected during these cruises (Willcox, Stagg, Davies, and others, 1988; Stagg and others, 1990) demonstrated that:

(1) Late Cretaceous spreading between Australia and Antarctica was directed N-S, although possible NW-SE strike-slip faulting beneath the outer margin of the Ceduna Terrace may reflect a NW-SE early continental extension direction.

(2) The Eyre Sub-basin is bounded to the south by a ridge of Precambrian basement overlying a probable south-dipping, primary detachment surface. Rotated blocks of a 4-6 km thick, probable Cretaceous and Tertiary sedimentary sequence overlie the basement block. This sequence contains at least nine unconformable seismic sequences, some of which clearly prograde southward.

(3) The Ceduna Terrace sequence includes a thick, progradational unit characterised by large-scale foreset beds, probably bounded by Cenomanian and Maastrichtian unconformities (Fraser and Tilbury, 1979).

(4) The Great Australian Bight Basin contains a Maastrichtian to Middle Eocene sequence of dominantly terrigenous marine sediments, with little non-marine sediment, overlain by a Middle Eocene to Quaternary sequence dominated by pelagic carbonate.

The *R/V RIG SEISMIC* southern margin sampling cruise described here was designed to complement this earlier work, as well as to advance our understanding of specific depositional, tectonic, magmatic, and geochemical processes. Work was focussed on the eastern and central Great Australian Bight region in expectation that a further *R/V RIG SEISMIC* survey, planned for 1992 but now unlikely to go ahead before late 1993, will concentrate on the western Great

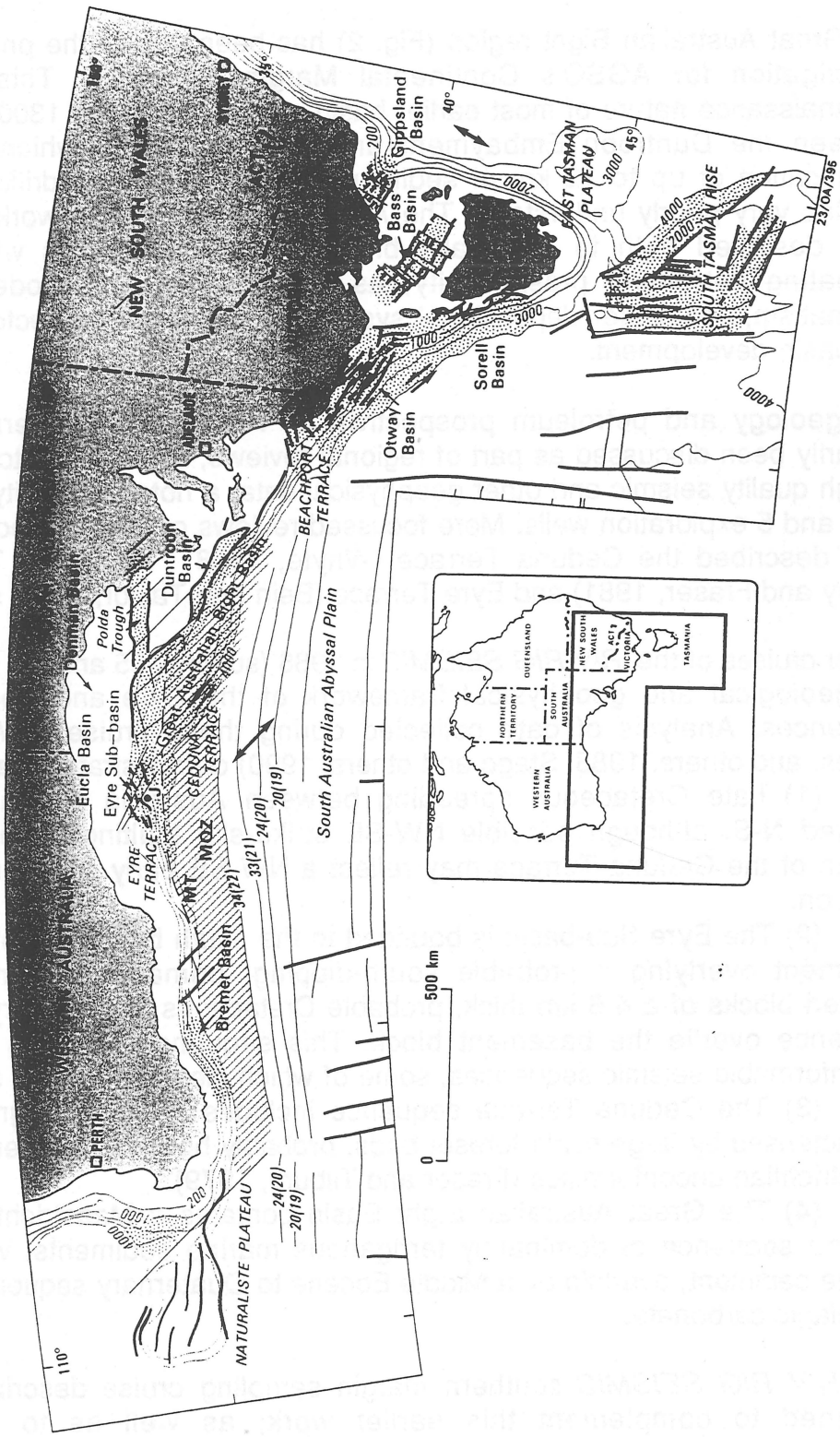

FIGURE 2. Southern margin sedimentary basins and major structural elements (after Willcox, 1990).

Australian Bight Basin, Bremer Basin, Diamantina Fracture Zone, and Naturaliste Plateau regions.

The program for the 1991 *R/V RIG SEISMIC* southern margin sampling cruise included work concentrated on the following geological themes, which in turn correspond to four specific geographic areas (Fig. 1). In order of priority, these are:
AREA A - to determine the biostratigraphy and sedimentary facies of the deep Ceduna Sub-basin sequence (45% of operational time);
AREA B - to determine the sedimentary characteristics and develop an appropriate facies model for high energy, cool-water Cenozoic carbonate deposition on the Eucla Shelf-Eyre Terrace (41% of operational time);
AREA C - to document the Late Quaternary paleochemistry of the southern margin, in order to evaluate the nature and extent of glacial/interglacial cyclicity as the control on sea-level variation, organic carbon fluxes, seafloor mineral accumulation, and continental weathering (7% of operational time);
AREA D - to determine the geochemical characteristics of Southern Ocean magmatism between the continent-ocean boundary and magnetic anomaly 13 (7% of operational time).

In order to maximise the scientific benefit from samples collected during cruise 102, requests to external organisations for their involvement resulted in shipboard and later shore-based contributions by G. Birch (Department of Geology and Geophysics, University of Sydney), T. Boreen (Department of Geological Sciences, Queen's University, Canada), and R. Lanyon (Geology Department, University of Tasmania). In addition, additional shore-based scientific contributions by N.F. Alley (South Australia Department of Mines and Energy), D. Almond, Y. Bone, and B. McGowran (Department of Geology and Geophysics, University of Adelaide), A.J. Crawford (Geology Department, University of Tasmania), and N.P. James (Department of Geological Sciences, Queen's University, Canada) are included in this report. The contributors to the scientific results presented in Section 6 are listed at the beginning of each report; AGSO personnel were responsible for the technical systems reports presented in Section 7. Unless otherwise attributed, additional material and editorial modifications are by D.A. Feary.

2. EXISTING DATA

Sample sites were located on the basis of existing seismic and bathymetric data. The following compilation and quality assessment of existing data used for site location is principally based on Willcox, Stagg, Davies, and others (1988) and Stagg and others (1990).

SEISMIC DATA

(1) AGSO Continental Margins Survey (1970-1973): Six-fold analogue seismic lines oriented N-S and E-W extend from the shoreward side of the continental shelf out to the abyssal plain at an average separation of about 35 km. These lines were recorded with a sparker source, and are of moderate to poor quality. Digital magnetic, gravity, bathymetry, and navigation data are also

available.

(2) *M/V PETREL* (Shell Development Australia Pty Ltd) (1972-1973): Moderate to good quality, 24-fold, airgun array, digital data in the form of zig-zag lines extending across the margin from the continental shelf out to the abyssal plain, with an average separation of approximately 100 km between the centre points of adjacent lines. Although recorded 24-fold, this material has not yet been stacked.

(3) Esso (1979): High quality, stacked 48-fold airgun array seismic data are available over much of the Eyre Terrace region.

(4) AGSO (1986): 3500 line km of high quality, stacked and migrated 24-fold airgun array seismic data are available over the Great Australian Bight Basin, Eyre Sub-basin, and Polda Trough.

(5) Japan National Oil Company (1989): JNOC recently collected seismic data over the Eucla Shelf-Eyre Terrace region. Neither this material, nor details of recording parameters and source type, were available when Cruise 102 took place. However, JNOC line location data were used as the basis for locating the Eucla Shelf-Eyre Terrace sampling transect, and it was intended that the JNOC seismic data complement the proposed but unsuccessful high-resolution seismic component of the cruise.

BATHYMETRIC DATA

(1) Between 1969 and 1972, Lamont-Doherty Geological Observatory collected magnetic and bathymetric data in many parts of the Great Australian Bight and throughout the Southern Ocean using the *USNS ELTANIN*.

3. GEOLOGICAL AND GEOPHYSICAL BACKGROUND

The following broad bathymetric and geological descriptions of Australia's southern margin and Great Australian Bight region are based substantially on earlier AGSO reports and reviews of the region by Willcox, Stagg, Davies and others (1988) and Stagg and others (1990).

3.1 BATHYMETRY

The bathymetry of the Great Australian Bight region (Fig. 3) has been described by Conolly and von der Borch (1967), Conolly and others (1970), and Willcox (1978). A detailed bathymetry map of the Ceduna Terrace was presented by Tilbury and Fraser (1981), and the margin west of the Great Australian Bight was described by Stagg and others (1990). Subsequently, Jongsma and others (1991, 1992) prepared detailed bathymetric maps for the shelf, slope, and abyssal plain between 126°E and 138°E, seaward from the continent to 38°S.

CONTINENTAL SHELF

The continental shelf is almost featureless, forming a gently sloping plain out to the shelf break at about 125-165 m depth. Minor changes in slope also occur at about 25 and 90 m depth. The shelf is 40-60 km wide from the vicinity of Albany to the

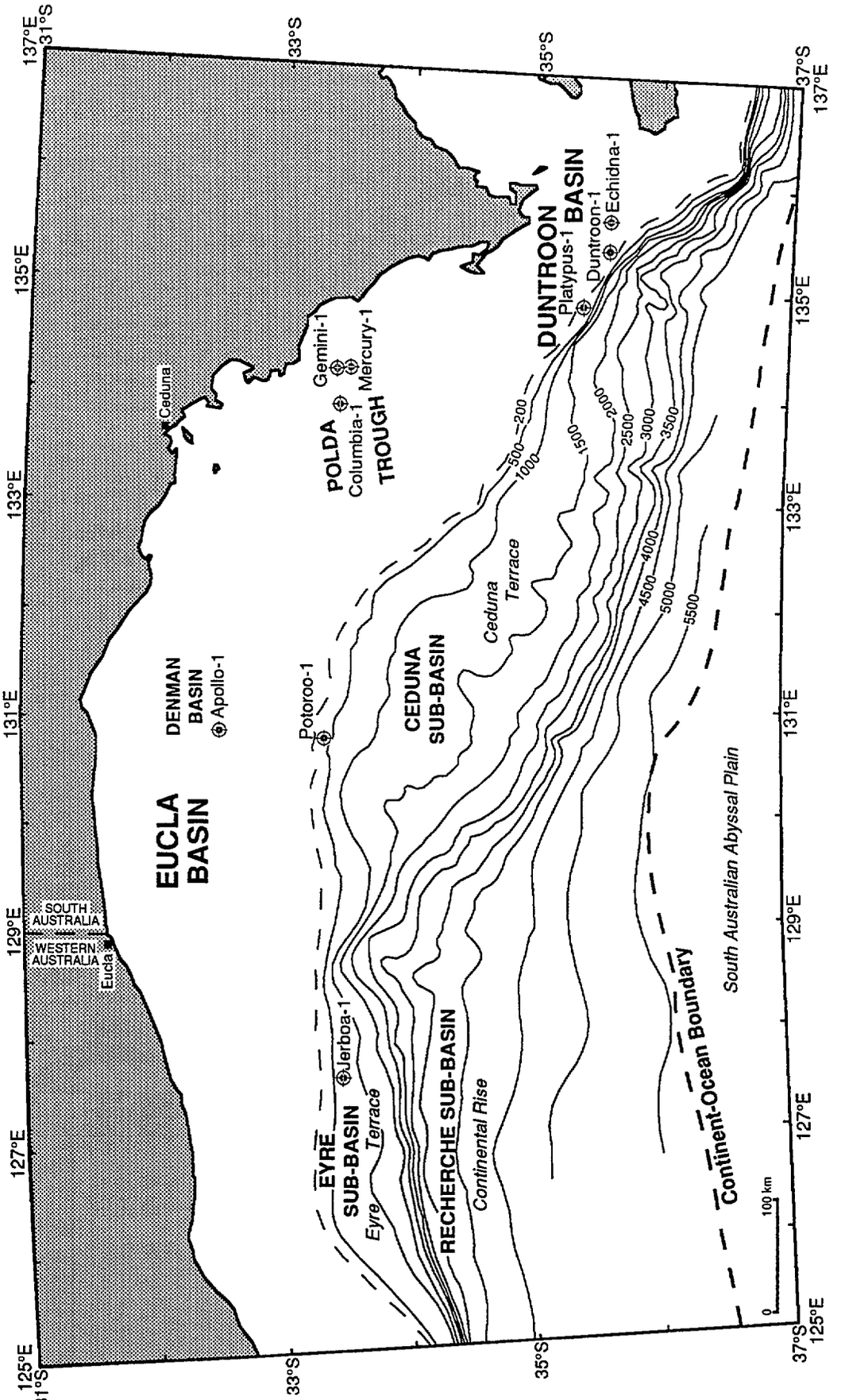

FIGURE 3. Bathymetry of the Great Australian Bight, showing sedimentary basins, sub-basins, and exploration wells.

western end of the Great Australian Bight, and the seabed falls away sharply below the shelf edge. Between the Archipelago of the Recherche and the Eyre Peninsula, the shelf forms a large arcuate plain with a maximum width of 300 km to the east of Eucla. Farther eastwards, the shelf width varies from 50 to 200 km, while in the extreme southeast it narrows to about 20 km. The shelf on the eastern side of the Great Australian Bight has been extensively modified by the Pleistocene courses of the Murray River.

CONTINENTAL SLOPE AND MARGINAL TERRACES

The continental slope is highly variable in width and gradient and is interrupted by several terraces. Gradients are up to 6° from offshore Albany to the western Great Australian Bight. Canyon development is extensive, particularly to the west of Esperance, although individual canyons are poorly defined due to the paucity of lines parallel to the slope.

The major part of the slope between Eyre and Ceduna is occupied by the Eyre and Ceduna Terraces. Offshore from Eyre, the continental slope dips at about 2° SSW from the shelf edge at 150-200 m. At 400 m depth it levels out to about 1° to form the Eyre Terrace, an oval feature about 60 km wide and 300 km long (Fig. 3). The outer limit of the terrace lies at about the 1600 m isobath. Below the outer margin, the slope steepens to about 5° and merges with the rise at about 3500 m. The southeasterly-trending Eyre Canyon extends from near the middle of the terrace onto the continental slope at its southern edge. The Eucla Canyon has cut several hundred metres into the continental slope at about 129°E, at the junction of the Eyre and Ceduna Terraces.

The Ceduna Terrace is sigmoidal in outline, some 70,000 km^2 in area, and up to 200 km in width and 600 km in length (Fig. 3). It is bounded to the north and northeast by an upper slope between the shelf break at 150-200 m and the 500 m isobath, and to the southwest by a lower slope between the 2500 and 4000 m isobaths. The surface of the terrace slopes gently to the southwest with an average gradient of 0.6°, compared with an average of 2° for the continental slope. The lower slope merges with the continental rise at about 4000 m.

The most striking features of the bathymetry of the Ceduna Terrace are the numerous submarine valleys which dissect its surface (Tilbury and Fraser, 1981). They are mostly broad and shallow and form a dendritic tributary system feeding steeper-walled canyons on the lower slope. The valleys originate on the upper slope as small channels; these channels coalesce to form valleys 5-10 km wide on the upper part of the terrace; and these valleys in turn converge on the lower slope to form larger valleys about 20 km wide that eventually feed the canyons of the lower slope. These canyons have been assigned names by Jongsma (1991); these names have been used in the geological report presented in Section 6.1.

To the east of the Ceduna Terrace, the continental slope off Kangaroo Island is similar to that on the western side of the Great Australian Bight, with gradients of up

to 8° and extensive canyon development. The slope here extends down to about 4600 m. It is extensively incised by the numerous paleo-channels and active channels of the Murray River canyon system; von der Borch and others (1970) have recorded the depth of the main canyon as about 1800 m below the adjacent seabed. Some canyons in this area are almost parallel to the slope, deepening westwards.

CONTINENTAL RISE AND ABYSSAL PLAIN

The continental rise is composed of a smooth apron of sediments lying between the continental slope and the abyssal plain (between the continental slope and the Diamantina Fracture Zone in the west). The upper boundary of the rise varies from about 4000 m off Albany, to about 3000 m south of the Archipelago of the Recherche, to as deep as 5000 m in the extreme southeast. South of the Eyre Terrace, the rise is abnormally broad, in excess of 200 km, with a gradient of about 0.5°. By contrast, south of the Ceduna Terrace, the rise is only about 50 km wide with a gradient of up to 2°.

The South Australian Abyssal Plain, in excess of 5500 m deep, is a relatively small area of ocean floor occupying the area between the rise, the Diamantina Fracture Zone in the west, and the rugged northern flank of the Southeast Indian Ridge. Pinnacles of oceanic crustal material rising through the smoother sediment-covered ocean floor were sampled in area D (see Section 6.4).

3.2 REGIONAL STRUCTURE AND SUBDIVISION OF BASINS

The southern margin of the Australian continent is a divergent, passive, continental margin, extending for 4000 km from the Perth Basin in Western Australia to the Sorrel Basin in Tasmania (Fig. 2). The margin developed during the Jurassic to Cretaceous by extension and rifting between the Australia and Antarctic plates. Seafloor spreading was initiated in the mid-Cretaceous (Cande and Mutter, 1982; Veevers, 1986; Veevers and others, 1990) and continues to the present day.

Stagg and others (1990) proposed the name **'Southern Rift System'** for the broad zone that has been affected by the Jurassic-Tertiary rifting and spreading event along Australia's southern margin. Within the Southern Rift System, a number of basins, sub-basins, troughs, and embayments have been identified and named in the past. In some cases, the sparsity of data (particularly in deep water) has resulted both in the overlooking of major sediment bodies and in the mis-identification or non-identification of the relationships between recognised sediment bodies. The following summary is based on the attempt by Stagg and others (1990) to rationalise the subdivision and nomenclature of sediment bodies within the western half of the Southern Rift System.

In the east, the **Duntroon Basin** (Fig. 2) (formerly also known as the Duntroon Embayment) is inferred to lie between two approximately NW-SE trending accommodation zones; the East Duntroon and West Duntroon Accommodation

Zones. The East Duntroon Accommodation Zone, immediately to the west of Kangaroo Island, is considered to be the boundary between the Duntroon Basin and the Otway Basin to the east, while the West Duntroon Accommodation Zone marks the junction of the Duntroon and Bight Basins. Both of these accommodation zones may have expression in the Polda Trough to the north.

The **Bight Basin** (Fig. 2) occurs almost exclusively beneath the continental slope and rise which underlies most of the Great Australian Bight west of the Duntroon Basin. Within the Bight Basin, three sub-basins can be identified. The main sediment accumulation underlies the bathymetric Ceduna Terrace and has been referred to in the past as the 'Great Australian Bight Basin' (e.g., Willcox, 1978; Fraser and Tilbury, 1979) or the 'Ceduna Depocentre' (Veevers, 1984); this feature is informally named the '**Ceduna Sub-basin**' by Stagg and others (1990). The **Eyre Sub-basin** is a discrete extensional basin 'perched' high on the continental slope on the western side of the Great Australian Bight, separated from the continental rise to the south by shallow basement, but apparently contiguous with the Ceduna Sub-basin to the east. The quite different structural styles of the Ceduna and Eyre Sub-basins warrants their continued separate names. The thick sediment accumulation beneath the continental rise, principally on the western side of the Great Australian Bight, has previously been referred to as the 'rise basin'. This sediment actually constitutes a sub-basin of the Bight Basin, being separated from the Ceduna Sub-basin to the northeast by the Southwest Ceduna Accommodation Zone; this feature was informally named the '**Recherche Sub-basin**' by Stagg and others (1990). The western limit of the Recherche Sub-basin is ill-defined, and it may continue well to the west of the Great Australian Bight.

To the west of the Great Australian Bight, the only easily-identified extensional basin is the **Bremer Basin**, which underlies the continental slope approximately between Albany and Esperance (Fig. 2). To the west, this basin terminates against shallow basement, while to the east it terminates against a major transfer fault or accommodation zone.

The northern and southern limits of the Southern Rift System are relatively easily defined. The northern margin is considered to be the major basement fault or monocline that marks the landward extent of the Duntroon, Bight, and Bremer Basins and which underlies the continental slope elsewhere. This fault system marks the northern limit of thick Cretaceous sediments. The southern boundary of the Southern Rift System is taken as the basement ridge beneath the abyssal plain that has been interpreted by Veevers (1986) as the continent-ocean boundary.

North of the Southern Rift System bounding fault in the Bight Basin, the continental shelf is underlain by a thin sequence of Cretaceous and Tertiary sediments that extend onshore to about 30°S. These sediments are very condensed in character, being related to stable platform deposition rather than a rifting regime. Such sediments are now included in the Tertiary-Cretaceous **Eucla Basin** which was formed in a continental platform sag regime, and dips gently towards the rifted

Bight Basin.

The Permian **Denman Basin** underlies part of the Eucla Basin. This basin occupies a north-south elongate depression between approximately 31-33°S and 130-131°E (Fig. 2). It appears to be coincident with the deepest depressions within the Eucla Basin and is probably related to an earlier zone of weakness.

The **Polda Trough** (or **Polda Basin**) is an east-west oriented elongate intracratonic basin, approximately 350 km long by 40 km wide. It extends onshore to 136°E and westward to 132°45'E where it debouches into the Bight Basin (Fig. 2). Its geographic location, structural trend, and Upper Proterozoic, Palaeozoic, and Jurassic sediment fill indicate that it formed within an ancient zone of crustal weakness, and was reactivated during formation of the Southern Rift System. However basement strength was apparently sufficient to block significant rift development and the basin remains as a Jurassic aulacogen.

In the nearshore areas on the eastern flank of the Great Australian Bight, large areas of shallow basement are covered by a thin veneer of Cenozoic (mainly Tertiary) sediments. Robertson and others (1979) used the term "Eyre-Encounter Bay Shelf" to describe these sediments. However, the seismic data in this area is both sparse and of poor quality and the relationship of the sediments to other basins, such as Eucla, Murray, St. Vincent, and Cowell remains to be determined before more formal basin naming is proposed.

3.3 SPREADING HISTORY

Magnetic lineations were first identified and mapped by Weissel and Hayes (1972), based on *USNS ELTANIN* data. These authors concluded that the oldest identifiable anomaly was anomaly 22, and that Australia-Antarctica breakup occurred in the Early Eocene, at about 55 Ma. In addition to the basic lineation pattern, Weissel and Hayes (1972) also identified several large-scale anomalous magnetic and/or morphologic features that have remained difficult to explain:

(1) The Australia-Antarctic Discordance (AAD) is a region of anomalously deep crust astride the Southeast Indian Ridge system south of the Great Australian Bight, containing subdued magnetic anomalies.

(2) The Diamantina Fracture Zone is a latitudinal band of extremely rough seafloor topography south of southwest Australia. The Diamantina Fracture Zone is most pronounced west of 125°E, and becomes progressively more buried by sediment towards the east so that its eastward extent is difficult to define.

(3) A broad Magnetic Quiet Zone (MQZ), bounded landward by a prominent magnetic trough, extends along the Australia's southern margin from the west of the continent, where the magnetic signature is relatively disturbed, to the eastern side of the Great Australian Bight, where it encompasses the oldest magnetic anomalies. The crust beneath the MQZ has variously been interpreted as continental (Falvey, 1974; Boeuf and Doust, 1975; Deighton and others, 1976) or hybrid "rift-valley" (Talwani and others, 1979) crust.

In a major reinterpretation of the oldest part of the magnetic anomaly record, Cande and Mutter (1982) suggested that the anomalies originally identified as 19-22 could be more appropriately modelled as anomalies 20-34, corresponding to a period of extremely slow spreading (approximately 4.5 mm/yr). On this basis, Cande and Mutter (1982) estimated that Australia-Antarctica breakup occurred at some time between 90 and 110 Ma. This revised, and now generally accepted interpretation provides explanations for many previously anomalous features off Australia's southern margin. The roughness of the Diamantina Zone can be attributed to the period of slow spreading; previous difficulties in identifying the oldest magnetic anomalies can be resolved; and this reinterpretation accounts for the period of rapid basin subsidence prior to 90 Ma identified along Australia's southern margin (Falvey and Mutter, 1981).

More recently, Veevers (1986, 1988) and Veevers and others (1990) have refined the estimate of breakup age to 96 ± 4 Ma (Cenomanian-Turonian) by proposing that Cande and Mutter's Anomaly 34 is, in fact, the continent-ocean boundary edge-effect anomaly, and by extrapolating the 4.5 mm/yr spreading rate (Figs 4, 5).

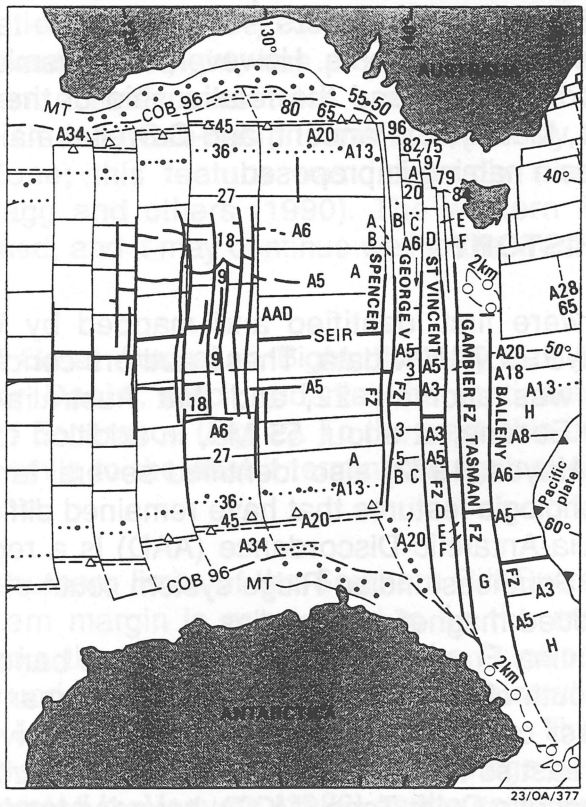

FIGURE 4. Australia-Antarctica magnetic anomalies and spreading history (after Veevers and others, 1990).

While Cenomanian breakup is now widely accepted, Stagg and others (1990) believe that there are still several potential problems that remain to be resolved, both with the breakup age and also with other aspects of the seafloor spreading

history. These problems, which are critical to a full understanding of the tectonic evolution of the southern margin, include:

(1) The deposition of interpreted Neocomian-Barremian sediments above crust oceanward of the continent-ocean boundary interpreted by Veevers (1986).

(2) The continental character of crust oceanwards of the continent-ocean boundary on some *R/V RIG SEISMIC* Survey 65 seismic lines (Stagg and others, 1990).

(3) The very poor correlation and identification of the oldest magnetic anomalies.

(4) The identification of several discrete subsidence events in the geohistory plots from wells in the Great Australian Bight (eg. Jerboa-1).

(5) The existence of a major tectonic event in the Late Cretaceous-Early Tertiary, reflected in seismic records margin-wide (Stagg and others, 1990). Stagg and others (1990) do not believe that this event can be ascribed to eustatic sea-level changes or to deep ocean currents.

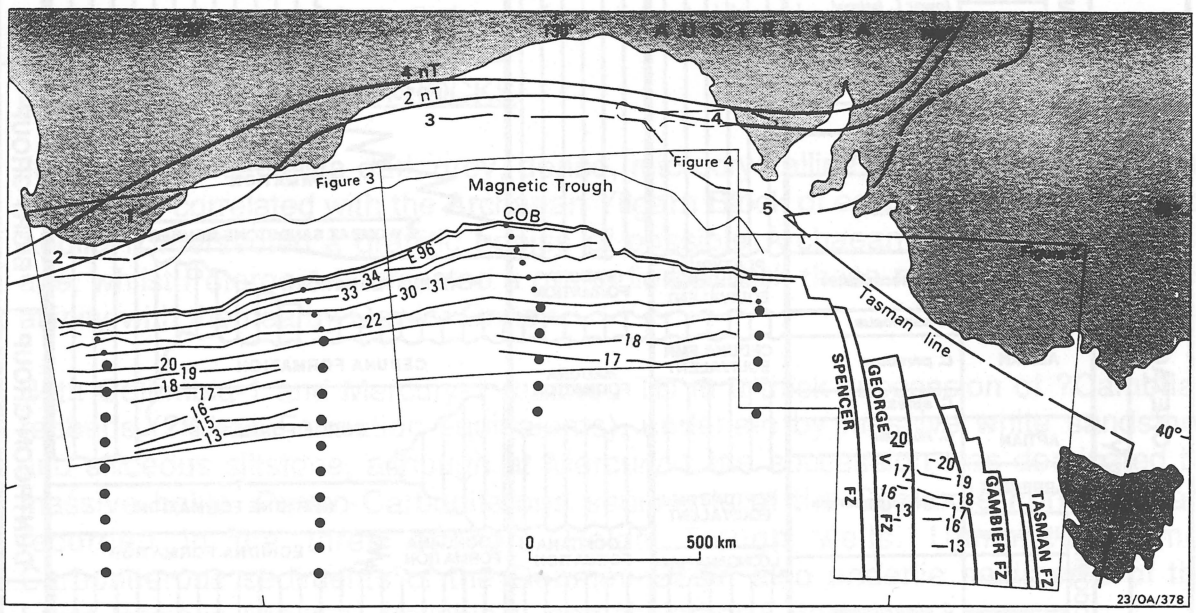

FIGURE 5. Magnetic trends and anomalies adjacent to Australia's southern margin (after Veevers and others, 1990).

3.4 REGIONAL STRATIGRAPHY AND PALEOENVIRONMENTS

Well control in the offshore portions of the platform-sag Eucla Basin, rifted Bight and Duntroon Basins, and intra-cratonic/rifted Polda Trough is limited (Fig. 3). Nine wells: Jerboa-1 and Potoroo-1 (Bight Basin), Apollo-1 (Eucla Basin), Duntroon-1, Echidna-1, and Platypus-1 (Duntroon Basin), and Gemini-1, Mercury-1, and Columbia-1 (Polda Trough), provide the basis for the region's stratigraphy.

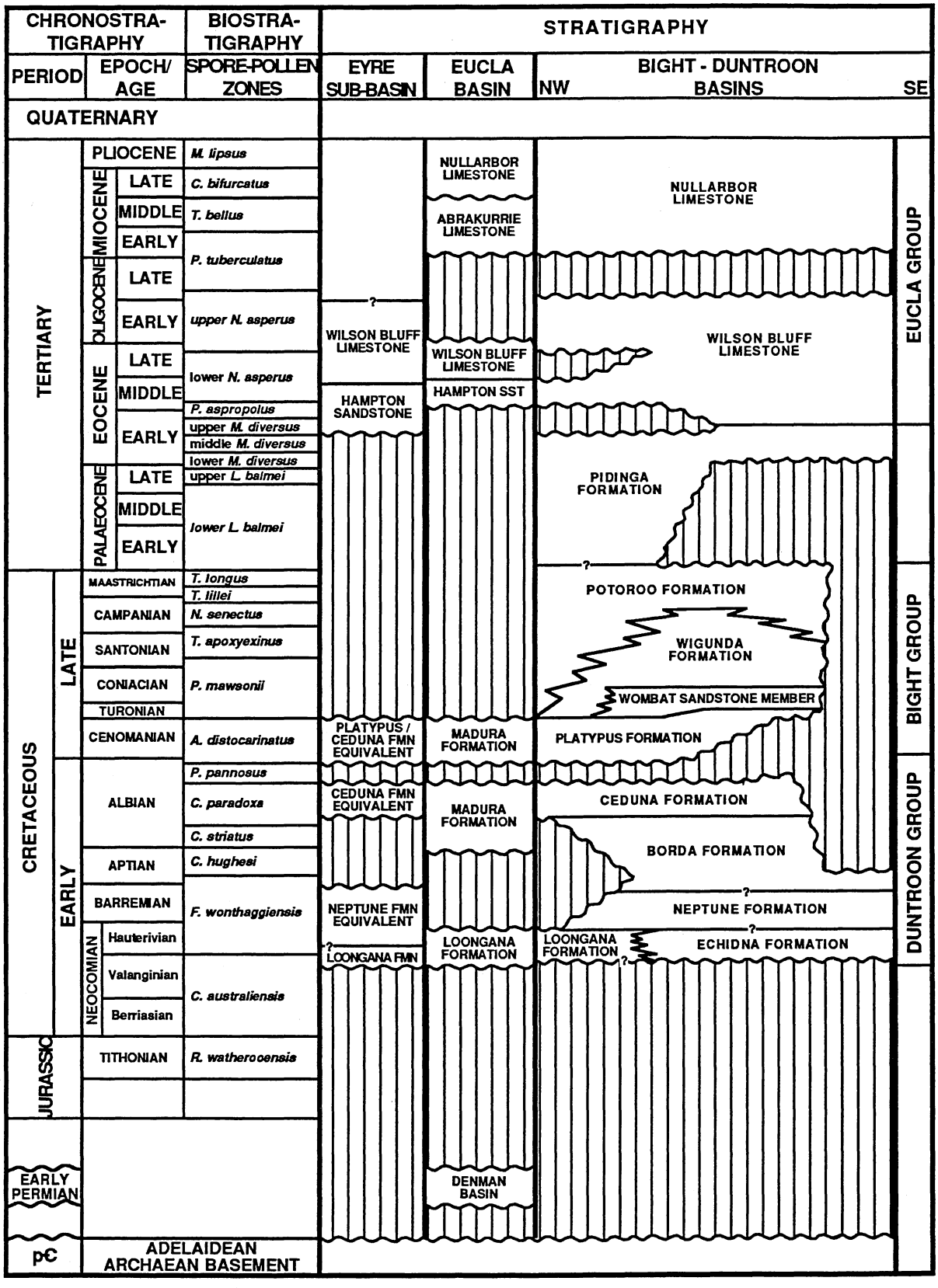

FIGURE 6. Summary of Great Australian Bight stratigraphy (after Stagg and others, 1990).

Previous workers (Lowry, 1970; von Sanden and Barten, 1977) provide the stratigraphic framework for the Cretaceous sequence, supplemented by seismic interpretation of key marker horizons between wells by Fraser and Tilbury (1979). A summary of the revised stratigraphy, incorporating the revised stratigraphic nomenclature of Hill (1989) and the revised palynological zonations of Morgan (1986), is presented in Figure 6.

There is an uncertainty with respect to age relationships between units across all basins, resulting from the lack of cored sections and the reliance upon drill-hole cuttings which, inevitably, can be grossly contaminated. Palynological investigations to date, excluding the work by Morgan (1986) on Duntroon-1, must be viewed with considerable caution, owing to revised palynological zonations for the Mesozoic (Helby and others, 1987). The absolute reliance upon palynological data for correlation and interpretation of the Mesozoic section in the Great Australian Bight by previous workers must also be treated cautiously, because of marked facies changes across the basins. The acceptance of palynological interpretations as an indicator of absolute time, irrespective of the fact that revisions in zonation and taxonomy occur periodically, casts doubt on previous burial history plots and predictions of continental breakup.

PALEOZOIC AND OLDER ROCKS

Jerboa-1 intersected a dark grey, dense, microcrystalline, amphibolitic basement, tentatively correlated with the Archaean Yilgarn Block of eastern Western Australia. Apollo-1 intersected a granitic gneiss of possible Archaean or Early Proterozoic age, whilst Potoroo-1 intersected a granodiorite; both these rock types show close affinity with the nearby Gawler Craton.

Both Columbia-1 and Mercury-1 reached TD in a thick succession of ?Cambrian redbeds (?Kilroo Formation equivalents), underlain by massive white sandstone and siliceous siltstone, although at Mercury-1 the succession was dominated by massive halite. Permo-Carboniferous sediments of the Coolardie Formation are recorded in the three offshore Polda Trough wells. Unnamed Permo-Carboniferous sediments of the Denman Basin also underlie sediments of the Eucla Basin in Apollo-1, Mallabie-1, and Nullarbor-8 Bore.

MESOZOIC SEDIMENTS

The first indication of Mesozoic sedimentation occurs in the Polda Trough. Fluviatile and lacustrine sediments of the Upper Jurassic **Polda Formation** have been intersected in the three offshore Polda Trough wells, and may represent early syn-rift deposition.

The earliest firm evidence of rift-related sediments recorded ubiquitously across the Southern Rift System is the Neocomian **Loongana Formation**. In Jerboa-1, the sequence consists of non-marine, interbedded sandstones, siltstones, and dark brown to black pyritic shales, assigned a Late to Middle Jurassic age (M.

florida Zone; Powis and Partridge, 1980). A fluvio-deltaic depositional environment with outbuilding of deltas into a deep lake that experienced localised anoxic conditions is envisaged. A similar but somewhat more condensed sequence occurs in Apollo-1 and Potoroo-1, where a basal sandstone and shale unit has been assigned to the Loongana Sandstone, but due to the strong affinities with Jerboa-1 is now referred to as the Loongana Formation; it represents a time equivalent of the Pretty Hill Sandstone of the Otway Basin.

In the Duntroon Basin, a sequence of dark brown to black shales interbedded with minor gritty sandstones, inferred to have been deposited in a proximal lacustrine environment, has been assigned to the **Echidna Formation** (Hill, 1989) and is a time equivalent of the Loongana Formation.

Non-marine conditions persisted across the region into the Barremian. A monotonous sequence of dark shales intersected in Echidna-1 is assigned to the **Neptune Formation** and is equivalent to a Neptune Formation equivalent in Jerboa-1. However, this unit was not penetrated, or was absent, in the remaining wells in the Duntroon Basin, and was absent in the Bight and Eucla Basins.

The first indication of marginal marine conditions is recorded within the Duntroon Basin during the Aptian. This involved the deposition of the **Borda Formation**, consisting of a thick sequence of shale with minor basal sands and coal. These sediments were deposited in a poorly drained floodplain that experienced minor marine ingressions, possibly resulting from the transgression of a shallow sea from the northeast (Veevers and Evans, 1975). No record of Aptian deposition is observed in the Bight and offshore Eucla Basins; marine influence in the Otway Basin is similarly transitory during the Aptian.

Predominantly marine conditions persisted during the early Albian in the Eucla Basin at Apollo-1 (Madura Formation; Fig. 6), but are not recorded in the Bight Basin. A hiatus in marine deposition between the Eucla and Duntroon Basins is apparent, reinforcing the notion of a transgression from the northeast possibly via the Eromanga Basin.

Shales and minor coals of the upper Borda Formation in Duntroon-1 were deposited in a non-marine, fluvio-lacustrine environment with one notable marine incursion (M. tetracantha dinoflagellate Zone; Morgan, 1986). Widespread marginal marine sedimentation is apparent during the middle Albian.

In the Duntroon Basin, the **Ceduna Formation** conformably overlies the Borda Formation and consists of distributary channel sandstones and siltstones deposited in a tidally-influenced deltaic complex that extended laterally to Platypus-1 (Dodd, 1986). Within the Bight Basin, the Ceduna Formation occurs as a nearshore marine facies that passes into a condensed sequence in Apollo-1 (Madura Formation), possibly due to clastic starvation. In the Eyre Sub-basin of the Bight Basin, Jerboa-1 contains a widely correlatable Albian section that comprises dark grey to black marine shales. It is assigned to the Ceduna Formation

equivalent.

A regional hiatus is apparent in the late Albian extending from the Bight Basin to the Duntroon Basin (Fig. 6). The hiatus marks the boundary between the Early Cretaceous Duntroon Group and the Late Cretaceous Bight Group (analogous to the Otway and Sherbrook Groups of the Otway Basin) and is also coincident with the presumed Australia-Antarctica breakup at 96 ± 4 Ma (Veevers, 1988).

In the Duntroon Basin, a major Cenomanian regression led to non-marine conditions and the deposition of sandstone, siltstone, and coaly facies of the **Platypus Formation**. Meanwhile, in the Bight Basin, nearshore marine facies of the basal Platypus Formation were deposited, passing into brackish and non-marine facies at the top in Potoroo-1. In Apollo-1, a condensed sandstone and shale sequence (upper Madura Formation) was laid down under marine conditions, while in the Eyre Sub-basin, Jerboa-1 intersected a correlatable sequence comprising dark shales and a basal sand deposited in a nearshore environment (Platypus Formation equivalents).

The **Wombat Sandstone Member** of the Wigunda Formation is restricted to the Duntroon Basin where it represents a thin, but laterally-extensive shoreface unit deposited on a marine shelf (Morgan, 1986). Stable marine conditions existed in the Duntroon Basin from the Turonian to the Campanian with the deposition of the strongly diachronous **Wigunda Formation**. The unit comprises prodelta siltstones and claystones and is analogous to the Belfast Mudstone of the Otway Basin. The unit is absent in Jerboa-1, Apollo-1, and Mallabie-1, suggesting that the proximal portions of the Eyre Sub-basin and Eucla Basin acted as a major bypass margin in the Late Cretaceous. Deighton and others (1976) and Fraser and Tilbury (1979) interpret this change to signify a probable eastwards encroachment of the sea along the floor of the rift valley. It is coincident with a major global sea level rise in the Turonian (Vail and others, 1977). The merging of the Platypus and Potoroo Formations is likely as the Wigunda Formation becomes more condensed to the north of the Bight Basin.

In the southwest part of the Ceduna Sub-basin, a thick prograding sequence with large-scale foreset beds (**Potoroo Formation**) was deposited in the Santonian-Campanian. The unit is equivalent to the Timboon Sand of the Otway Basin. Significant upbuilding of topset beds is indicative of relative sea level rise which Fraser and Tilbury (1979) attribute more to sediment loading than to eustacy. The formation is strongly diachronous (Fig. 6), ranging in age from Cenomanian to Maastrichtian in the west to late Campanian to Maastrichtian in the east (Forbes and others, 1984). Depositional environments were paralic in the northeast and bathyal in the southwest.

Within the Duntroon Basin, the Potoroo Formation is divisible into a basal nearshore marine sand, middle massive brackish-water shale, and an upper interbedded sand and shale sequence deposited in a delta plain environment. Fraser and Tilbury (1979) suggest a high rate of terrigenous influx as being a

contributing factor for this regression. A similar sequence is encountered in Potoroo-1 in the Ceduna Sub-basin. Seismic data indicate that the Potoroo Formation regression was followed by a transgression resulting in a seaward thinning wedge of paralic facies sediments cutting across the top of the prograded sequence and extending over most of the Ceduna Sub-basin (Willcox, Stagg, Davies and others, 1988).

TERTIARY SEDIMENTS

The Potoroo Formation is unconformably overlain by the transgressive marine sands of the Tertiary **Pidinga Formation** in the Duntroon Basin, whilst no apparent unconformity can be recognised in the Bight Basin (von Sanden and Barten, 1977). Environments of deposition range from shallow subtidal to lagoonal. In the Eyre Sub-basin and the Eucla Basin, the **Hampton Sandstone** unconformably overlies the Upper Cretaceous Bight Group sequence and is considered to be a correlative of the Pidinga Formation.

Open marine conditions in the Early Eocene extended from the Eyre Sub-basin to the Duntroon Basin with the deposition of the **Wilson Bluff Limestone** of the Eucla Group which conformably overlies the Hampton Sandstone to the west and the Pidinga Formation to the east.

A regional hiatus, due to either non-deposition or erosion, is apparent across the region in the Lower Oligocene. Stable open marine conditions prevailed with deposition of the **Nullarbor Limestone** from the Early Miocene until the latest Tertiary (Fig. 6). Since their deposition, the limestones of the Eucla Group have been elevated and tilted gently to the east and south. At the Head of Bight, they are overlain by Pleistocene aeolinites (Ludbrook, 1969).

3.5 SUMMARY OF TECTONIC HISTORY

Stagg and others (1990) proposed the following speculative tectonic history for the Great Australian Bight region, and for the Southern Rift System in general:

(1) Lithospheric extension in the ?pre-Valanginian, and probably as old as the Permian, was on a NW-SE azimuth. This extension, which is well-documented on the western margin of Australia, probably reached at least as far east as Kangaroo Island, and may have affected the entire Southern Rift System. Movement would have been predominantly strike-slip or transtensional in the nascent Otway Basin, and in the Bass Strait/west Tasmania area.

(2) Permian to Jurassic sedimentary basins developed along the embryonic Southern Rift System (for example, underlying the Recherche Sub-basin), and were filled largely by fluvio-lacustrine syn-rift sediments. The sediment fill was at least partially indurated.

(3) Neocomian 'breakup' lead to subsidence of the margin and the onset of marine deposition in the deeper parts of the rift basins. The developing ocean basin was underlain by crust which ranged from highly-extended continental, through mixed slivers of oceanic and continental material, to purely oceanic. Crust

with greater oceanic affinity was probably more prevalent in the west. At about this time, lithospheric extension appears to have occurred in the Gippsland Basin of southeastern Australia along a NNE-SSW azimuth, almost orthogonal to coeval extension in the west.

(4) A huge pile of clastic sediment (?3000 m thick), rapidly deposited in the Ceduna Sub-basin and Duntroon Basin areas during mainly Barremian to Albian times, was probably a shelf/slope deposit on the incipient continental margin.

(5) Continued breakup and the onset of thermal sag during the Cenomanian led to renewed block-faulting in the Ceduna Sub-basin and Duntroon Basin, and reactivation of deep-seated transfer fault zones. The pile of under-compacted sediment was put under transpression and/or slumped to create a zone of nappe and overthrust structures along the southwestern flank of the Ceduna Sub-basin. This covers an area of approximately 60,000 km^2.

(6) Gradual reduction in tectonic subsidence during the Late Cretaceous allowed the aggradation and outbuilding of massive delta complexes, particularly in the southwest Ceduna Sub-basin. Continued movement within the underlying incompetent sediment pile caused diapirism throughout the Late Cretaceous. In the Otway/Tasmania area, the proximity of the spreading ridge thermal anomaly to the plate boundary (as a result of numerous ridge offsets) and contact between parts of the Australia and Antarctica Plates, led to transpression and uplift of some of the oceanward tilt-blocks.

(7) Extensive uplift and erosion appears to have taken place in the Late Cretaceous and ?earliest Tertiary when, for example, the `outer high' formed in the Ceduna Sub-basin and the Echidna-Koala Structures (see Stagg and others, 1990) formed in the Duntroon Basin. Several thousand metres of sediment were probably eroded from the tops of these structures. Stagg and others (1990) could offer no satisfactory explanation for the origin of this uplift, since from calculations of the degree of extension and the rate of seafloor spreading, it would appear that the plates were separated by several hundred kilometres at this stage.

(8) The Tertiary was a period of minimal deposition, or deposition and subsequent erosion, in the Great Australian Bight area, with only a few hundred metres of Paleogene terrigenous sediment and Neogene carbonate being preserved. In the Otway area, Paleogene deltaic sediments were being laid down. During the Late Eocene and possibly earliest Oligocene, major wrench-related anticlines developed on the Otway continental slope, corresponding to the onset of fast seafloor spreading. These complexly-faulted structures occupy an inboard position on the slope (that is, away from the plate boundaries and contact), suggesting that they are caused by re-activation at the heads of major basin-forming detachment faults.

(9) Nearly all faulting and related tectonic movements ceased abruptly during the mid-Oligocene when the Australia and Antarctic Plates cleared each other in the South Tasman Rise area.

4. CRUISE PLAN

A summary of the cruise plan, as outlined in Feary (1991), is as follows:

1) Transit from Fremantle (departure 0000 hrs 12/6/91).
2) Dredging of northwestern ocean crust geochemistry site.
3) Shooting of two high-resolution seismic lines, together with short tie lines, across the Eucla Shelf and Eyre Terrace; a total of 650 line km.
4) Vibrocoring (in shallow water - <350 metres) and gravity coring (in deeper water - 350 to 1000 metres) on the Eucla Shelf and Eyre Terrace, at sites located on the high-resolution seismic lines.
5) Gravity coring for geochemical traverse from 500 - 3500 metres water depth.
6) Dredging and gravity coring of deep Ceduna Terrace sequence (>3500 m water depth).
7) Dredging of remaining three ocean crust geochemistry sites.
8) Transit to Fremantle (arrive 2330 hrs 10/7/91).

5. CRUISE 102 OPERATIONAL SUMMARY

The actual operational record for cruise 102 diverged little from the cruise plan detailed above, with the exception of the abandoned high resolution seismic component.

Departure from Fremantle was delayed slightly and departure finally occurred at 1600 hours on 12th June 1991, followed by a 44 hour transit to the first sampling site. The first dredge site, in 5000 m water depth, recovered a large quantity of manganese nodules and crusts, but no oceanic crustal rocks.

Following the long transit to the start of the Eucla Shelf transect, attempts to deploy the seismic streamer and begin seismic data recording were delayed first by attempts to locate the cause of 8 dead channels in the streamer, and then by the continued failure of the seismic acquisition system during numerous attempts at data recording. After 24 hours of intense but fruitless efforts, in abnormally slight seas ideal for seismic data collection, this component was deferred and the coring transect commenced. A total of 11 gravity cores (all except one successful, ranging from 0.22 m to 4.90 m recovery) and 14 vibrocores (7 successful, ranging from 0.30 m to 1.37 m recovery) established an excellent record of Quaternary cool-water carbonate deposition across the Eyre Terrace-Eucla Shelf. The hope that some of these cores might penetrate a thin veneer of Quaternary sediment into older Cenozoic deposits was unrealised. During the transit back to the middle shelf to recommence attempts at seismic acquisition, a series of 7 seafloor photographic stations were occupied, between 22 m and 91 m water depth. The seismic streamer was re-deployed, after the faults causing dead channels had been corrected, and attempts to begin acquisition recommenced. However, the seismic acquisition system, which had operated for many hours in test mode, once again failed as soon as real data collection began. After a further 18 hours of fruitless attempts to locate the problem, this component of the program was abandoned.

Prior to transit to the western Ceduna Terrace geochemical transect (Area C), a single dredge haul recovered medium to coarse sand from the previously unsampled zone between the Area B gravity core and vibrocore traverses, confirming that the nature of the substrate prevented gravity core penetration.

The first gravity core in Area C was unsuccessful, almost certainly because of a coarse, sandy seafloor. However the remaining 6 cores, in water depths from 1000 to 3500 m, were all successful, with cores of between 2.13 m and 5.20 m recovered. Although these cores constitute an excellent upper slope sedimentological traverse, an assessment of their usefulness for the Australian continental margin paleochemistry program still awaits further shore-based studies.

Sampling operations in Area A, to sample the Ceduna Sub-basin sequence, were of mixed success. A series of cores designed to sample possible diapiric features on *RIG SEISMIC* Survey 65 multichannel seismic lines predominantly recovered Quaternary cover sediments; however, one core did contain shale fragments which may represent either outcropping indurated sedimentary rocks, or a shale diapir. A total of 6 dredge sites were occupied in canyons deep on the lower slope. In most cases existing bathymetric data, particularly the Jongsma and others (1991) bathymetric map of the offshore Ceduna area (which was found to be generally highly accurate), indicated that the eastern sides of the canyons were the steepest sides, and were therefore the prime targets for dredging. However, rough seas and strong winds from the WSW during much of this part of the operation made accurate dredging almost impossible, with the result that only three dredges recovered Ceduna Sub-basin sediments. Nevertheless, these rocks yielded Late Cretaceous (Campanian to latest Maastrichtian) and Middle Eocene to mid-late Oligicene ages. Attempts to penetrate apparently thin surficial Quaternary sediments with a short-barrelled gravity corer at 9 sites were only marginally successful, with only two sites yeilding pre-Quaternary faunas.

Completion of sampling in the Ceduna Terrace region was followed by transits to the two eastern abyssal plain sites to dredge steep-sided pinnacles rising from oceanic basement through a cover of sediment (Area D). These dredges were spectacularly successful, yielding excellent samples of oceanic crust basalts and, in the case of the more seaward of the sites, an enigmatic assemblage of gabbroic rocks which is likely to make a significant contribution to our understanding of Australian-Antarctic seafloor spreading processes.

The transit back towards the western oceanic crust sites was sited to collect bathymetric data for the AGSO's Offshore Resource Mapping Series (ORMS) project. Despite rough seas, some 913 line km of good quality bathymetric data was collected.

6. GEOLOGICAL RESULTS OF CRUISE 102

6.1 - AREA A: BIOSTRATIGRAPHY AND SEDIMENTOLOGY OF THE DEEP CEDUNA SUB-BASIN SEQUENCE

The earlier *R/V RIG SEISMIC* cruises in the Great Australian Bight extended the existing seismic coverage in the Ceduna Terrace area (Survey 65), and carried out an extensive sampling program, using coring, dredging, and heatflow techniques (Survey 66) in the shallow Ceduna Terrace sequence. This earlier program was designed to further evaluate the hydrocarbon potential of an area considered to possess fair to good hydrocarbon prospectivity (Fraser and Tilbury, 1979). Fraser and Tilbury (1979) recognised two main possibilities in the Great Australian Bight Basin that may be favourable for hydrocarbon generation, migration, and entrapment:

(1) The top part of the faulted Lower to mid-Cretaceous sequence where structural entrapment may exist in tilted blocks by a combination of dip closure and faulting. While both source (marine beds within the blocks) and seal (fine-grained sediments of the Wigunda Formation) may be present, Potoroo-1 did not contain indications of appropriate reservoir facies. However Potoroo-1 was sited on the far northern edge of the Ceduna Terrace sequence, and cannot be considered a truly representative facies sequence.

(2) Juxtaposition of a thick Upper Cretaceous sequence, interpreted to contain interbedded sands and shales, directly above a probable fine-grained, shallow marine sequence. The deeper marine sequence provides a potential source, with any generated hydrocarbons having a simple migration path into sand bodies forming stratigraphic traps within the delta sequence. However Willcox (1981) suggested that the sand bodies may be too shallow for maturity, and that the delta shows no proximal downwarping or closure.

The existing biostratigraphic and sedimentologic facies information for the Ceduna Terrace sequence is based on the sequence encountered in Potoroo-1, lying on the northern margin of the terrace, and on dredge and core data from *R/V RIG SEISMIC* Survey 66, from the shallow outer margin of the terrace on the upper continental slope. The sampling program proposed for Cruise 102 was for a series of dredge samples to be taken from the deepest exposed parts of the Ceduna Terrace sequence, from deeply eroded submarine canyons primarily concentrated on the central and eastern parts of the terrace. The objective of this program was to describe the biostratigraphy and sedimentary facies of the interpreted Cretaceous sequence, in order to determine whether facies variations between Potoroo-1 and the southern margin of the sequence enhance the prospectivity of this sequence.

As noted above, the extremely poor weather conditions encountered during much of the time in Area A resulted in poor sample recovery. As a consequence of this poor weather, some of the dredge sites were abandoned and, rather than heave-to, were replaced by short-barrelled gravity core sites in an attempt to "punch" through any Quaternary cover and recover older underlying sediments. However all such gravity cores recovered only Quaternary material.

The following reports (Sections 6.1.1 and 6.1.2) detail the sedimentological characteristics of samples recovered in Area A. Biostratigraphic results from this area are described in Section 6.5.1.

6.1.1 SEDIMENTOLOGY OF THE DEEP CEDUNA SUB-BASIN DREDGE SITES

G. Birch (Department of Geology and Geophysics, University of Sydney)

DREDGE LOCATIONS AND RESULTS

Six dredge stations were occupied on the lower slope of the Ceduna Terrace (Fig. 7). Two stations (102DR03 and 102DR04) were located in the central Terrace region and the remaining four stations (102DR05, 102DR06, 102DR07, and 102DR08) were located in submarine canyons (in Pearsons Canyon, Widbey Canyon, and two in Topgallant Canyon) in the east. Due to the poor weather conditions, only three (102DR03, 102DR05 and 102DR07) of the dredges attempted in this area were successful. A total of approximately 270 kg of rock was recovered.

SEDIMENTARY FACIES

Rocks from the three successful sites are grouped into three sedimentary facies: terrigenous siliciclastic facies, carbonate facies, and dolomite facies.

(i) Terrigenous Siliciclastic Facies: Terrigenous siliciclastic rocks were recovered from all three dredge sites.They comprise black mudstones, indurated siltstones and bioturbated iron-rich mudstones.

Black mudstones are widespread (recovered from all 3 sites) and individual samples from each site are indistinguishable. Typically, they are well-rounded, weakly consolidated, tabloid and thinly coated with manganese. Outer surfaces are smooth, but often bored. They are composed almost wholly of mud with minor silt-sized quartz, organic material, and minor glauconite. They are texturally homogeneous with no distinct sedimentary structures. Minor burrowing indicates a marine, possibly lagoonal environment.

Indurated siltstones were encountered at all three dredge sites. Typically, they possess an Fe-rich orange outer crust up to 8 mm thick, which is in turn coated with a thin Mn layer. These rocks are texturally uniform, but minor compositional changes produce subtle colour variations. Very small scale, poorly formed low angle ripples and erosion surfaces are present. *Chondrites* burrows are indicative of a possibly estuarine marine environment.

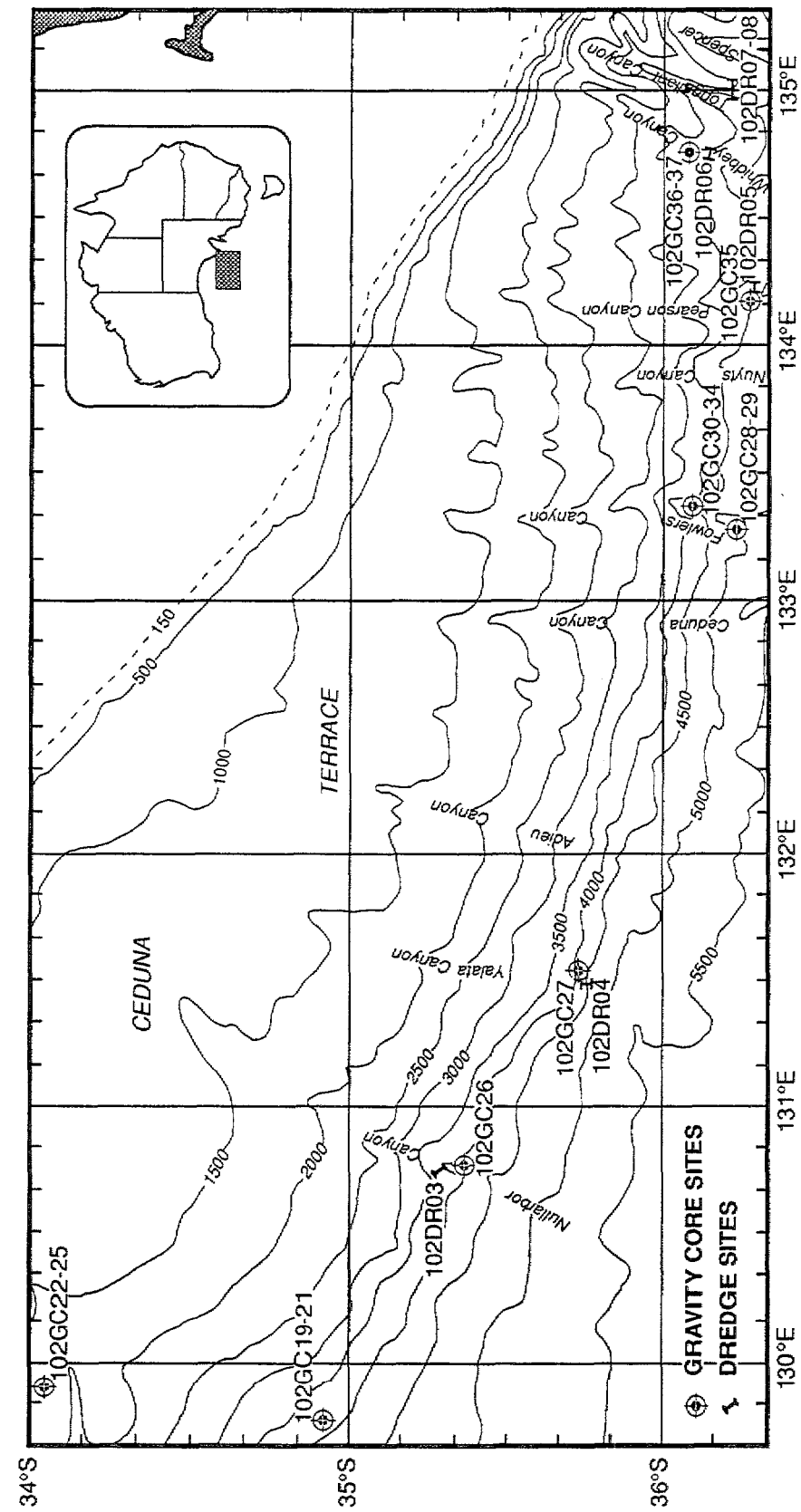

FIGURE 7. Cruise 102 dredge sites and core locations in Ceduna sub-basin (Area A).

The highly bioturbated calcareous mudstones are moderately indurated and well-rounded with very thin Mn outer veneers. The rocks are mainly comprised of clay, silt-sized quartz, and glauconite with minor organic fragments and mica. A pervasive orange colouration suggests a Fe-rich matrix. A high mud content and the presence of burrows and glauconite suggests a low energy marginal marine, possibly tidal flat depositional environment. Possible ?haematitic cementation indicates subareal exposure and pedogenic activity.

These terrigenous rocks are predominantly smooth and well rounded, indicating considerable post-erosional reworking, whereas the ubiquitous Mn-coating is evidence of extensive ocean floor mineralisation.

(ii) Carbonate Facies: calcareous rock was only recovered from site 102DR07. These rocks include foramineral ooze/chalk and calcarenites/calcisiltites.

Semi-lithified, white, foraminiferal ooze/chalk is comprised mainly of planktonic foraminifers, silt-sized to very fine sand-sized quartz, minor glauconite, sponge spicules, benthic foraminifers, and mica. Grains are sometimes Fe- and Mn-stained, and the matrix is probably micritic. Burrows are undiagnostic. The abundance of planktonic foraminifers and minor glauconite suggests an open marine, possibly shelfal environment with restricted terrigenous supply.

Well-indurated, light to dark grey calcarenites and calcisiltites are comprised of foraminifers, sponge spicules, quartz, glauconite, minor echinoid spines, organics, mica, Fe ?authigenic clay aggregates, and altered calcareous matrix. The calcarenites are grainstones with graded laminae defined by grainsize and composition. Small scale ripple troughs and low angle cross-stratification is present. The calcisiltites are burrow-mottled with possible small-scale, low-angle ripple lamination. Evidence of dissolution and replacement by Mn-oxides and cementation by microcrystalline carbonate is pervasive. Calcareous sedimentation with minor glauconite and quartz is suggestive of a marine shelfal environment with suppressed terrigenous influx in an area of slow sedimentation.

(iii) Dolomite Facies: a large volume (>22 kg) of dolomite boulders was recovered from site 102DR07. The rocks are rounded with smooth outer surfaces covered by up to 2 mm of a brownish weathered Fe- and Mn-stained crust. They are comprised of highly birefringent dolomite crystals rimmed with Mn and Fe material and subordinate fine quartz. The rocks are possibly tidal flat wackstones with a weathering rind of iron oxide formed during extensive exposure on the sea floor.

AGE OF ROCKS

Nannofossil dating of seven subsamples from dredge 102DR07 indicates ages between Middle Eocene and Mid-late Oligocene for the carbonate rocks (see Section 6.5.1). Palynological data indicate that the terrigenous rocks are of Late Cretaceous (Campanian to late Maastrichtian) age (see Section 6.5.1).

DISCUSSION

The calcareous and terrigenous rocks recovered from the lower slope of the Ceduna Terrace represent various sedimentary environments from terrigenous shallow water estuarine/lagoonal and mud flats to deeper, purely calcareous shelfal sedimentation. The Late Cretaceous ages for the terrigenous mudstones and siltstones indicate that these rocks are correlatives of the Potoroo Formation. The calcareous rocks are time equivalents of the Wilson Bluff Limestone of the Eyre, Eucla, and Bight Basins and of the Eucla Group limestones in Potoroo-1 and Platypus-1. The shelfal carbonates dredged during the current survey would thus support the general open marine conditions postulated for the Bight Basin from the Early Eocene to the Middle Oligocene.

ROCK DESCRIPTIONS:

DREDGE 102DR03 - west-central Ceduna Terrace.
Water depth: 4180-3660 m. Recovery: ~10 kg.

A - (90% of recovery). Very dark grey (10YR3/1) to black (10YR2/1) mudstone. Well-rounded, moderately consolidated tabular rocks, typically 100-150 by 10-25 mm thick. Patchy, very thin Mn coating on all rocks; probably completely coated by Mn prior to dredging. Outer surfaces bored and internally burrowed. Comprised almost wholly of mud with minor silt-sized quartz, organic matter, and possibly glauconite. Homogeneous texture, no distinct sedimentary structures, but inconclusive evidence of rootlets. Burrowing indicates a marine influence; possibly estuarine. Barren of nannofossils; palynological data indicate Campanian to Maastrichtian age.

B - (10% of recovery; one rock). Greyish brown (10YR5/3), well-rounded cobble (120x80 mm) of siltstone. Outer surface smooth and covered on one side by Fe-rich mineral layer up to 5 mm thick which is in turn mantled by a thin coat of black manganese.The rock is a well consolidated, well sorted claystone to siltstone containing minor ?pyrite and organic matter. The texture is generally uniform, but minor changes in composition produce subtle colour variations. A subtle erosion surface is evident with possible low angle ripples outlined by elongate organic particles. *Asterosoma*, *Chondrites*, and *Planolites* burrows indicate a probable estuarine environment. No age data.

C - pipe dredge 1. Light grey(10YR7/2) nannofossil ooze with small rock fragments similar to above. Comprised of mainly planktonic foraminifers, echinoid fragments, sponge spicules, benthic foraminifers. Age: Quaternary.

D - pipe dredge 2. Very dark greyish brown (10YR3/2) mud with minor silt-sized quartz, mica, organics. Orange Fe-rich streaks evident. Barren of nannofossils; palynological data indicate a Campanian to Maastrichtian age.

DREDGE 102DR05 - Pearson Canyon.
Water depth 5206-4376m. Recovery: ~8 kg rocks; 5 kg mud (pipe dredge).

A - (90% of recovery). Very dark grey (10YR3/1) to black (10YR2/1) mudstone. Well-rounded, moderately consolidated, tabular rocks. Patchy, very thin Mn coating on all rocks, probably completely coated prior to dredging. Outer surfaces bored and internally burrowed. Comprised almost wholly of mud with minor silt-sized quartz, organic matter, and possibly glauconite. Homogeneous texture, no distinct sedimentary structures. Burrowing trace fossils indicate a marine influence, possibly estuarine. Barren of nannofossils; palynological data indicate a late Maastrichtian age. Indistinguishable from 102DR03A.

B - (10% of recovery). Greyish brown (10YR5/3), well rounded cobble (120x80mm) of siltstone. Outer surface smooth and covered on one side by Fe-rich mineral layer up to 5 mm thick which is in turn mantled by a thin coat of black manganese. The rock is a well consolidated, well sorted, claystone to siltstone containing minor ?pyrite and organic matter. The texture is generally uniform. *Chondrites* burrows indicate a probable estuarine environment. Barren of nannofossils; palynological data indicate a late Maastrichtian age. Indistinguishable from 102DR03B.

C - pipe dredge 1. Top: Brown (7.5YR5/4) foraminiferal ooze. Mainly planktonic foraminifers, with subordinate benthic foraminifers, echinoid fragments, and ostracods. Base: Fine to coarse skeletal sand comprising planktonic foraminifers, catenicellid bryozoans, benthic foraminifers, echinoid fragments, cyclostome bryozoans, pteropods, thin-walled mollusca, and ostracods. Age: Quaternary.

D - pipe dredge 2. Unconsolidated, very dark greyish brown (10YR3/2) mud with very fine grained quartz, mica, organics, and calcareous fragments. Small red/brown clumps of Fe-stained aggregates. Barren of nannofossils; palynological data indicate a late Maastrichtian age.

DREDGE 102DR07 - Whidbey Canyon.
Water depth 4380-3660 m. Recovery: ~250 kg rocks; ~2 kg mud (pipe dredge).

A - (~5% of recovery). White, semi-lithified, foraminiferal ooze to indurated chalk. Lithification probably due to compaction and microcrystalline carbonate cementation. The rock comprises planktonic foraminifers, silt- to very fine sand-sized quartz, glauconite, sponge spicules, echinoid spines, Fe-stained mud aggregates, mica, and ostracods. Sedimentary structures are rare and include borings and non-diagnostic burrows.The environment of deposition is interpreted as deep, open-water marine.

B - (<5% of recovery). Dark grey (5YR4/1) to light grey (10YR7/1) calcarenite/ calcisiltite. Well indurated grainstone with graded laminae defined by grain size and compositional variations. Basal scour with ripple trough and low angle cross-stratification is evident. The calcisiltite rocks are burrowed with possible low angle ripple laminations. Compositionally, these rocks are similar to calcarenites with

notable glauconite, sponge spicules, quartz grains, echinoid spines, organics, and mica in a highly altered calcareous matrix. Its origin is possibly quiet-water marine with low terrigenous influx.

C - (<5% of recovery). Very dark grey (10YR3/1) to black (10YR2/1) mudstone.Well-rounded, moderately consolidated, tabular rocks. Very thin discontinuous Mn coating on all rocks, probably completely coated prior to dredging. Outer surfaces bored and internally burrowed. Comprised almost wholly of mud with minor silt-sized quartz, organic matter, and possibly glauconite. Homogeneous texture, no distinct sedimentary structures. Burrowing indicates a marine influence, possibly estuarine. Barren of nannofossils; palynological data indicate a Campanian to latest Maastrichtian age. Indistinguishable from 102DR03A.

D - (~70% of recovery). Grey (7.5YR4/2) dolomite. Smooth, rounded rocks (up to 400x230mm) have outer rims of up to 2 mm brownish, weathered, Fe- and Mn-stained material. They comprise highly birefringent subhedral dolomite crystals rimmed with Mn - and Fe-stained material and subordinate fine quartz. Dark irregular patches and veins of dark Mn-staining are also evident.

E - (20% of recovery). Grey (10YR5/1) to dark grey (10YR4/1), rounded and ellipsoidal boulders of lithified claystone. Outer surfaces coated with Fe-rich material up to 10 mm thick. The rocks are comprised of finely laminated clay with silt-sized organic fragments and quartz. Bioturbation (*Chondrites*) and microfractures are present. Light green (?sulphide) mineralisation is possibly associated with layers of higher organic content. The rocks are non-calcareous and barren of nannofossils and their age is indeterminate.

F - (<5% of recovery). Highly bioturbated, slightly calcareous mudstone. The rock is well rounded with a thin Mn coating on one surface. Burrows are infilled with moderately calcareous mud. The rock is comprised of rounded, medium sand-sized and silt-sized quartz, mica, organic fragments, possibly glauconite, and clay. The overall colour is light to dark orange (7.5YR6/6 to 7.5YR5/4) indicating a moderate iron content.

6.1.2 SEDIMENTOLOGY OF THE CEDUNA CANYONS GRAVITY CORE SITES

G. Birch (Department of Geology and Geophysics, University of Sydney)

Thirteen of nineteen gravity cores taken on the slope of the Ceduna Terrace (Fig. 7) were successful. A total of 12.72 m of core was recovered with a maximum length of 2.68 m and an average length of 1.16 m (Fig. 8).

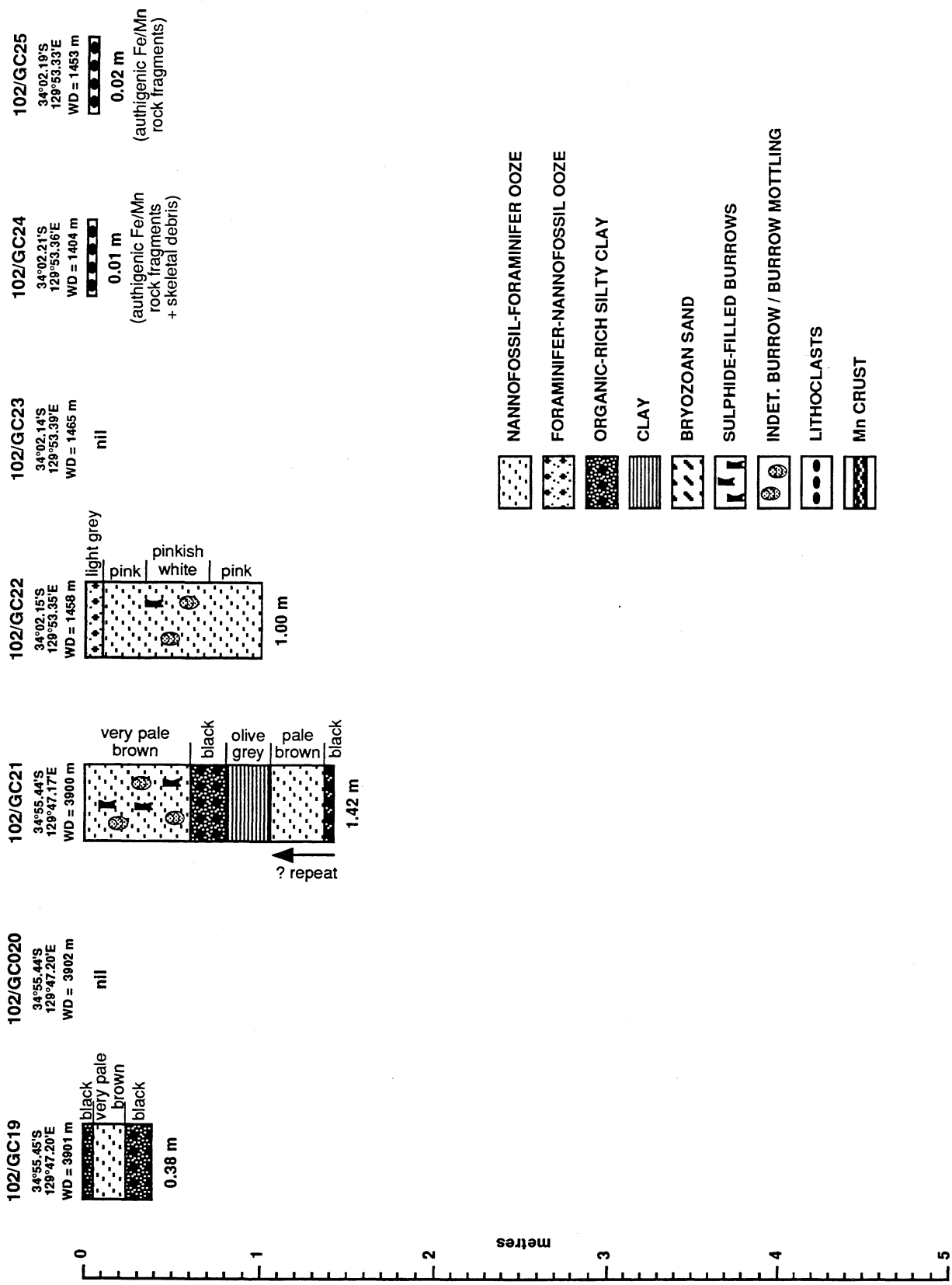

FIGURE 8. Sedimentological logs of Ceduna Sub-basin (Area A) gravity cores.

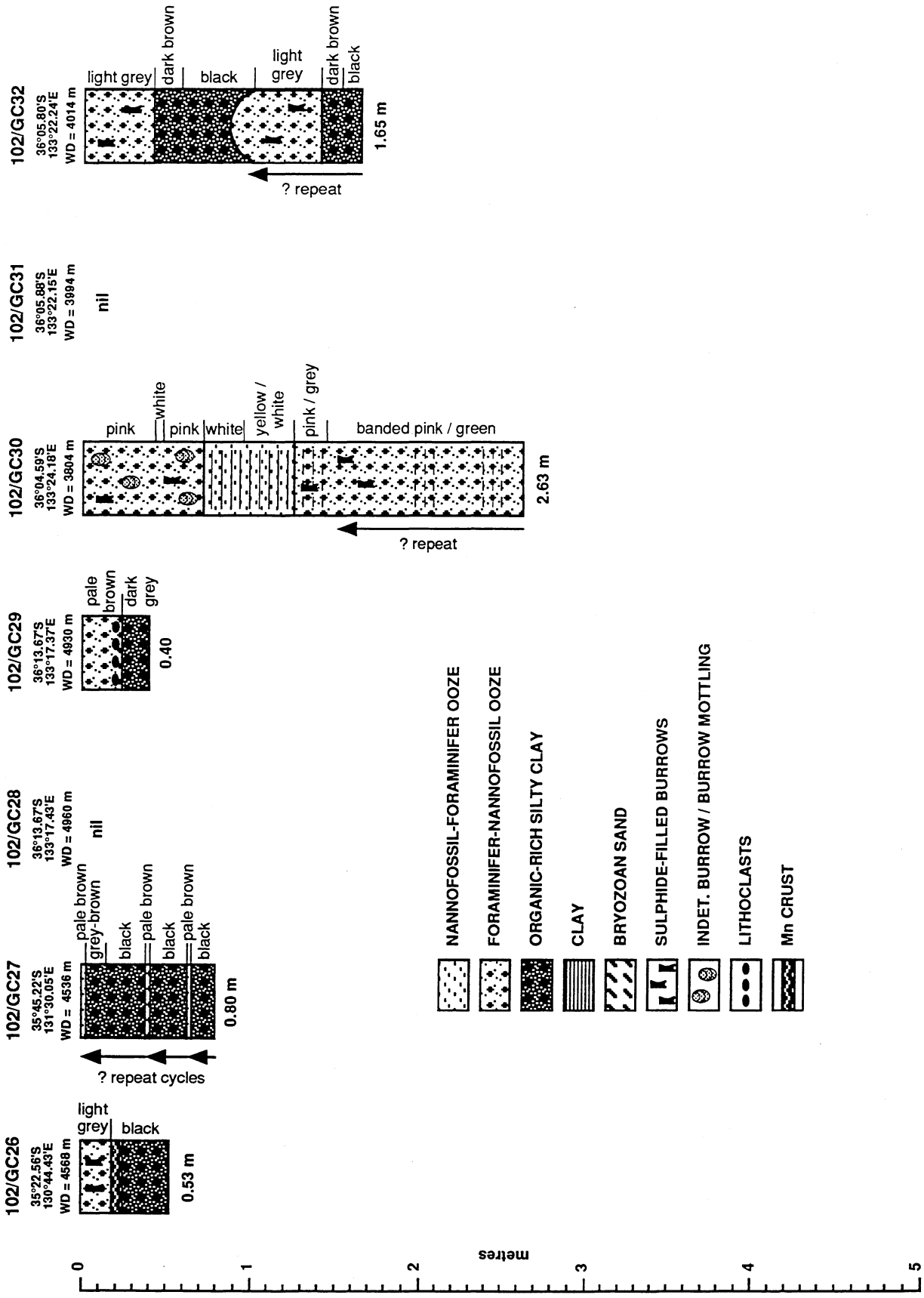

FIGURE 8. Sedimentological logs of Ceduna Sub-basin (Area A) gravity cores (cont.).

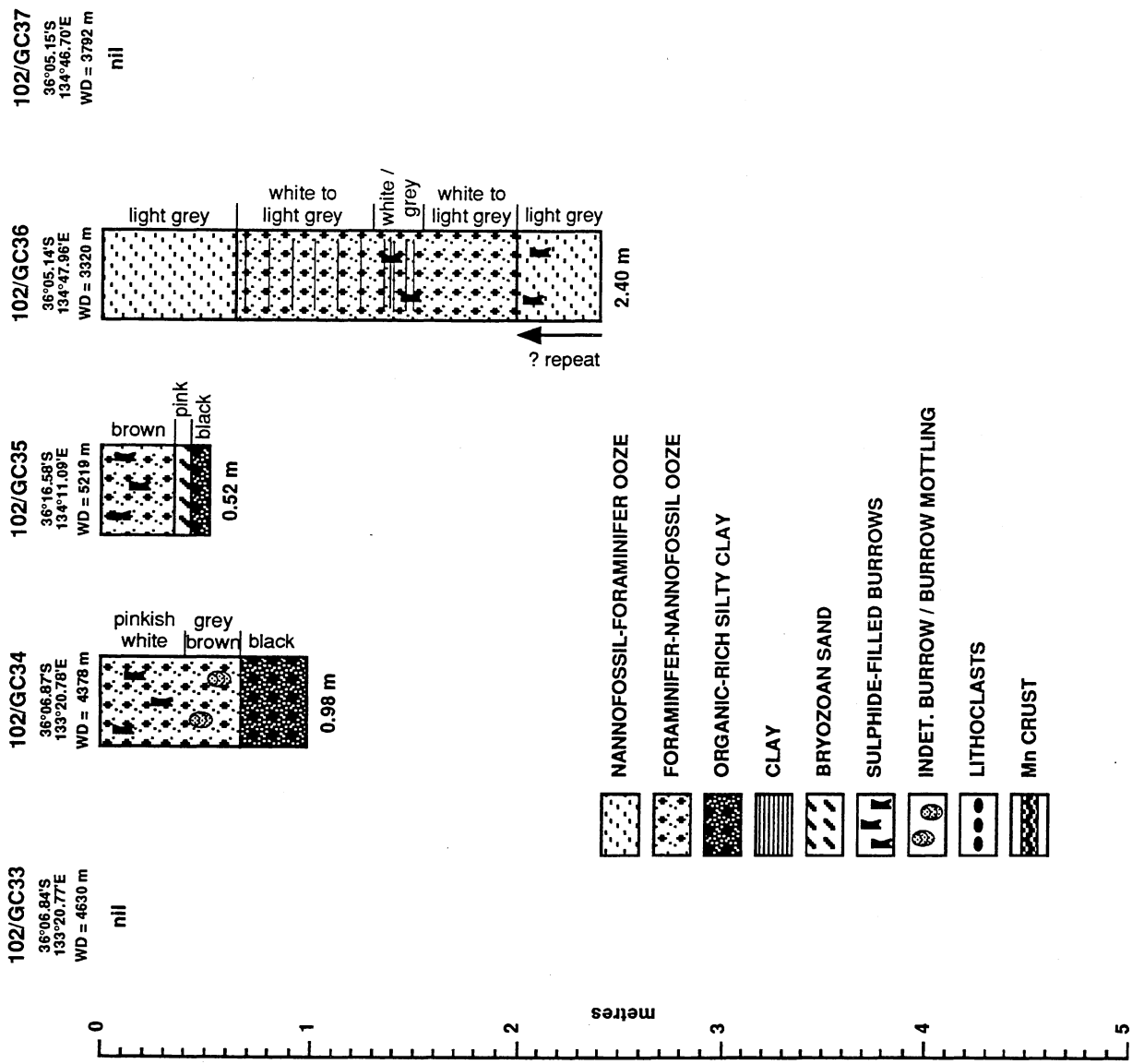

FIGURE 8. Sedimentological logs of Ceduna Sub-basin (Area A) gravity cores (cont.).

All but one of the core targets was the Cretaceous of the lower Ceduna Sub-basin. Four gravity cores (102GC22 to 102GC25) were targeted on a seismic anomaly on the central Terrace. This anomaly consists of a steep-sided, positive bathymetric feature (several tens of metres above the surrounding sea floor). Seismic reflectors are disrupted below this feature (Fig. 9). Hypotheses for the cause of this feature include diapiric or intrusive origins.Two cores (102GC24 and 102GC25) recovered calcareous debris (bryozoans, ahermatypic coral, foraminifers) and small rock fragments. These fragments rock are red/brown to black, indurated but friable, and comprised of a number of ?authigenic minerals, fine sand-sized quartz, and lithified pink calcareous ooze. They are covered with a hard Mn crust up to several millimetres thick. The authigenic minerals include a translucent, botryoidal/rhombic mineral; a fine-grained, massive, red/brown vitreous mineral; and black ?Mn crusts on intraclasts. Although the core cutter was substantially damaged during coring, the recovered material is probably only an authigenic crust and the true composition of the feature was probably not tested.

The remaining ten gravity cores (Fig. 8) were sited along a 260 nautical mile (480 km) swathe on the lower slope, in water depths from 3320 to 5219 m. One core was sited at the western end of the Terrace; two in the central part; and seven were sited in three canyons (Fowlers, Pearsons, Widbey) in the east (Fig. 7).

SEDIMENTARY FACIES

Two major and two minor facies are identified in the gravity cores from the lower Ceduna Terrace; a foraminiferal/nannofossil ooze; a dark terrigenous mud; a shelfal bryozoan sand; and a foraminiferal quartzitic muddy sand.

(i) Foraminiferal/nannofossil Ooze Facies: The majority (8.52 m or 67%) of recovered material was foraminiferal/nannofossil ooze or nannofossil/foraminiferal ooze (these two sedimentary types are grouped together in this report). The colour of this material is most commonly very pale brown (10YR7/3) or light grey (5YR7/1), but pink (7.5YR7/4), pinkish white (7.5YR8/2), white (7.5YRN8), yellow (7.5YRN6), and dark brown (10YR4/3) colours also occur. It often displays a uniform texture, but mottling and more distinct burrowing are common (e.g. 102GC21, 102GC30, 102GC34). Gradual changes in colour, mainly from light grey to pale brown (102GC35) or from pinkish white to white (102GC22, 102GC36) occur. Distinct, unbroken banding or laminations are well developed in some cores; either finely laminated pink and grey (102GC30: 0.7-2.0 m) or white and grey (102GC36); or alternating wide bands of pink and grey (102GC30 below 2.0 m). Occasionally, light grey (5Y7/1), greenish grey (102GC36) and yellowish green (102GC30) mottling or laminations are evident. These colourations may be indicative of Mn and sulfide authigenic mineralisation related to alternating oxidising/reducing conditions. The sand-size fraction of the nannofossil/foraminiferal ooze is predominantly (95%) planktonic foraminifers (*Orbulina*, *Globerotalia* etc.), with minor benthic forms (*Uvigerina*), echinoid debris, sponge spicules and ostracods. Planktonic tests sometimes display a pinkish colouration. The non-calcareous, silt-sized fraction is comprised of quartz, sponge spicules, and echinoid debris, with

minor mica, glauconite, pyrite, orange ?Fe minerals, vitreous clay aggregates (?faecal pellets), and ?organic fragments. The composition of the foraminiferal/ nannofossil ooze is similar to the above with perhaps a lower planktonic content and more fine fraction.

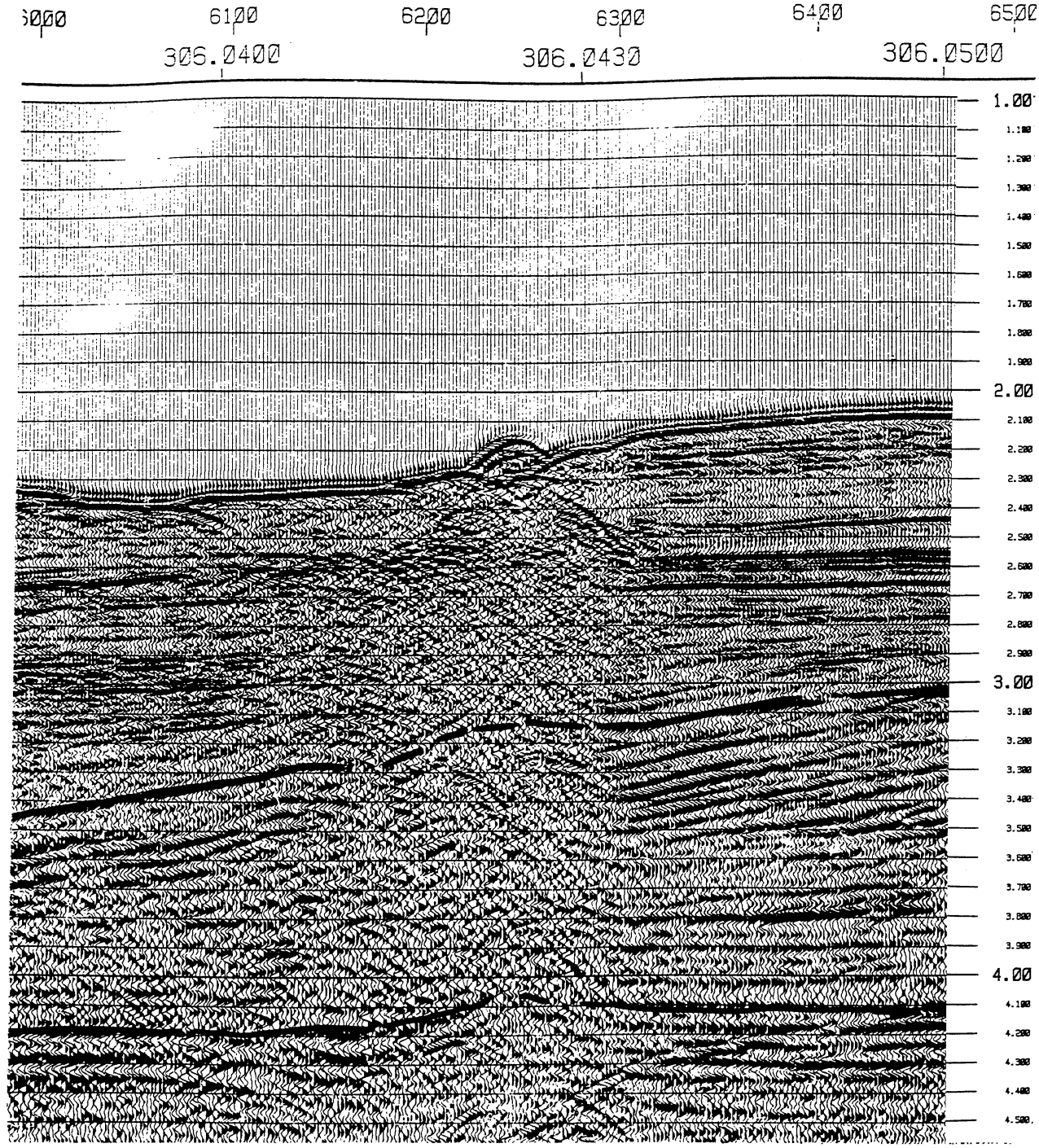

FIGURE 9. Seismic section (AGSO Line 65/7P1; S.P.'s 6000-6500) showing the diapiric structure which was targeted by cores 102GC22 to 102GC25.

(ii) Dark Terrigenous Mud Facies: Altogether, 4.04 m of terrigenous mud was recovered from eight of the ten gravity cores from the Ceduna Terrace. Its colour ranges from very dark grey (10YR3/1) and dark grey (5Y4/1) to olive grey(5Y4/2) to black (7.5YR2/0). The sediment is comprised mainly of silt and clay, but the very fine sand fraction includes quartz, (including some large, Fe-stained grains in 102GC29), organic fragments, mica, glauconite, Fe-stained clay clasts, "limonitic" clay streaks (102GC21 and especially 102GC32), and pyrite (a 3 mm large nodule in 102GC27). The sediment is typically firm and occasionally 'sticky'. It is usually uniform and homogeneous showing no signs of internal bioturbation, although burrowing does occur at its boundaries with adjacent sediment (102GC19). The organic content varies from subordinate for the grey muds to moderate (?10%) for the black muds.

(iii) Shelfal Bryozoan/Foramineral Sand Facies: A small amount (0.11 m) of bryozoan/foramineral sand was recovered from one core (102GC35) located in Pearson Canyon. The very pale brown (10YR7/2), medium to coarse sand is comprised mainly of bryozoans, planktonic and benthic foraminifers (30%), echinoid fragments, minor bivalves, gastropods, and poorly-sorted, angular to rounded Fe- stained quartz. The relict component includes red/orange-stained quartz, fragmented and corroded calcareous debris, and authigenic materials are glauconite and dolomite rhombs and possibly (?)phosphatic clay aggregates/ pelloids (?faecal pellets).

(iv) Foramineral Quartz Muddy Sand Facies: One very minor (10 mm interval) of foraminiferal quartz muddy sand was recovered from the top of core 102GC19. This olive grey (5Y4/2) sediment contains planktonic foraminifers, abundant silt-sized quartz, minor glauconite, echinoid fragments, pyrite, organic fragments, mica, and brown Fe-rich clay aggregates. Non-calcareous material constitutes over 60% of the total sediment.

In addition to the above facies, authigenic minerals are fairly common in these slope sediments. Minor glauconite and possibly phosphate are found in the foramineral/nannofossil ooze facies, and pyrite and a red/orange ?Fe mineral are commonly found in the terrigenous mud facies, especially core 102GC32. A hard Mn-rich crust is located at the interface between the terrigenous muds and carbonate sediments in core 102GC26.

DISTRIBUTION OF SEDIMENTARY FACIES

Before discussing the distribution of sedimentary facies, it is important to draw attention to the frequency with which the upper part of some gravity cores are repeated at depth. Notable are 102GC19, 102GC20, 102GC27, 102GC30, 102GC32, and 102GC36. A clear example of this is exhibited in 102GC32 where the outline of the core catcher is evident at about 0.9 m and inclined bedding with subtle textural detail is repeated. It is believed that the lower section is recovered by the core bouncing back into the sea bed upon retrieval as a result either of the ship pitching with the swell, or by cable stretch and rebound on pullout. It is

inconceivable that this could occur three times on pullout, therefore at least two of the three repeat sections of 102GC27 must be real.

No clear regional facies distribution trends are evident with the small number of cores available. All the cores have a mantle of calcareous nannofossil foraminifer ooze, except for 102GC19. However, 102GC21 is taken at the same locality and in this core there is 0.6 m of calcareous surficial sediment, indicating either that the distribution of surficial terrigenous mud is very restricted or that the upper nannofossil/foraminiferal ooze has been lost from the top of 102GC19.

In terms of depth distribution, there is a weak decrease in the thickness of surficial calcareous sediment with depth and the only two cores with no terrigenous mud are the shallowest cores taken (<3800 m water depth). This may indicate a minor CCD (carbonate compensation depth) effect at about 4000 to 4500 m depth.

The widespread regional distribution of terrigenous mud is worth noting. This facies was intersected in all cores except 102GC32 and 102GC36, which are located near the shelf edge where biogenic sedimentation can be expected to be higher. In previous times, terrigenous mud therefore mantled the entire lower slope of at least the Ceduna Terrace region of the Great Australian Bight.

AGE OF FACIES

Subsamples were taken from the core cutter of all gravity cores for age dating. Nannofossil results indicate that all sediments are Quaternary, with the exception of late Maastrichtian palynomorphs from the core catchers of 102GC26 and 102GC27 (see Section 6.5.1).

DISCUSSION

Although the gravity core material provided little information on the deeper section of the Ceduna Sub-basin, it has provided important data on the climatic effect on sedimentation. The repeated alternation from carbonate to terrigenous sedimentation on the continental slope is presumably a response to climatic change, possibly superimposed on the effects of fluctuations in the CCD.

During glacial times, extensive areas of the southern margin shelf would be exposed and terrigenous material, especially from the Murray River, would bypass the shelf and be exported to the heads of submarine canyons which are mapped to the shelf break in this area. A southward shift of the weather belts would probably increase rainfall and sediment supply from the Great Australian Bight hinterland. Anoxic, nutrient-rich Antarctic bottom water would be reduced due to fresh water being 'ice-locked'. Relatively more anoxic water would thus sweep the lower slope of the Bight, promoting the production of pyrite and preserving organic matter in the surficial sediment. Shallow, warmer shelf water would promote formation of authigenic minerals on the shelf such as phosphatised calcareous debris and glauconite and Fe-rich minerals, as found in the slope muds.

Antarctic bottom water flow would increase with the transgression associated with interglacial periods. Enhanced nutrients and dissolved oxygen would promote high bioproductivity and increase carbonate sedimentation on the slope. Manganese mineralisation found in these sediments may be evidence of such oxygenated environments. The shelf would be flooded, terminating direct terrigenous supply. During transgression, calcareous debris perched on the shelf edge would be destabilised and transported by mass flow down the sides of submarine canyons. Foramineral/bryozoan sand intersected in core 102GC35 and obtained in pipe dredges may be evidence of such occurrences. These sediments are clearly shelfal as depicted by catenicellid bryozoan fragments and Fe-stained quartz. Subtle graded bedding in this core is also suggestive of turbiditic flow. Pebbles at the interface between terrigenous mud and carbonate sediments in 102GC29 support mass flow in Fowlers Canyon.

At least one, and possibly two eustatic cycles are evident in 102GC27, and very thin (20 mm) carbonate interbeds between terrigenous mud suggests substantial dissolution during glacial periods.

Terrigenous, dark brown muds recovered from a pipe dredge on *Rig Seismic* Survey 66 from the Ceduna canyon area contain Miocene foraminifers. Foraminiferal/nannofossil ooze associated with muds of similar composition obtained during the current survey are Quaternary based on nannofossil evidence. The above discussion is based on the cored material recovered on the current survey being Quaternary, and would have to be revised should they prove to be older.

6.1.3 PALEOCLIMATIC AND SEA LEVEL IMPLICATIONS OF QUATERNARY SEDIMENTATION IN THE CEDUNA CANYONS AREA

T. Boreen (Department of Geological Sciences, Queen's University, Kingston, Ontario, Canada).

Cores from the canyon transects of Area A show a consistent sequence of Quaternary sedimentation related to climatic cyclicity. Most of the core attempts were targeted at canyon walls, but two cores penetrated deeper water canyon floor sediments. With minor variations, the cores which penetrated Quaternary sediments show a consistent downward subsurface transition from 1) surficial pinkish brown foram/nanno oozes, to 2) a thin layer rich in authigenic clays, organics, iron-stained quartz granules, glauconite, and shelf-derived calcareous skeletal debris, to 3) black terrigenous clay with abundant quartz silt, organics, mica, and pyrite framboids. Contacts between the successive units are abrupt. Stacked occurrences of two or more cycles were present in several cores. If the repeated cycles are not an result of the coring procedure, then both carbonate and terrigenous lithologies are Quaternary in age based upon nannofossil assemblages contained in the pelagic oozes (see Section 6.5.1). Similar sequences have been recorded from the Otway shelf to the east (Heggie and O'Brien, 1988). The widespread occurrence of this repeated sequence of

lithologies can be interpreted in the framework of documented Quaternary paleoclimatic patterns.

The role of the extensive canyon systems on the South Australian continental margin in the supply of terrigenous and calcareous sediment to the continental rise and abyssal plain has largely been a matter of speculation. Previous examination of shelf edge deposits indicates that calcareous sediments are presently entering canyon mouths near the shelf edge (von der Borch and Hughes Clarke, 1993); however, downslope movement of these sediments was not determined. Samples recovered from the canyon transects in Area A indicate that:
(1) Much if not all of the Ceduna Canyons transport system is currently dormant.
(2) Highstand deposition within the canyons is dominated by pelagic calcareous deposition. Pinkish brown foram/nanno oozes have accumulated up to several tens of cm thick since the beginning of the Holocene transgression. In deeper water areas, the presence of the lysocline and CCD significantly reduces the thickness of this pelagic veneer.
(3) Regressive and lowstand deposition is represented by fine-grained, terrigenous deposition on canyon walls and mixed coarse-grained, calcareous/ terrigenous deposition in more axial and canyon floor localities.
(4) Transgressive episodes record starved deposition, minor mixed terrigenous/ calcareous sedimentation, and authigenic mineral growth in canyon wall locations; and episodic downslope movement of shelf-derived, coarse-grained calcareous and terrigenous material in more axial locations.
(5) Highstand deposition is currently occurring under strongly oxidising conditions in the bottom water depositional environment.

6.2 AREA B: SEDIMENTARY CHARACTERISTICS OF COOL-WATER CENOZOIC CARBONATE DEPOSITS ON THE EUCLA SHELF-EYRE TERRACE

In recent years there has been a growing appreciation that modern tropical carbonate systems do not constitute a universally applicable analogue for ancient carbonate hydrocarbon reservoirs (c.f. Nelson, 1988). Throughout much of the Phanerozoic, and especially the Paleozoic, carbonate deposition was characterised by the absence of the large metazoans capable of forming reef build-ups to produce rimmed shelves (James, 1983). Instead, non-rimmed platforms or distally steepened ramps (Read, 1986) appear to have been more common (Wilson, 1975). The best modern analogues for these non-rimmed carbonate deposits are carbonate shelves outside the tropics (James and von der Borch, 1991). However, lack of detailed information on the geometry and facies characteristics of such shelves, relative to the better known tropical shelf deposits, has meant that non-rimmed carbonate facies models have been little used. In addition, there is now an appreciation that studies of modern and Cenozoic shelf deposits can provide a record of past climatic variation, contained within the facies and isotopic characteristics of carbonate deposits (Marshall and Davies, 1978; Davies and others, 1988; Feary and others, 1991).

The Eucla Shelf (Fig. 3) is the largest modern contiguous area of cool water carbonate sedimentation, and has been the site of predominantly cool water carbonate deposition since Eocene time. Accordingly, this area provides the potential to make a significant contribution to our understanding of the origin, accumulation history, and diagenesis of cool water carbonate deposits; to enable the formulation of facies models of critical importance for the interpretation of cool water carbonates in onshore and offshore Australian Cenozoic basins; and to act as analogues for Paleozoic shelf and slope limestone deposits.

Reconnaissance work on the Eucla Shelf-Eyre Terrace and Lacepede Shelf areas (Conolly and von der Borch, 1967; Wass and others, 1970; Lowry, 1970; Davies and others, 1989; James and von der Borch, 1991) have demonstrated the general characteristics of the modern southern margin shelf facies. The Eucla Platform is a high energy shelf with a relatively deep shelf-slope break. A sigmoidal prograding seismic geometry visible on airgun seismic sections suggests that shelf margin accumulation rates exceed subsidence rates. The surficial sediments are dominated by bryozoans with accessory mollusc and foraminifer components. There is little terrigenous input, primarily because the platform borders the limestone karst Nullarbor Plain. The near shore sediments (down to 80 m water depth) are coarse-grained, rippled, bioclastic sediments reworked by long period storm waves. Deeper sediments are progressively finer grained and more poorly sorted, with proportionately greater planktonic foraminifer, sponge, and pteropod components.

The aim of this component of the program was to provide a description of facies belts, across the Eucla Shelf and Eyre Terrace, relative to energy, water depth, and substrate; to provide an assessment of the role of relict components in shelf sediment dynamics; to determine the intensity and style of sea floor diagenesis in bioclastic sediments; and to document the nature of the shelf margin bryozoan community and its history relative to Quaternary sea level fluctuations. The intention was to record a high-resolution seismic grid to define the geometry and seismic facies of the Cenozoic sequence. This was to be oriented to complement the recently collected Japan National Oil Corporation airgun seismic lines which show the deeper structure. Subsequently, a transect of vibrocores and gravity cores collected across the width of the shelf, terrace, and upper slope were to be used to provide biostratigraphic and sedimentary facies control, and to enable the compilation of a three-dimensional facies model for high energy cool water shelf and upper slope carbonate deposition. Failure of the seismic acquisition system (see Section 7.3) meant that the high resolution seismic component of the program was abandoned. Despite having to sample "blind", the sampling program of vibrocores and gravity cores, together with a single dredge, were successfully completed. The sedimentology of these samples are described in the following section; biostratigraphic aspects of these samples are discussed in Section 6.5.1 below.

6.2.1 SEDIMENTARY CHARACTERISTICS OF THE COOL-WATER CENOZOIC CARBONATE DEPOSITS ON THE EUCLA SHELF

N.P. James (Department of Geological Sciences, Queen's University, Kingston, Ontario, Canada), Y. Bone (Department of Geology and Geophysics, University of Adelaide), and T. Boreen (Department of Geological Sciences, Queen's University, Kingston, Ontario, Canada).

The vibrocore transect was run along the longitude line 128°01.50'E (Fig. 10), which intersects the shoreline at ruins of the telegraph line on Mundrabilla Station. At each site, a van Veen grab was deployed to determine the characteristics of bottom accumulations and assess their applicability for vibrocoring. Despite this precaution, only eight of eleven vibrocore attempts successfully recovered sediment, and the six metre vibrocore barrel provided a maximum core length of only 1.37 m. These modest core recoveries were primarily due to the thinness of the Holocene succession over either Tertiary carbonates or older Pleistocene. Tenacious coring attempts resulted in several penetrations of the surface and recoveries of on-shelf Tertiary and Quaternary limestones.

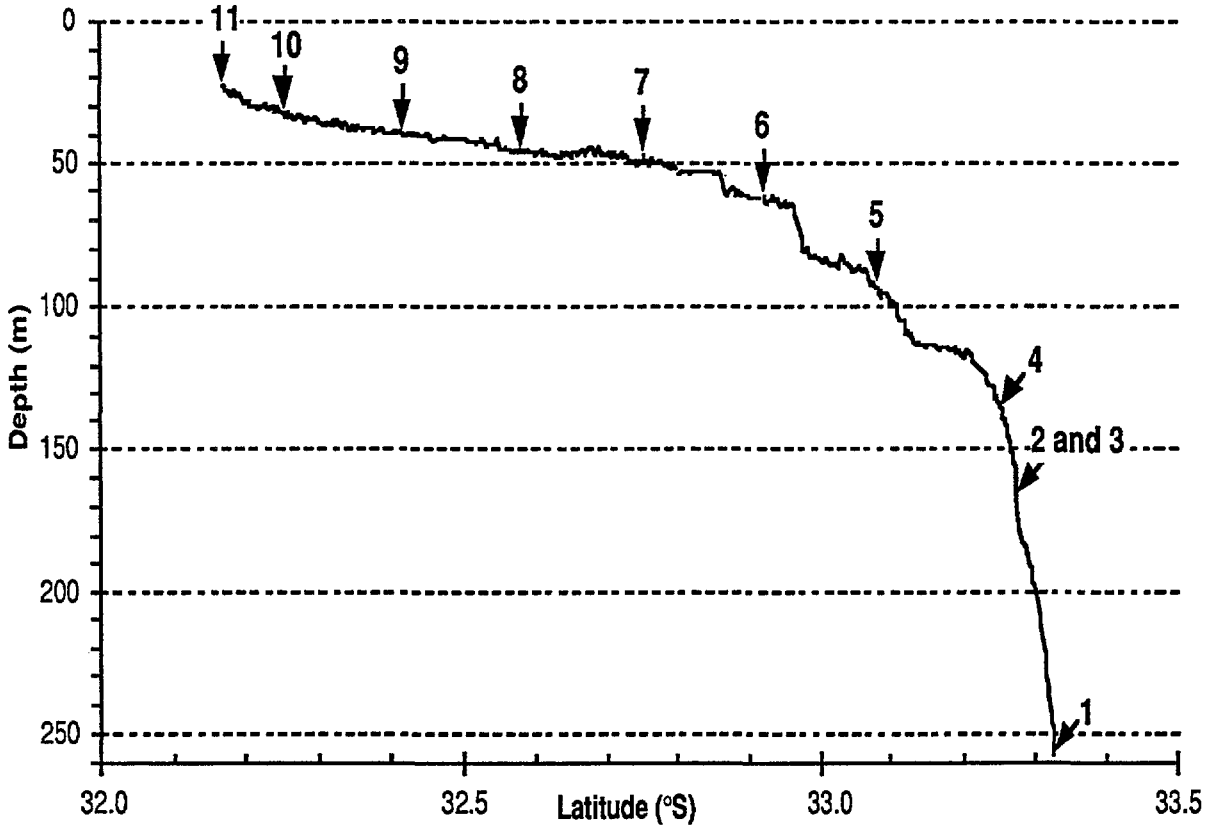

FIGURE 10. Bathymetric profile across the Eucla Shelf showing vibrocore locations.

Descriptions of the vibrocores and grabs from the Eucla Shelf transect follow. For each location the tandem vibrocore and associated grab sample are listed and described together. Since grab samples represent disturbed and homogenised

bulk accumulations which lack the resolution and stratigraphic trends detectable in cores, priority is given to description of the vibrocore samples. In locations with both vibrocore and grab recoveries, the cores are generally described in some detail, with only a brief grab sample description. Locations with minimal or no vibrocore recovery are given more lengthy grab sample analysis.

Sample 102VC01 Method: Vibrocore Lat: 33°20.00'S
Depth: 277 m Recovery: 1 gm in core catcher Long: 128°01.50'E

Sample Description 102VC01 -
Core catcher: living delicate branching cyclostome bryozoans. Sand-size bioclastic grains of benthic foraminifers, bivalves, serpulids, pteropods and delicate branching cyclostomes and cheilostomes. Orange (relict) opercula.

Comments: Bent core barrel - probable hardground (not preceded by grab).

Sample: 102VC02 Method: Vibrocore Lat: 33°16.49'S
Depth: 184 m Recovery: 29 cm Long: 128°01.53'E

Grab: 102GR01 - Fine to medium-grained, pale olive, bryozoan sand.

Core: 14 cm of rhodolith (coralline algal nodule) gravel overlain by 15 cm of pale olive, fine- to medium-grained, foram-echinoid-bryozoan bioclastic sand.

Sample Description 102VC02 -
(1) Rhodolith gravel:
- Very pale brown (10YR8/3); rhodoliths, from one to four cm. in diameter and tightly packed; encrusting bryozoans; serpulid worm tubes; small bivalves; turretellid gastropods; reteporiform bryozoans; cheilostome rods; and planktonic foraminifers. Small, extremely well-preserved *Katelysia* bivalves occur as nested accumulations in cracks between nodules. The presence of loose bryozoan and bivalve-rich sediments at the base of the core, beneath the main accumulation of cemented nodules, suggests that the nodule layer may overlie recent unconsolidated sediments. An alternative explanation of filtration during the vibrocoring process is less likely, given the apparent gradational transition from well cemented surficial hardground to underlying mixed smaller nodules and sediment.

(2) Foraminifer, bryozoan, medium grained, bioclastic sand (surface):
- Pale olive (5Y6/4); 5% relict fraction consisting of orange/yellow-stained grains with notable benthic foraminifers, echinoid debris, and serpulid fragments.
- Bulk Sample: silt-fine sand fraction consists of 20% quartz, 20% planktonic foraminifers, 20% sponge spicules, 30% unidentified fragments, 15% glauconite (internal molds), and trace organics; Med-coarse sand fraction consists of 15% benthic foraminifers, 15% planktonic foraminifers, 20% echinoid fragments, 5% bivalves, trace turreted gastropods, 5% sponge spicules, 15% serpulids, trace pteropods, 10% unidentified fragments, 5% delicate branching cyclostomes, trace

cheilostome rods, and 15% catenicellid bryozoans.

^{14}C Age: Rhodoliths at base - 9,250 ± 110 years B.P.

Sample: 102VC03	Method: Vibrocore	Lat: 33°16.48'E
Depth: 184 m	Recovery: 28 cm	Long: 128°01.53'S

Core: 8 cm of very pale brown rhodolith gravel overlain by 20 cm of fine to medium grained pale olive bryozoan sand.

Sample Description 102VC03 -
(1) Rhodolith gravel:
- similar to core 102VC02. The nodules form a framework between which there is medium to coarse bioclastic sand composed of abraded and worn particles.
- Bulk sample: Silt and fine sand-size fraction (20 %) consists of 20% ostracodes, 20% planktonic foraminifers, 10% catenecellids, 10% sponge spicules, and 30% unidentifiable grains. The medium to coarse sand fraction (80%) is 20% benthic foraminifers, 30% coralline algae rods, 10% fragments, 10% cyclostome rods and 30% unidentifiable grains.

(2) Fine, microbioclastic sand:
- Olive (5Y5/3), 10% relict particles consisting of yellow and grey particles including benthic foraminifers, rods and clasts.
- Bulk sample: Silt and fine sand fraction (80%) consists of 10% ostracode valves, 20% benthic foraminifers, 30% planktonic foraminifers, 10% sponge spicules 10% catenecellids and 10% unknowns. Medium to coarse sand (20%) is 20% bivalves, 20% serpulids, 20% benthic foraminifers, 10% cyclostomes, 10% cheilostome rods and 10% lunulitiform cheilostomes.

^{14}C Age: (1) bivalves and gastropods at base - 9,110 ± 80 years BP; (2) bivalves at base - 9,990 ± 80 years BP.

Sample: 102VC04	Method: Vibrocore	Lat: 33°15.03'S
Depth: 152 m	Recovery: 1.34 m	Long: 128°01.50'E

Grab: 102GR02 - Fine to coarse grained bryozoan-bivalve bioclastic sand.

Core: 26 cm of pale yellow rhodoliths overlain by a thin bivalve lag; remainder of core is olive, muddy, fine microbioclastic sand with pockets and layers of medium to coarse sand. There is a sharp contact at 80 cm, but no obvious change in lithology.

Sample Description 102VC04 -
(1) Rhodolith gravel (1.08-1.34 cm):
- Pale yellow (5Y8/3); Coralline algal nodules are morphologically similar to 102VC02 and 102VC03, but the upper 7 cm consists of loose nodules that are grey-stained and extremely corroded in appearance. Bivalve fragments which

overlie the upper surface are also extremely corroded and encrusted by serpulids and bryozoans. Sediment between nodules is 20% fine microbioclastic sand (see below) and 80% medium to coarse sand consisting of 10% relict grey particles, 20% benthic foraminifers (including *Homotrema*), 30% coralline algae rods, 10% cheilostome rods and trace delicate cyclostome, escharifom, lunulitiform and adeoniform cheilostomes, and small ahermatypic corals.

(2) Muddy, fine, microbioclastic sand (100 cm):
- Olive (5Y5/3); 10% relict fraction (all grains have a worn chalky appearance) consists of grey, stained particles with notable cheilostome rods, bioclasts, bryozoan debris, and mollusc fragments.
- Bulk Sample: mud 10%; silt-fine sand fraction (90%) consists of 5% quartz, 20% planktonic foraminifers, 10% infaunal echinoid fragments, 20% sponge spicules, 35% unidentified hyaline fragments, 10% catenecellid bryozoans, trace gastropods and bivalves. Medium to coarse sand fraction (10%) consists of trace lithoclasts, 10% benthic foraminifers (agglutinated, *Cibicides)*, 5% planktonic foraminifers (*Orbulina, Bulloides, Pachyderma?*), 10% echinoid fragments, 10% bivalves *(Katelysia)*, 5% gastropods, 5% serpulids, trace ostracods, 5% unidentified fragments, 5% delicate branching cyclostomes, 5% cheilostome rods, 5% adeonid bryozoans, trace lunulites bryozoans, and 20% coralline algae rods.

^{14}C Age: (1) Rhodoliths at base - 13,000 ± 100 years BP; (2) Bivalves at 90 cm 7,950 ± 70 years BP; (3) Bivalves at 30 cm - 970 ± 70 years BP.

Sample: 102VC05	Method: Vibrocore	Lat: 33°05.00'S
Depth: 113 m	Recovery: 1.04 m	Long: 128 01.50'E

Grab: 102GR03 - Fine to coarse grained, bryozoan, bivalve, foraminifer, bioclastic sand.

Core: 15 cm of very pale brown coral boundstone abruptly overlain by 16 cm of light grey fine to medium grained bryozoan/foraminifer bioclastic sand; 40 cm light olive-grey bryozoan/bivalve medium to coarse grained bioclastic sand; and 20 cm pale brown bryozoan/foraminifer medium to coarse grained bioclastic sand.

Comments: Upper two units display significant boudinage-style contorted bedding and mixing of lithologies due to either 1) vibrocoring process (three vibrocoring pulses to attempt penetration of basal hardground: 1 min, 2 min and 2 min), 2) burrowing or 3) downslope slumping. The main sediment appears to be fine microbioclastic sand with irregular isolated areas of coarser sands.

Sample Description 102VC05 -
(1) Scleractinian coral boundstone (100 cm):
- Very pale brown (10YR8/3); 7 cm nodular disc of highly indurated limestone, weathered surface grey-green and corroded in appearance; macrofauna include scleractinian colonial coral (*Montastrea?*) with encrusting bryozoans, serpulid worm tubes, and large (3 cm) boring bivalve *(Lithophaga)* infilled by fine grained,

white, calcareous matrix with floating skeletal particles. All mineralogy is still original, ie. aragonite and high-magnesium calcite, suggesting that the material is Pleistocene in age. Other coarse fragments include *Adeona* fronds encrusted with serpulids and other bryozoans, epifaunal echinoid spines, gastropod fragments and bivalves (*Glycymeris* and *Katalysia*).

(2) Fine, microbioclastic sand (80 cm):
- Pale Brown (10YR6/3); <5% relict (stained) material with notable grey-stained benthic foraminifers, delicate branching cheilostome bryozoans, red algal plates; no living material.
- Bulk sample: Silt/fine sand fraction (90%) consists of 5% quartz, 10% benthic foraminifers, 30% planktonic foraminifers, 10% echinoid fragments, 10% sponge spicules, trace ostracods, trace pteropods, 30% catenecellid fragments, 5% glauconite, 10% catenicellid bryozoans and trace dolomite rhombs. Medium to coarse sand fraction (10%) consists of 15% benthic foraminifers, 15% planktonic foraminifers, 10% echinoid fragments, 5% thin-walled bivalves, 5% sponge spicules, 5% serpulids, 30% delicate branching cyclostomes, 5% delicate branching cheilostome rods, 20% unidentifiable grains, and trace fish vertebrae.

(3) Bryozoan, bivalve, coarse grained, bioclastic sand (66 cm):
- Light olive grey (5Y6/2); 60% relict grains consisting of yellow-orange and grey-green stained particles with notable benthic foraminifers, catenicellid bryozoans, aggregate lumps, the benthic foraminifers *Marginopora*, adeonid bryozoans, and mollusc fragments. No living material.
- Bulk Sample: All particles badly worn and abraded; Silt to fine sand fraction consists of 5% quartz grains, 5% benthic foraminifers, trace planktonic foraminifers, 10% echinoid fragments, 10% sponge spicules, 20% catenecellid fragments, 40% unidentifiable fragments, trace glauconite (foraminifer molds). Medium to coarse sand fraction consists of 10% benthic foraminifers (including *Marginopora*), 15% echinoid fragments, 10% bivalves, trace coralline algae, trace serpulids, 15% unidentified fragments, 40% coralline algae rods, 10% lunulites bryozoans. Gravel fraction is dominated by robust bivalve fragments, with notable regular echinoid spines.

^{14}C Age: (1) bryozoans at base - 9,910 ± 80 years BP; (2) bivalves at base - 8820 ± 80 years BP.

Sample: 102VC06/6A	Method: Vibrocore	Lat: 32°55.00'S
Depth: 79.7 m	Recovery: 50 grams	Long: 128°01.50'E

Grab: 102GR04 - Bivalve, bryozoan, coarse-grained, bioclastic sand.

Core: Four small pieces of rock and a small amount of skeletal sand.

Comments: Two vibrocore attempts; both bent the aluminium core barrel.

Sample Description 102GR04 and 102VC06A -
(1) Palimpsest bioclastic foraminiferal sand (102GR04):
- Light Yellowish Brown (10YR6/4); 50% relict material consisting of yellow/orange stained grains with notable lithoclasts, polished rods and spheres, mollusc fragments, bryozoan fragments, benthic foraminifer tests (including *Marginopora*), and coralline algal fragments. All particles are highly worn and abraded, both stained "relict" and unstained "modern" making estimation of skeletal abundances difficult.
- Bulk Sample: silt to fine sand fraction negligible; Medium to coarse sand fraction (80%) consists of 5% quartz grains (well rounded), 30% benthic foraminifers (including *Homotrema* and *Marginopora*), 10% bivalves, 15% red algae (encrusting, plates and rods), trace sponge spicules, 20% unidentified fragments, trace dolomite rhombs, trace delicate branching cyclostomes, 10% cheilostome rods, trace reteporiform bryozoans. Gravel fraction (20%) consists of abundant bivalve fragments and adeoniform bryozoans, common gastropods, trace lunulites bryozoans, and Fe-stained worn and bored pebble clasts.

(2) Gravel-sized skeletal fragments and limestone clasts (102VC06A, core catcher):
- Living encrusting coralline algae.
- Mollusc fragment, badly worn and abraded (1.3 cm long axis).
- Fragments of colonial coral (underlying coral boundstone?).
- Lunulites bryozoan.
- Two small limestone clasts (2 cm long axis); well rounded, bored and encrusted by serpulid worms and red algae; red-brown Fe-stained (possibly Eocene dolomitic limestone clasts).
- Skeletal grainstone clast (5 cm long axis), well indurated, rounded, pale brown (10YR6/3), bored and encrusted by red algae and serpulid worms. Clast composed of cemented skeletal grains including planktonic and benthic foraminifers, echinoid spines, cheilostome rods, delicate branching cyclostomes, quartz grains. Dolomite rhombs are conspicuous.

Sample: 102VC07	Method: Vibrocore	Lat: 32°45.00'S
Depth: 67.3 m	Recovery: 1.3 m	Long: 128°01.50'E

Grab: 102GR05 - Medium-grained, palimpsest, bivalve-foraminiferal, bioclastic sand.

Core: 1.3 m of brown to very pale brown, bivalve-foraminifer, medium to coarse grained bioclastic sand; basal accumulation of nested bivalves; decreasing gravel-sized mollusc fragments upward through the core; surface layer of fine grained microbioclastic sand.

Comments: Nested bivalve accumulation at base of core almost certainly directly overlies a hardground surface responsible for stopping the vibrocore.

Sample Description 102VC07 -
(1) Medium to coarse grained bivalve foraminifer bioclastic sand (120 cm):
- Brown (10YR5/3); 60% relict material with common yellow-orange staining and lesser dark brown to dark grey grains. Most relict particles are very badly abraded and occur as unidentifiable rods and polished grains apparently similar in composition to the unstained but highly polished and abraded "modern" components.
- Bulk Sample: silt to fine sand fraction is volumetrically insignificant and consists of traces of quartz silt. Medium to coarse sand fraction consists of trace quartz grains (up to 20% at base), 40% benthic foraminifers (including *Marginopora*), 10% echinoid fragments, 10% bivalve fragments, trace gastropods, 5% coralline algal plates, trace serpulids, 30% coralline algal rods and polished grains, trace delicate branching cyclostomes, trace polished cheilostome rods, trace *Adeona sp.* bryozoan, and 5% catenicellid bryozoans. Gravel fraction is dominated by bivalve fragments including abundant nested shells, and notable *Chlamys* fragments with *Homotrema* encrustation, and *Katelysia*..

(2) Fine, microbioclastic, foraminifer-bryozoan sand (surface):
- Very pale brown (10YR7/3); 20% relict material, mostly yellow-orange stained, very fine to fine sand-sized, polished skeletal fragments.
- Bulk sample: silt to fine sand fraction (80%) consists of trace quartz, 10% benthic foraminifers, 5% echinoid fragments, 10% sponge spicules, 10% bivalve fragments, 30% catenecellid fragments, 10% ostracode valves, 20% polished unidentifiable fragments, trace glauconite (aggregates), trace dolomite (single clear rhombs). Medium to coarse grained fraction (20%) consists of 30% benthic foraminifers (including *Homotrema*), 20% echinoid fragments, 15% bivalve fragments, trace gastropods, 5% coralline algal plates, trace serpulids, trace ostracods, 25% polished unidentifiable fragments, 5% delicate branching cyclostomes and cheilostome rods, and trace fish vertebrae.

Sample: 102VC08	Method: Vibrocore	Lat: 32°35.00'S
Depth: 69.2 m	Recovery: 0.75 m	Long: 128°01.50'E

Grab: 102GR06 - Medium to coarse grained, palimpsest, bivalve, bioclastic sand.

Core: Pale brown, medium to coarse grained, bivalve-bryozoan, bioclastic sand; basal bivalve lag with clasts of dolomitic white limestone, becoming slightly finer-grained with reduced bivalves up core; thin cap of fine microbioclastic sand.

Comments: As with 102VC07, the presence of the basal mollusc accumulation and associated clasts of dolomitic limestone undoubtedly indicate the presence of a hardground surface which limited penetration of the vibrocore. Clasts suggest hardground composition of Eocene dolomitic limestone (see Section 6.5.1). Fragments of possible calcrete at base.

Sample Description 102VC08 -
(1) Medium to coarse grained, bivalve, quartzose, bioclastic sand (60 cm):
- Pale brown (10YR6/3); 40 -50% relict material consisting of 70% orange-yellow to brown polished rods and grains, and 30% grey-green stained polished rods and grains; phosphatic pellets, and skeletal intraclasts. Both stained and unstained particles are all badly abraded and polished.
- Bulk Sample: silt to fine sand fraction (<5%) consists of traces of quartz, polished and abraded unidentifiable skeletal fragments. Medium to coarse grained fraction (80%) consists of 10% well-rounded and well-sorted quartz grains (up to 20% at base), 20% benthic foraminifers (including *Marginopora*), 5% echinoid fragments, 15% bivalves, trace coralline algal plates, 20% coralline algae rods, 30% unidentifiable polished and rounded skeletal grains, trace encrusting and adeoniform bryozoans, trace dolomite rhombs. Gravel fraction (20%) dominated by worn and broken bivalve fragments (abundant *Katalysia*). Conspicuous (but <5%) small, sand-sized lithoclasts consisting of sand grains bound by fine white microcrystalline carbonate.

(2) Fine, microbioclastic sand:
- Very pale brown (10YR7/3); 10% relict material. Fine sand-size consists of 10% bivalves, trace gastropods, trace echinoid spines, 20% benthic foraminifers, 10% sponge spicules, 10% ostracodes, 5% faecal pellets, 20% catenecellid fragments, 30% unidentifiable grains, trace bryozoan rods.

^{14}C Age: (1) Bivalves (*Katalysia*) at base - 2,780 ± 110 years BP; (2) Bivalves (*Katalysia*) at base - 2,600 ± 100 years BP; (3) bivalve and gastropod fragments at 10 cm - 2,400 ± 60 years BP.

Sample: 102VC09	Method: Vibrocore	Lat: 32°25.00'S
Depth: 58 m	Recovery: Nil	Long: 128°01.50'E

Grab: 102GR07

Sample Description 102GR07 -
(1) Medium-coarse, quartzose, bivalve, bioclastic sand:
- Living small crustacean.
- Pale brown (10YR6/3); 60% relict material consisting of yellow/orange and dark brown/grey stained, highly polished and abraded skeletal fragments including echinoid fragments, cheilostome rods, benthic foraminifers, and red algal plates.
- Bulk Sample: silt to fine sand fraction negligible but includes catenecellid bryozoans; medium to coarse sand fraction consists of 10% quartz grains, 5% lithoclasts (white matrix with red/brown skeletal grains), 20% benthic foraminifers, 5% echinoid fragments, 10% bivalves, 30% coralline algal rods, trace sponge spicules, 20% unidentified polished grains, 5% dolomite rhombs (rhomb clusters and single rhombs, clear and pink/orange stained). Gravel fraction (20%) dominated by abundant whole and fragmented bivalves (mainly *Katalysia*).

Sample: 102VC10 Method: Vibrocore Lat: 32°15.00'S
Depth: 31.2 m Recovery: core catcher Long: 128°01.50'E

Core 102VC10: A few small clasts of Eocene dolomitic limestone (see sample description 102VC11 for detailed description of Eocene dolomitic limestone) with maximum 2.6 cm long axis, and coarse grained, abraded, skeletal clasts (limpet *Cellena* and serpulid tubes). Living fauna include branching and encrusting coralline algae and encrusting cheilostome bryozoans.

Grab: 102GR08

Sample Description 102GR08 -
(1) Medium-coarse grained, quartzose, bivalve, dolomitic, bioclastic sand:
- Living branching and encrusting red coralline algae, small crustacean, encrusting cheilostome bryozoans, serpulid worms, catenicellid bryozoans, adeonid bryozoan.
- Pale brown (10YR6/3); 50% relict material consisting of yellow/orange, red/brown, and dark grey/brown stained grains, all badly abraded and highly polished.
-Bulk Sample: Silt to fine sand fraction negligible; medium to coarse sand fraction consists of 20% quartz grains (very well rounded), 10% benthic foraminifers, 10% echinoid fragments, 20% bivalves, 5% gastropods, 5% red algae plates, trace serpulids, 25% unidentified polished grains, trace delicate cyclostomes, 10% dolomite (single and clustered rhombs, high % of stained rhombs, most fine to medium sand-size), 5% cheilostome rods, trace reteporiform bryozoans, 5% catenicellid bryozoans. Gravel fraction consists of 15% corroded clasts, 10% regular echinoid spines, 25% bivalves (*Lima, Glycymeris*?, keyhole limpets), 15% gastropods (turreted, fusiform, turbiniform), 5% brachiopods (*Terebratulid*), 25% branching and encrusting red algae, trace cheilostome rods, and 10% adeonids.

Sample: 102VC11 Method: Vibrocore Lat: 32°10.00'S
Depth: 22.2 m Recovery: 0.76 m Long: 128°01.52'E

Grab: 102GR09 - Fine to medium grained, bryozoan, bivalve, echinoid, foraminifer bioclastic sand.

Core: 6 cm of white Eocene dolomitic limestone overlain by a bivalve lag and grey, well-sorted, fine to medium grained, quartzose bioclastic sand. Decreasing relict grains, quartz, dolomite, and grain size upward.

Comments: Microfossils in the basal limestone indicates a poorly-preserved, recrystallized, late Middle Eocene to late Eocene nannofossil assemblage, with a high probability of latest Eocene age (see Section 6.5.1). The component skeletal assemblage indicates a probable mid to outer shelf depositional environment (planktonic foraminifers, nannofossils, branching cheilostome and cyclostome bryozoans, benthic foraminifers, fine to medium quartz grains).

Sample Description 102VC11 -
(1) Eocene dolomitic limestone (foraminifer, bryozoan, microbioclastic wackestone to packstone):
- White (10YR8/1), indurated, circular disc 8 cm diameter cut by vibrocorer and smaller fragmented clasts. Matrix is microcrystalline white limestone with small, zoned, dolomite rhombs, glauconite grains, bivalve fragments (up to 2 cm), bryozoan fragments (delicate branching cyclostomes, cheilostome rods, adeonids), echinoid spines, benthic foraminifers, planktonic foraminifers, quartz grains and sponge spicules. Dolomite occurs as fine to medium sand-size single rhombs and rhomb clusters (3-6 intergrown rhombs); both whole pristine rhombs and worn fragmented grains may be clear to yellow-stained (there is evidence of rhombs encasing sponge spicules). Glauconite occurs both as aggregate grains and as internal molds of benthic foraminifers (agglutinated, *Cibicides*), planktonic foraminifers, and bryozoans. Quartz grains are fine to medium sand-size, very well sorted, very well rounded, low to moderate sphericity, with minor rose quartz grains. Organics are present in trace amounts and are very fine grained, smooth, black ovoid pellets. The surface of the limestone is bored with vertical to subhorizontal tubes 4-5 mm diameter and up to 25 mm in length which are partially encrusted by bryozoans (a modern seafloor exposure phenomenon). Overlying and filtered between cracks in the limestone are numerous worn, abraded and encrusted mollusc fragments and whole valves including small (1-2 cm) involute, obconic, fusiform and turreted gastropods, and 1.5-2 cm shells of the bivalves *Mactra australis, Pholas australasiae, Donax,* and *Katelysia.*

(2) Medium grained, dolomitic, quartzose, bivalve bioclastic sand (70 cm):
- Grey (10YR5/1); 30% relict grains consisting of 30% black to grey and 70% dull-brown to yellow/brown stained grains, mostly irregular and rod-shaped, highly abraded and polished particles difficult to identify precisely.
- Bulk Sample: silt to fine sand fraction minor; medium to coarse sand fraction consists of 25% quartz, 10% benthic foraminifers, 5% echinoid fragments, 5% small bivalves, trace sponge spicules, trace serpulids, 20% coralline algal rods, 30% unidentifiable fragments, 5% dolomite rhombs (10% at base), trace delicate branching cyclostomes, trace glauconite grains, trace cheilostome rods, *Adeona* sp. and catenicellid bryozoans. Gravel fraction (<5% bulk sample); 15% dolomitic limestone clasts, trace regular echinoid spines, 70% bivalve fragments including *Glycymeris, Pholas*, cockle *Anadora*, pipi *Donax.*, 10% small turreted and turbiniform gastropods, 5% crustacean fragments, and trace reteporiform bryozoan.

(3) Fine bioclastic sand (surface):
- Light grey (10YR7/1); no relict grains
- Bulk Sample: silt to fine sand fraction negligible; medium to coarse sand fraction consists of 5% quartz, 5% benthic foraminifers, trace echinoid fragments, 5% small bivalves, trace sponge spicules, trace serpulids, trace ostracods, 70% unidentifiable fragments, 5% delicate branching cyclostomes, 5% catenicellid bryozoans. Gravel fraction negligible.

^{14}C Age: Bivalves at base - 1,140 ± 50 years BP.

ANALYSIS AND INTERPRETATION

General Overview

The shelf can be divided into (i) shallow, inboard, bedrock-floored (shoreline to 80 m depth), and (ii) deep, outboard, sediment-veneered (80 to 200 m). The rock-floored shallow shelf is irregular, with areas of shallow sediment alternating with bare limestone (Figs 11, 12). The inner part is floored by Tertiary limestone, mainly Wilson Bluff Limestone and equivalents, to a distance of, on average, 35 km offshore. The strata dip gently seaward. This seems to be overlain by a quite different limestone composed of hermatypic corals, probably faviids, abundant coralline algae and benthic foraminifers. This limestone occupies a band some 40 km wide between depths of 60-70 m and possibly to 80 m. The composition of this limestone suggests warmer water conditions than are present on the shelf today. Lack of green calcareous algae, however, still suggests cool water. The lack of any diagenetic alteration implies that the strata are probably Pleistocene in age (all Tertiary carbonates onshore are altered to low magnesium calcite; James and Bone; pers. obs.). It is possibly a seaward facies of the Roe Calcarenite (Lowry, 1970), a Pleistocene bivalve-rich unit whose inboard facies is a thin veneer on Cenozoic bedrock across the Roe Plain, immediately onshore from this transect.

The deeper, outer shelf (25 km wide) is thinly veneered with sediment, but the vibrocorer did not penetrate below a depth of 1.4 m because coring was halted by a widespread layer of Holocene coralline algal nodules.

Holocene Sediments

Holocene sediments are relatively simple in composition and comprise 2 major facies; inboard medium to coarse-grained, palimpsest, quartzose bioclastic sand facies and outboard fine to very fine grained , muddy, microbioclastic sand facies.

The modern components fall into three distinct size classes, whose composition is a function of the size of the component calcareous skeletons. *Fine to very fine sands* are mainly composed of ostracode valves, planktonic foraminifers, benthic foraminifers, siliceous sponge spicules, infaunal echinoid spines, pteropod cones, and the singlets of catenecellid bryozoans. There are variable, generally trace amounts of delicate branching cyclostome and cheilostome bryozoan rods, delicate bivalve fragments and tiny gastropods. *Medium to locally coarse sands* are made up of lithoclasts, benthic foraminifers, coralline algal rods, and bivalve fragments. Lithoclasts are a variety of bored, rounded and abraded individual and/or compound skeletons of coralline algae, benthic (especially encrusting) foraminifers, and molluscs and/or bioclastic wackestone. They contain intraskeletal cements and are of unaltered sedimentary mineralogy. Present in minor amounts are gastropods, serpulid worm tubes, regular echinoid fragments and spines,

gorgonian spicules, large planktonic foraminifers and adenoiform, escharifform, reteporifirm, robust branching and vagrant lunulitiform cheilostomes. Many of these particles are polished and worn. *The gravel fraction* is almost entirely fragmented bivalves and minor Adeona or other robust branching cheilostome bryozoa.

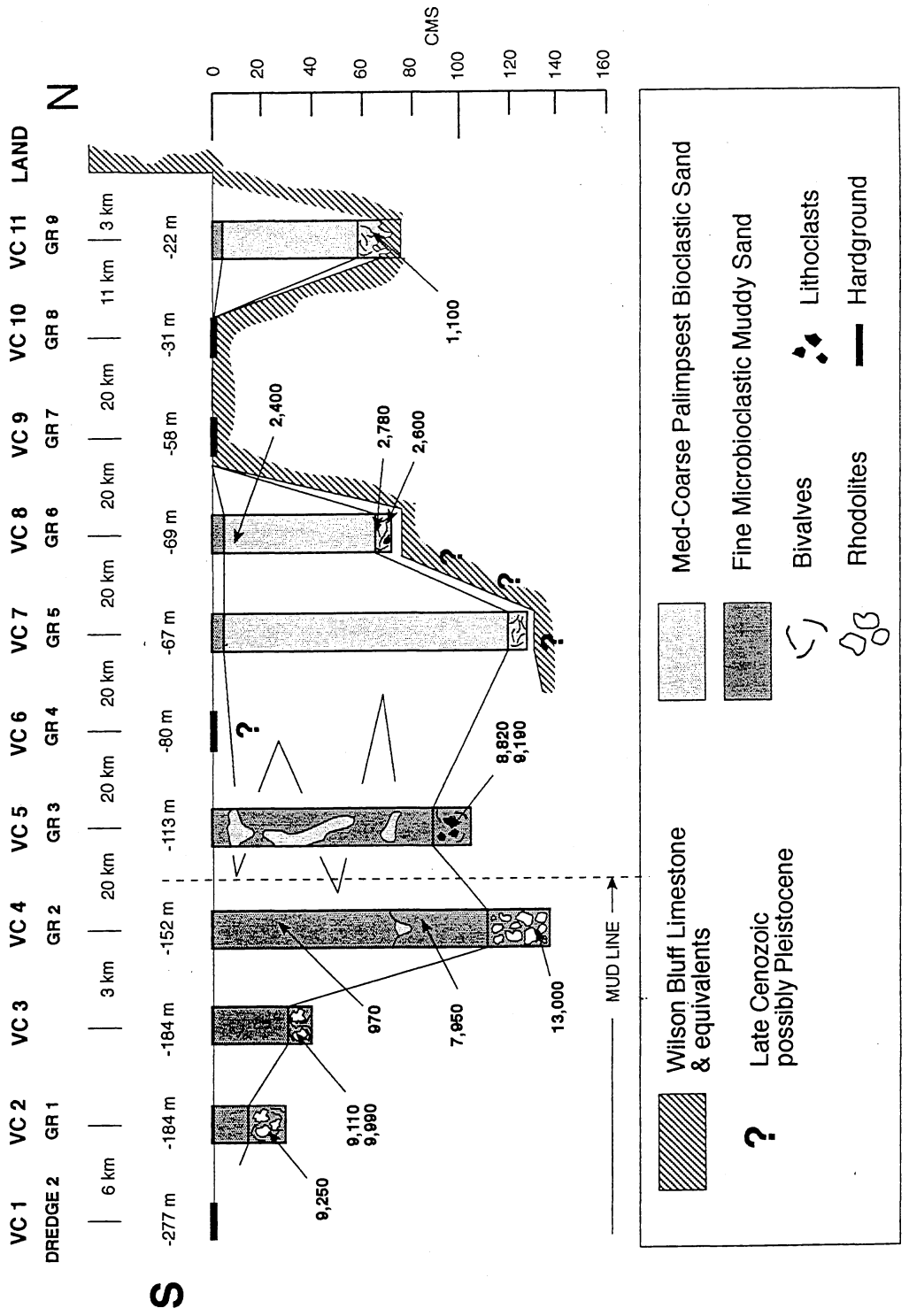

FIGURE 11. Sedimentology of Eucla Shelf (Area B) vibrocores.

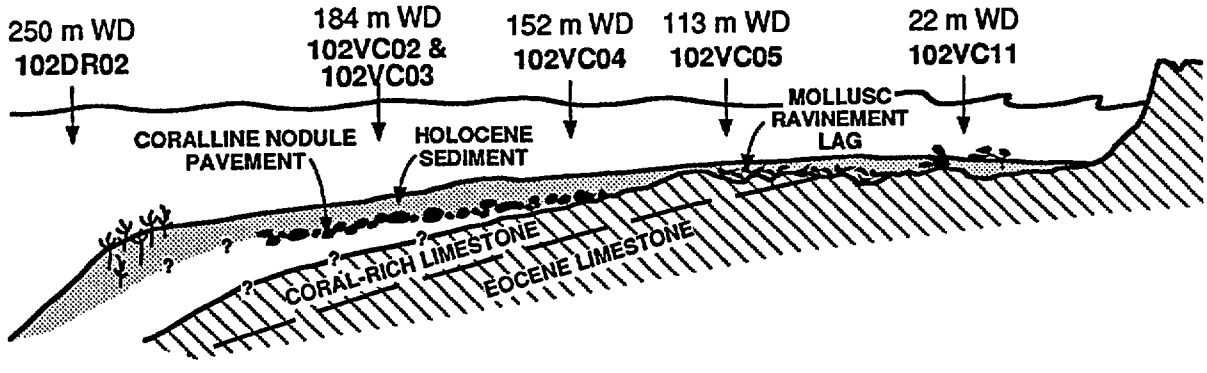

FIGURE 12. Schematic interpretation of the Eucla Shelf vibrocore transect.

Palimpsest Quartzose Bioclastic Sand Facies
These sands have a distinct yellow to buff colour and are speckled with dark grey particles. These colours are due to the 40 to 60% relict component of polished and fragmented grains. It is difficult to resolve the precise composition of the relict particles but most modern grain types can be recognized. The relative abundance of relict particles remains constant throughout. Quartz is generally rounded to subrounded and polished, and decreases in abundance seaward from 25% near the shore to less than 5% at 70 km near the outer shelf. Dolomite rhombs are abundant only to distances of 30 km offshore. The Holocene component is dominated by benthic foraminifers, coralline algal rods, and unidentifiable fragments. Bryozoa are generally unimportant in depths shallower than 80 m.

Microbioclastic Muddy Sand Facies
These sediments are dominated by the finer-grained particles and are mostly singlets of catenecellid bryozoa, pelagic foraminifers and sponge spicules with locally abundant ostracode valves and infaunal echinoid spines. The skeletons are generally whole in deeper water but are highly fragmented in depths shallower than 60 m. All sediments are mud-free in depths shallower than 113 m (102VC05), and contain from 10% to 20% mud deeper than 152 m (102VC04), indicating that the mud line lies somewhere between 113m and 152m.

Three attributes: 1) lack of bryozoans, 2) abundance of coralline algae, and 3) presence of *Marginopora* distinguish these sediments and separate them from deposits at similar depths to the east on the Lacepede and Otway margins. Medium and coarse sand-sized sediments on the continental shelves east of Kangaroo Island are all dominated by bryozoa, both inboard and along the shelf edge (James et al, in press; Boreen et al, in press). Coralline algae are, by contrast, not common in sediments on shelves to the east, except locally adjacent to bedrock highs and in the Gulfs. *Marginopora* is not present in any sediments

except those in Spencer Gulf and Gulf St. Vincent. These differences likely reflect both regional and local environmental conditions. The abundance of bedrock substrates inboard on the Eyre Shelf is certainly conducive to coralline algal growth. The predominant downwelling of oceanic waters and accompanying low nutrient levels may inhibit the growth of many bryozoans. The warmer waters of this area, produced by the Leeuwin Current allow the warm water foraminifer *Marginopora* to proliferate and possibly are more conducive to the growth of corallines.

A relatively high percentage of relict (stained and abraded) grains are present in all cores, reaching a maximum of 75% in some inner shelf areas. In many samples, a marked decrease in the percentage of stained grains occurs upcore; a trend that undoubtedly reflects the transition from Holocene transgressive ravinement to highstand deposition. Planktonic foraminifers and glauconite are absent from inner shelf sediments, and increase in abundance progressively towards the outer shelf edge. Glauconite occurs both as aggregate grains and as internal skeletal molds.

Abundant quartz is present in inner shelf areas (up to 20% - 102VC11). These sediments were likely brought onto the shelf during lowstands. Beaches along the modern Eucla Coast are all quartz-rich, due to longshore transport from the west. The relative amount of quartz in the modern sediments of the Eucla platform, even in inner shelf areas is, however, lower than that of the adjacent Central Gulf and Otway/West Tasmanian regions. This is undoubtedly due to the lack of regional drainage conduits and presence of only older Tertiary carbonate sediments in eroding coastal areas. Outer shelf sediments have significantly lower abundances of quartz which are dominated by silt and very fine sand sizes.

Shelf Edge Sediments

The shelf edge was sampled in one dredge (102DR02; 250-180 m depth) and three vibrocores (102VC01-277 m depth; 102VC02/03-184 m depth). The tandem pipe dredge which recovered sediment undoubtedly filled upon initial emplacement and thus records a 250 m assemblage. The vibrocores recovered a combined total of less than 0.5 m of sediment due to the shallow subsurface rhodolith layer. The olive-coloured unconsolidated sediments present in all samples are bimodal in aspect, with 10-15% well-preserved, gravel-sized, skeletal clasts in a matrix of very fine to medium sand-sized bioclastic sand.

The skeletal constituents have a high diversity and include: whole small echinoids, plates and spines, small fusiform, involute and conical gastropods, free-living (lunulites) bryozoans with conical, disc-shaped and spheroidal growth forms, small serpulid worm tubes, several species of ahermatypic corals including *Scolymia australis, Monomyces radiatus, Flabellum pavoninum, and Charyophillia sp.*, crustacean parts, reteporiform and catenicellid bryozoans, delicate branching cheilostome and cyclostome bryozoans, scaphopods (*Dentalia*), scallops (*Lima, Pectin, Chalmys*), thin-walled bivalves (*Katelysia, Glycymeris, Tellina sp.*), sponge spicules, glauconite aggregates, benthic and planktonic foraminifers, pteropods,

and terebratulid brachiopods. The relict component is less than 5% in all cases, and while many skeletal components are fragmented, they are generally not highly abraded.

A diversity of living organisms were recovered in samples 102DR02 (250-180 m) and 102VC01 (277 m) including: Catenicellid bryozoans, delicate cheilostome and cyclostome bryozoans, encrusting cheilostome bryozoans, thin-walled bivalves, abundant sponges, scallops, benthic foraminifers, crustaceans, the echinoid *Ophiothix,* pteropods, and numerous polychaete worms. Several of the bryozoan species have dense and long chitinous root masses at their bases which can effectively bind loose sediment particles and undoubtedly contribute to increased sediment stability in outer shelf and shelf edge areas. It is conceivable that the failure of the vibrocorer to penetrate at site 102VC01 in 277 m water depth may be related to the presence of some form of hardground upon which cyclostome bryozoans were growing.

The Cellepora packstone facies is quite prevalent on the Lacepede and Otway shelf edges in depths between 150-250 m. The reason for its apparent absence on the Eyre margin may be related to the slightly less vigorous shelf edge current regime in the Bight region, or lack of recognition caused by the low core and dredge density at the shelf edge. The occurrence of large *Cellepora* in coarse-grained slope apron deposits of Thevenard Canyon (BMR cruise 66) indicates that the Cellepora facies is undoubtedly present along the eastern edge of the Bight shelf.

Dolomite Rhombohedra

Dolomite rhombohedra were found in most of the vibrocore and grab samples recovered from the Eucla Shelf, especially inboard samples. The dolomite occurs as individual rhombs and as amalgamated clusters of up to 14 rhombohedra. The rhombs vary from very fine to coarse sand-size (dominantly fine to medium sand-size), are translucent/white to orange/yellow stained, and form both well-preserved euhedral crystals and highly fragmented and rounded grains. The densest accumulation (20% sand fraction) occurs in the shallowest vibrocore (102VC11 - 22 m water depth) at 70 cm depth directly overlying Eocene limestone. The percentage of dolomite decreases markedly upward through the core to 5% at the surface, and the relative percentage of stained rhombs and dolomite clusters decrease in a similar fashion. Progressively decreasing amounts of dolomite also occur in an offshore direction with trace amounts recorded in water depths of 67 - 152 m (102VC07-102VC04), and an apparent disappearance of rhombs at shelf edge depths (184 m -102VC03/02).

The close correlation between sedimentary dolomite rhombs in the modern shelf sediments and compositional variations in the underlying strata suggests that there may be a strong palimpsest control on the occurrence of dolomite in the modern marine sediments. The greatest accumulations undoubtedly occur above exposed and shallowly-burrowed outcrops of white Eocene limestone rich in dolomite

inclusions. The Eocene dolomite occurs as a mixture of stained and unstained, zoned rhombs and rhomb clusters which weather out of a white fine-grained calcareous matrix. A preliminary examination of limestone constituents (glauconite, benthic and planktonic foraminifers, nannofossils, cyclostome bryozoans, sponge spicules, well-rounded quartz grains) suggests a relatively deep shelf, Eocene, temperate carbonate depositional environment.

At present it is unclear whether the dolomite is 1) reworked from Tertiary carbonates, 2) a precipitate on reworked Tertiary nucleii, 3) Quaternary, 4) coated Quaternary nucleii, or 5) Holocene. Dolomite is known from the Wilson Bluff Limestone onshore, both beneath the Nullarbor Plain (James and Bone; pers. obs.) and along the shoreline (Lowry, 1970). Identical dolomite in Holocene sediments on the Lacepede Shelf have a late Pleistocene age and are thought to be precipitating today in shallow subsurface sediments (Bone et al, 1991).

Holocene Stratigraphy and Sediment Dynamics

Radiometric age dates from the vibrocores provide a chronostratigraphic framework for the accumulation of this sedimentary package.

Lithostratigraphy. The irregular topographic surface of the shallow shelf to water depths of 80 m is either bare carbonate or variably covered with up to 1.3 m of sediment. The 3 cores which were successful, at 3 km (22 m depth), 54 km (69 m depth) and 74 km (67 m depth) from land, all illustrate the same stratigraphic succession. A basal bivalve 'lag' overlies lithified substrate. The bulk of the sediment is medium to coarse grained, palimpsest, quartzose bioclastic sand. The succession is capped by a 2 to 4 cm-thick unit of fine to very fine microbioclastic sand.

The deep shelf to depths of 184 m is variably veneered with up to 1.4 m of sediment. In this area the package is floored by a rhodolith gravel. At a depth of 113 m (114 km from land), the sediments are a mixture of the coarse, palimpsest, shallow shelf sediments and the finer, deeper water microbioclastic sands. Although the sediments in this core are disturbed, and it is unresolved whether this is natural or a product of vibrocoring, the presence of both lithologies indicates in place production and episodic offshelf transport. The succession at 152 m and 184 m depth is the same, consisting of rhodolith gravel overlain by muddy, fine, microbioclastic sand.

Chronology. All ^{14}C dates are Holocene. Rhodoliths and bivalves at the base of the deep shelf succession are early Holocene (13.0 to 8.8 Ka). Bivalves from the base of cores on the shallow shelf are much younger, all yielding late Holocene dates (2.6 to 1.1 Ka). The sedimentation rate on the deep shelf ranges from 5.7 to 8.0 cm/ky (core 102VC08). The upper sediments in this core seem to be somewhat reworked. On the inner shelf, the homogeneous age dates throughout the core suggest extensive physical and/or biological reworking.

Comparison with the general Holocene sea level curve for this region (Collins, 1988) indicates that there was a considerable lag time before sediment began to accumulate. On the deep shelf, at 152 m depth for example, sedimentation began at 13.4 Ka, but at that time sea level was at 80 m, i.e. this location was at a depth of 72 m. This seems to support the contention that the depth of wave abrasion is a critical parameter limiting sediment accretion on open, wave-swept shelves. Sediment does not seem to have begun to accumulate on the shallow shelf until ca. 3 Ka, at which time sea level was approximately where it is today and had been there for some 4, 000 years.

SUMMARY

1) The Eyre shelf is variably veneered with a thin (<2.0 m) veneer of Holocene sediment which overlies Tertiary bedrock or ?Pleistocene carbonate (Fig. 12). Much of the shallow shelf inboard of 60 m water depth is bedrock which is being scoured by waves, bored by endolithic organisms, and colonised by attached calcareous and non-calcareous benthos.

2) A thin mollusc and lithoclast lag deposit covers bedrock on the shallow shelf and a rhodolith pavement mantles the deep outer shelf.

3) The thin patchy cover of Holocene sediments consists of two facies. Palimpsest, quartzose, bioclastic sand composed of benthic foraminifers, coralline algae, bivalve fragments, lithoclasts and trace amounts of bryozoans together with, on average, 50% relict grains veneers the mid- to inner-shelf to depths of 80 m, some 90 km from shore. The deeper outer shelf is covered by fine, microbioclastic, muddy-sand rich in catenecellid bryozoans, pelagic foraminifers, ostracodes, and infaunal echinoid debris.

5) The presence of the large foraminifer *Marginopora*, both modern and relict, suggests that the overall environment of deposition is somewhat warmer than that to the east.

6) The shelf edge (~150-200 m water depth) is the site of prolific and diverse carbonate production in the form of bryozoans, bivalves, ahermatypic corals and sponges.

7) Detrital dolomite concentrations in modern shelf sediments are intimately related to exhumed Eocene dolomitic limestones on the inner shelf plain, which may act as a nucleation source and catalyst for modern marine dolomite formation.

8) The upper 2 m of sediment, over bedrock on the mid- to inner-shelf and above a rhodolith layer on the outer shelf, is all Holocene. The rhodolith layer is ca. 9 ka to 13 ka. The inner shelf package is younger, generally less than 3 ka.

6.2.2 SEDIMENTOLOGY OF THE EYRE TERRACE AND WESTERN CEDUNA TERRACE GRAVITY CORE TRANSECTS

T. Boreen (Department of Geological Sciences, Queen's University, Kingston, Ontario, Canada).

Two gravity core transects were carried out to investigate sedimentary and geochemical aspects of upper slope and deep water Quaternary sedimentary records on the Eyre and Ceduna Terraces. Specific objectives included 1) the documentation of Quaternary glacial/interglacial cycles within continental margin sediments, 2) the determination of bulk sedimentation rates and accumulation rates of biogenic and terrigenous components, and 3) the documentation of glacial/interglacial organic carbon sources and fluxes.

Eyre Terrace coring recovered sediment at eleven sites (102GC01 to 102GC11), along a continuation of the vibrocore transect (along 128°01.50'E) into deeper water, at depths from 529 m to 3615 m (Fig. 13). The western Ceduna Terrace transect involved gravity coring seven stations (102GC12 to 102GC18) in water depths ranging from 500-3500 m, at 500 m intervals (Fig. 14). Although the western Ceduna Terrace transect lies in Area C, the substantial similarities in the material recovered from similar depth ranges on both transects makes a combined description reasonable. Only one core (102GC12 - western Ceduna Terrace) failed to recover sediments, in 498 m water depth, undoubtedly due to sandy bottom conditions. A total of 51.56 m of Quaternary sediment was collected in 18 gravity cores. The average core length was 2.86 m; the longest core was 5.17 m.

Quaternary sediments on the Ceduna and Eyre terrace margins are almost exclusively pelagic calcareous ooze, compositionally dominated by planktonic foraminifers and calcareous nannoplankton. Subtle variations in the ratios of the nannofossil and foraminifer components and colour banding were the characteristics used in this first-order subdivision of the cores (Figs 13, 14).

The nannofossil-foraminifer oozes which dominate the Ceduna and Eyre Terrace margins generally consist of 20-40% sand-sized material in a fine-grained calcareous matrix. Compositionally, the sands are almost entirely planktonic foraminifers with accessory benthic foraminifers (*Uvigerina*) and delicate infaunal echinoid spines. A poorly-sorted mixture of very fine to coarse sand-size grains is typical, with a characteristic temperate assemblage including *Globigerina bulloides, Globorotalia truncatulinoides* and large *Orbulina*. Non-calcareous input is generally minor, and rarely exceeds 10% of the bulk sample. Constituent grains include very fine sand-sized to silt-sized particles of quartz, sponge spicules, organics, mica, and red-brown/grey clay aggregates. Scattered solitary corals (*Charophyllia)*, fusiform gastropods and lunulitid cheilostome bryozoans are notable in upper slope cores (102GC06 to 102GC09).

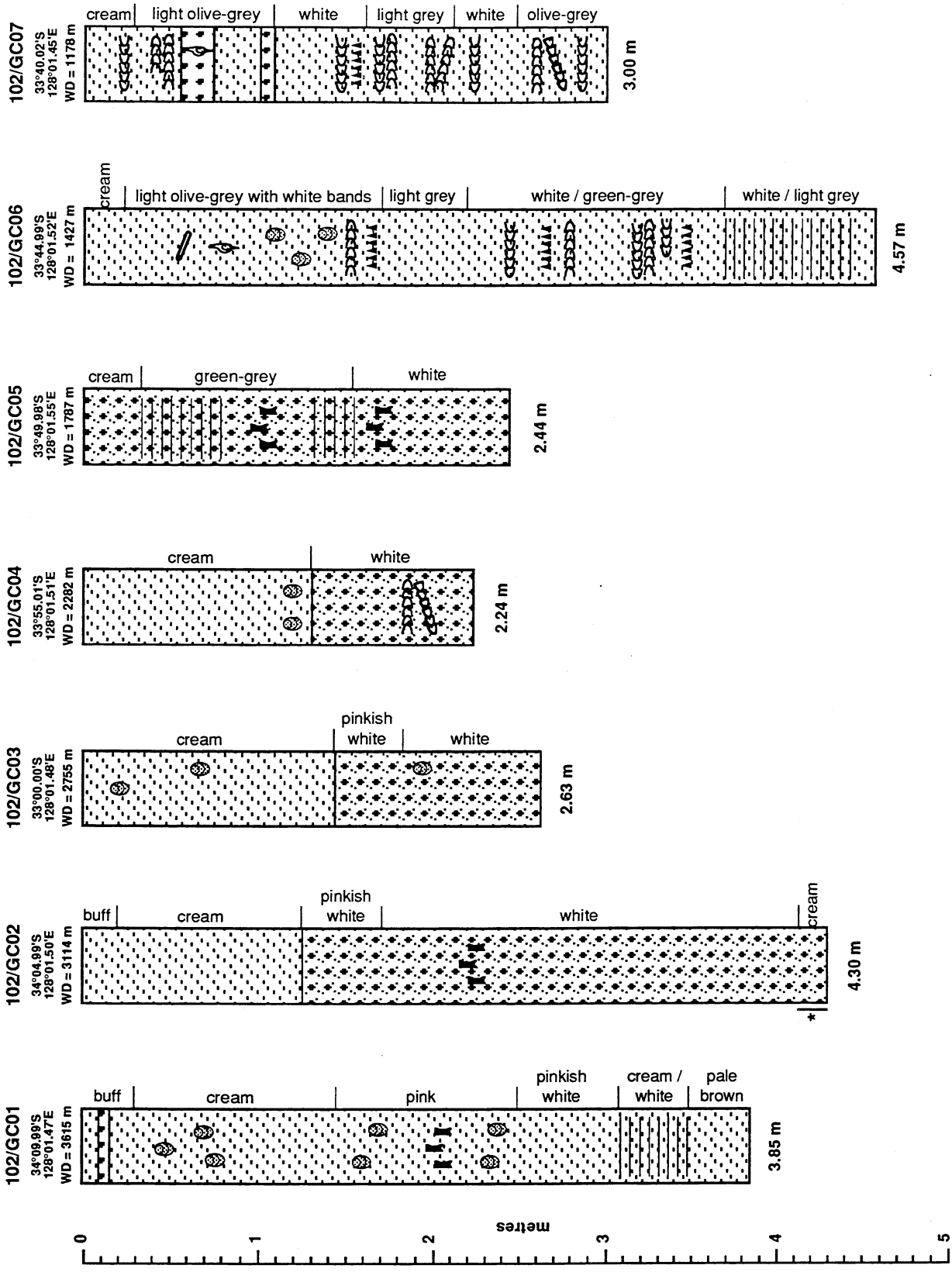

FIGURE 13. Sedimentology logs for Eucla Shelf - Eyre Terrace (Area B) gravity cores.

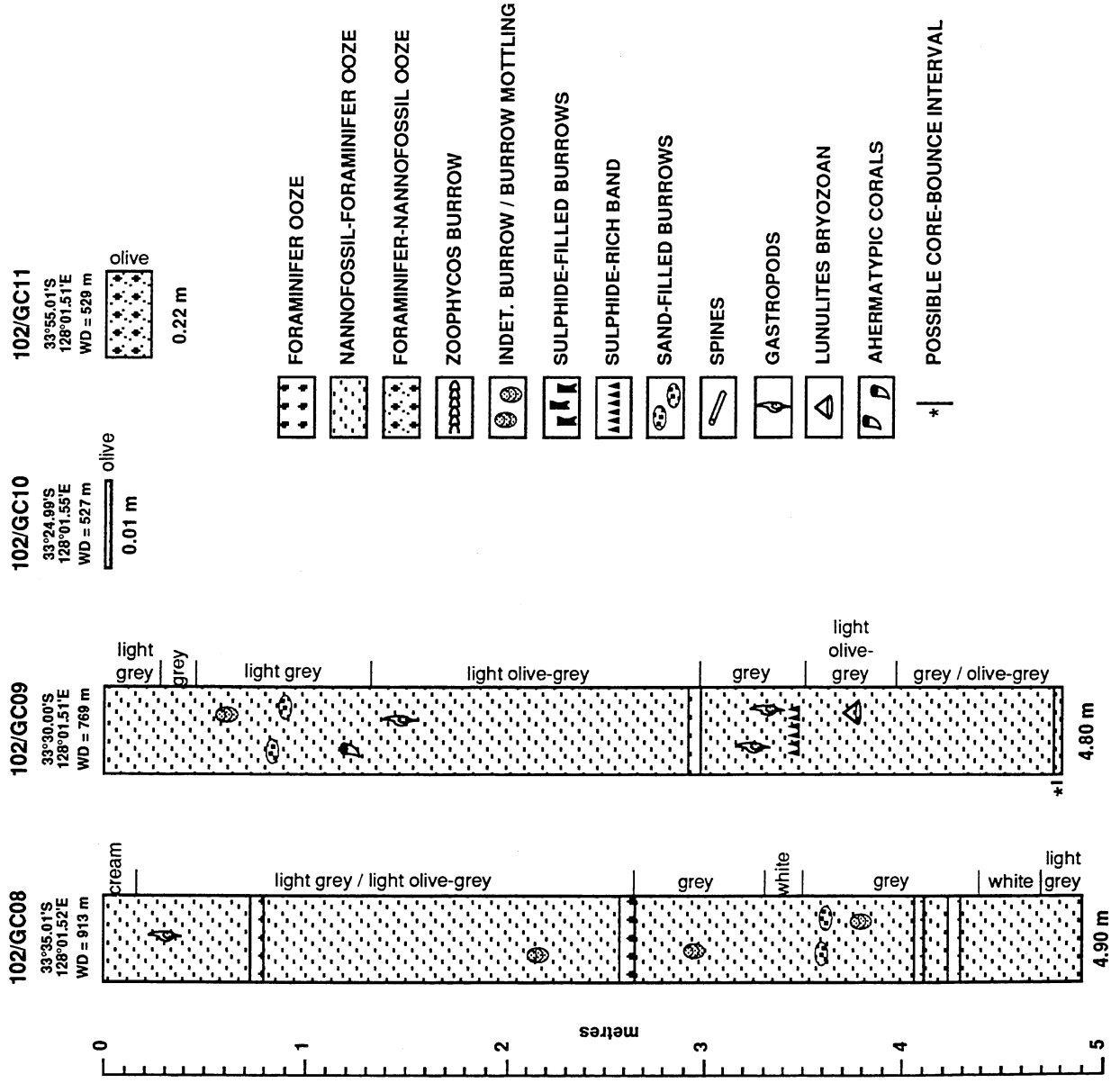

FIGURE 13. Sedimentology logs for Eucla Shelf - Eyre Terrace (Area B) gravity cores (cont.).

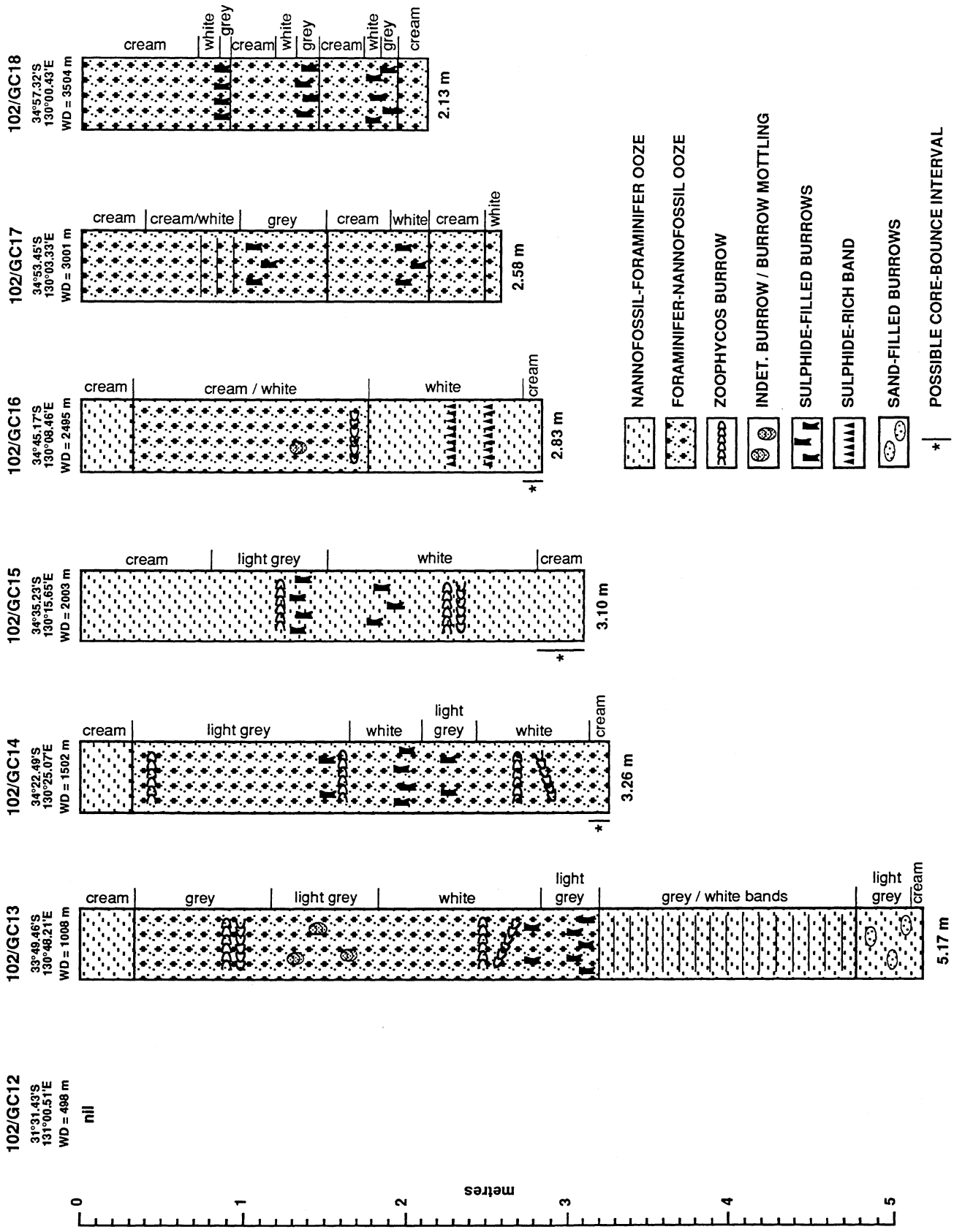

FIGURE 14. Sedimentology logs for western Ceduna Terrace (Area C) gravity cores.

Physical structures in the calcareous oozes are rare and consist of cm-scale, sharp-based sandy beds with normal grading (turbidites), and homogenised sand-rich bands, probably resulting from grainflow deposition. These structures are most prominent in cores from the upper slope of the Eyre Terrace, in depths of less than 1000 m (102GC07 to 102GC09). Skeletal assemblages in these resedimented layers are generally rich in planktonic foraminifers and have variable amounts of shelf-derived, fragmented, skeletal particles dominated by fine-grained bryozoan debris, delicate echinoid spines, thin-walled molluscs, and pteropod husks. Occasional structureless pockets of foraminifer-rich sandy debris in deeper water mid to lower slope cores may be the remnants of biologically-reworked turbidites and resedimented flows.

Biogenic structures are much more prevalent. Transect cores show variable intensities of ichno-disturbance, from sparsely burrowed and burrow-mottled, to completely bioturbated. The most common traces include *Planolites, Zoophycos,* and small sulphide-filled burrows. In addition, an abundance of taxonomically non-diagnostic burrows occur throughout, including mottles, blebs, spots, streaks, tubes, and pockets. A broad depth-related zonation of burrow types, previously documented in similar sediments from the Otway basin, appears also to be present in the Eyre and Ceduna Terrace cores. Intensive homogenisation and bioturbation occurs in outer shelf/upper slope sediments (less than 1000 m); *Planolites*- and *Zoophycos*-dominated burrowing at midslope depths (1000 to 2500 m); and sparse burrow-mottling and sulphide-filled burrows predominate in lower slope regions (2500-4000 m). Colour banding is inversely related to burrowing intensity, and is increasingly prominent at greater depths.

All gravity cores from the western Ceduna and Eyre Terraces display a surficial band of light cream to pinkish-brown oxidised sediment, which passes downcore into grey-green/white oozes, often with dark grey sulphide-burrows and bands. This colour change is consistent with a transition from oxidising to reducing conditions below the sediment water interface. At upper slope depths on the Eyre Terrace, the oxidised layer is restricted to a band within 0.3 m of the sediment-water interface, and widens significantly in downslope areas to more than 1 m in 102GC02 to 102GC04. This trend may reflect the influence of increased circulation of oxygen-rich Antarctic bottom waters at greater depths. Two cores in deeper mid- to lower-slope depths in the Ceduna Terrace area (102GC17 and 102GC18) show an apparently cyclic repetition of this same colour-banded sequence at 50 -100 cm intervals, with up to 3 distinct cycles per core (Fig. 14).

Easily detectable compositional variations between oxic and anoxic layers are not readily apparent. In some cores, the grey/white bands appear to have a slightly increased abundance of clay-sized material. Shipboard petrographic analysis of the sand fractions of consecutive cycles in core 102GC18 revealed very similar compositions and grain size trends between the sand-sized components of consecutive oxic/anoxic bands. The only clearly visible variations are transitions from pink-stained foraminiferal walls (Mn-oxides) with accessory red-brown Fe-oxides, to light grey-tinted foraminifer tests, infilled with grey coloured fine material

(sulphides?). Variable dissolution effects were not observed. The fact that the most prominent expression of the oxic/anoxic signature occurs in the sediments of the deep slope would appear to be consistent with the presence of a strong but episodic influx of cold, oxygen-enriched Antarctic bottom water during interglacial episodes.

TABLE 1. Gravity core locations and descriptions - Eyre and western Ceduna Terraces.

Core	Depth (m)	Length (m)	Latitude	Longitude	Summary Description
<u>Eyre Terrace</u> (see Fig. 13)					
GC01	3615	3.85	34°09.99	128°01.47	385 cm banded cream to pinkish white nanno-foram ooze with burrow mottling and one sandy turbidite
GC02	3114	4.30	34°05.00	128°01.50	126 cm cream nanno-foram ooze over 304 cm pinkish-white to white foram-nanno ooze
GC03	2757	2.63	33°00.00	128°01.50	144 cm cream nanno-foram ooze over 119 cm pinkish-white to white foram-nanno ooze
GC04	2282	2.24	33°55.01	128°01.51	130 cm cream nanno-foram ooze over 94 cm white foram-nanno ooze with *Zoophycos* burrows
GC05	1787	2.44	33°49.98	128 01.55	33 cm cream foram-nanno ooze over 120 cm banded grey-green foram-nanno ooze and 91 cm white foram-nanno ooze
GC06	1424	4.57	33°44.99	128°01.52	23 cm cream nanno-foram ooze over 148 cm light grey and white burrowed and banded nanno-foram ooze,198 cm light grey, *Zoophycos* burrowed nanno-foram ooze, and 88 cm banded grey and white nanno-foram ooze
GC07	1178	3.00	33°40.02	128°01.45	28 cm cream nanno-foram ooze over 272 cm light olive-grey nanno-foram ooze with abundant *Zoophycos* burrows and 2 sandy turbidites

GC08	913	4.90	33°35.01	128°01.52	17 cm cream nanno-foram ooze over 473 cm grey to olive-grey nanno-foram ooze with 4 thin turbidites and pockets of shelf-derived skeletal debris (benthic and planktonic foraminifers, echinoid, pteropod, mollusc, bryozoan, sponge spicules, and large fusiform gastropod)
GC09	769	4.80	33°30.00	128°01.51	480 cm light grey-olive grey nanno-foram ooze with one thin turbidite and pockets of shelf-derived debris (benthic and planktonic foraminifers, echinoid, brachiopod, mollusc debris, lunulites bryozoan, gastropods and ahermatypic solitary coral)
GC10	527	0.01	33°24.99	128°01.55	0.01 m olive homogenous foram-nanno ooze
GC11	529	0.22	33°55.01	128°01.51	0.22 m olive homogenous foram-nanno ooze
western Ceduna Terrace (see Fig. 14)					
GC12	498	nil	31°31.43	131°00.51	no recovery
GC13	1008	5.17	33°49.46	130°48.21	33 cm cream nanno-foram ooze over 287 cm grey to white foram-nanno ooze with *Zoophycos*, burrow mottles and sulphide burrows, 157 cm banded grey-white nanno-foram ooze, and 40 cm light grey nanno-foram ooze with pockets of sandy debris
GC14	1502	3.26	34°22.49	130°25.07	32 cm cream nanno-foram ooze over 294 cm of alternating bands of cream to white foram-nanno ooze with *Zoophycos* and sulphide burrows
GC15	2003	3.10	34°35.23	130°15.65	80 cm cream nanno-foram ooze over 71 cm light grey *Zoophycos*-burrowed nanno-foram ooze and 159 cm white nanno-foram ooze with sulphide-filled burrows
GC16	2495	2.83	34°45.17	130°08.46	32 cm cream nanno-foram ooze over

					144 cm banded light grey-white foram-nanno ooze and 107 cm white ooze with sulphide bands
GC17	3001	2.58	34°53.45	130°03.33	3 successions (150 cm, 64 cm, 44 cm) cream foram-nanno ooze over grey banded to mottled foram-nanno ooze and white foram-nanno ooze with sulphide-filled burrows
GC18	3504	2.13	34°57.32	130°00.43	3.5 successions (91 cm, 54 cm, 49 cm) of cream foram-nanno ooze over grey and white foram-nanno ooze with sulphide-filled burrows

SUMMARY

1) Shelf sediments periodically move downslope as turbidity currents and grainflows, but shelf-derived deposition appears to be confined to upper slope (<1000 m) and deep canyon-accessed slope apron locations.

2) Mid to lower slope deposition is dominated by pelagic sedimentation (foram-nanno oozes), with only minor terrigenous input. Bioturbation decreases down slope, with inversely-related preservation of colour banding. A yellow-brown, surface-oxidised layer increases in thickness downslope from <30 cm in upper slope cores to >100 cm at 3000 m depth, and reflects the increased effect of oxygenated bottom waters at greater depths.

3) There is a general zonation of ichnofacies downslope: <1000 m homogenisation by bioturbators; 1000-2500 m dominated by *Zoophycos*- and *Planolites*-style burrowing; 2500-4000 m burrow mottling and sulphide-filled burrows.

4) Cyclic repetition of oxic/anoxic colour banding is apparent in lower slope cycles and may be related to climatic fluctuations in Antarctic bottom water - pink Mn-oxide staining associated with interglacial periods and increased oxygenated bottom waters; grey sulphide-filled burrows associated with reduced circulation glacial episodes.

6.3 AREA C: LATE QUATERNARY PALEOCHEMISTRY OF THE AUSTRALIAN CONTINENTAL MARGIN: BIOGENIC FLUXES AND CONTINENTAL WEATHERING RATES

The organic carbon cycle and the flux of biogenic elements in the ocean have important implications both for climatic change and for the accumulation of some seafloor minerals, e.g. phosphorites, manganese nodules. The rates of organic

carbon production in surface water, organic flux to the seafloor, and the degradation of organic matter in surficial sediment and ultimate burial by sediment are key factors in these cycles.

Organic carbon burial in seafloor sediment is a long-term control on the oxygen content of the atmosphere, and organic carbon burial on continental margins, estimated to be 20-25% of primary productivity, is likely to be an important control on atmospheric carbon dioxide content. Glacial/interglacial changes in oceanic circulation patterns, on a 10^3-10^5 year timescale, have caused variations in sea surface temperature, nutrient concentration, oceanic primary productivity, organic carbon fluxes to the sediment, and the chemistry of the water column and the atmosphere. Furthermore, the occurrences and concentrations of seafloor minerals (e.g. phosphorites of Eastern Australia; metallic nodules and crusts on the South Tasman Rise and western Tasmanian margin), have been linked to the dynamics of major current systems, organic carbon flux to the seafloor, and the cycling of organic carbon and bioactive constituents in the sediments.

The western Ceduna Terrace geochemical sampling transect forms one component in a proposed series of transects around Australia designed to document the Late Quaternary paleochemistry of continental margin sediments. These coring transects will examine the effects of past climatic change, as reflected in sea-level variations, on the oceanic organic carbon cycle on Australia's continental margin. The western Ceduna Terrace transect will form part of a series of southern margin transects, with additional coring proposed for the Naturaliste Plateau, the South Australian - west Tasmanian margin, and the South Tasman Rise. Sediment on these margins has been influenced by variations in the location of the Sub-Tropical Convergence, by the Leeuwin and Flinders Currents, and by the West Wind drift. Specific objectives of this program are:

(1) To document Quaternary glacial/interglacial cycles within continental margin sediments.

(2) To determine bulk sedimentation rates, and accumulation rates of biogenic and terrigenous components.

(3) To document glacial/interglacial organic carbon sources and fluxes, and to determine the consequent implications both for paleoproductivity and nutrient flux, and for coastal upwelling and circulation pattern variations.

(4) To investigate the influence of glacial/interglacial cycles in ocean biogeochemistry and continental weathering on the accumulation and/or formation rates of seafloor minerals.

Results of analyses from Western Australian margin coring transects, including the Exmouth Plateau and Perth Basin, record interglacial minima and glacial maxima in calcium carbonate content, and document glacial/interglacial cycles in the oxygen isotopic ratios of planktonic foraminifer tests. These cores record variations in sediment accumulation rates, sediment composition (biogenic and terrigenous components and bioactive trace metals), and water column chemistry. Radiochemical studies indicate sedimentation rates of about 2.5 cm/kyr, and dramatic variations in authigenic uranium content indicate changes in organic

carbon fluxes (McCorkle and others, 1990).

Gravity cores were collected at approximately 500 m intervals between 500 and 3500 m water depth (102GC12 to 102GC18). Because of the considerable lithological similarities between these cores and the transect of gravity cores collected on the lower slope of the Eyre Terrace, the sedimentology of cores from both transects are described together in Section 6.2.2 above. The biostratigraphic results from all cruise 102 samples are discussed in Section 6.5 below.

6.3.1 REPORT ON GEOCHEMICAL ANALYSES - WESTERN CEDUNA TERRACE GRAVITY CORES (AREA C).

J. Lane and D. Heggie (AGSO, Canberra).

INTRODUCTION

The primary purpose of the western Ceduna Terrace gravity core sampling program was to determine whether this part of the Australian margin was a suitable locale to examine glacial/interglacial oceanographic variations, particularly oceanic productivity underlying the SubTropical Convergence. If appropriate, this part of the Australian continental margin could be used as a 'window' into the Southern Ocean, providing important clues to fluctuations in Southern Ocean oceanography. This work is being undertaken on a collaborative basis between scientific staff at AGSO, Dr. H. Veeh at Flinders University of South Australia and Dr. D. McCorkle at Woods Hole Oceanographic Institution, USA; the present report is a summary of preliminary analytical work only.

Specific objectives included: (i) to determine glacial/interglacial variations in oceanic productivity, (ii) to examine glacial/interglacial variations in the vertical nutrient structure in the water column, (iii) to determine glacial/interglacial variations in sedimentation rates and bulk chemical compositions that may be related to changes in terrigenous inputs and local oceanography and, (iv) to seek evidence of geochemical tracers that may be both direct and indirect indicators of glacial/interglacial variations in particle fluxes (biogenic and terrigenous) and local oceanography; specifically, to test radioactive tracers (uranium and thorium abundance) as indicators of organic carbon input. The sedimentology of cores from this transect are summarised in Table 1 above. Two cores were selected for preliminary sampling and analyses from the western Ceduna Terrace (Table 2). In addition, a further core from the Eyre Terrace, from 769 m water depth, was also analysed.

METHODS

Cores were analysed for porosity, % water content (by mass), wet and dry bulk density, $\%CaCO_3$, total magnetic susceptibility, and grainsize.

TABLE 2. Location and geochemical analysis summary.

Core	Water Depth (m)	Latitude	Longitude	Recovery (m)
102GC09	769	33°30.00'S	128°01.51'E	4.80
102GC14	1502	34°22.49'S	130°25.07'E	3.26
102GC17	3001	34°53.45'S	130°03.33'E	2.58

Core	NUMBER OF SAMPLES ANALYSED						
	Porosity	Water Content	Wet Bulk Density	Dry Bulk Density	CaCO3	Magnetic Suscept.	Grainsize
102GC09	78	78	78	78	78	78	5
102GC14	55	55	55	55	55	55	5
102GC17	41	41	41	41	41	41	5

Bulk Chemical Composition:
The procedure for the determination of percent calcium carbonate using the "carbonate bomb" is as follows. The samples were oven dried overnight, then ground into a fine powder. Approximately 10 ml of concentrated hydrochloric acid was placed in the bomb; one gram of sediment was added; and the bomb was sealed and connected to a digital pressure monitor. The bomb was then swirled gently to allow the samples and acid to react. This reaction produces carbon dioxide gas, with the gas pressure read off the monitor. A number of standards were run to check the accuracy of the bomb. The precision of the analyses (expressed as the coefficient of variation) determined from analyses of 5 aliquots of a sample was found to be ±1-2%.

Grainsize:
Grainsize analyses were performed to determine the different fractions of mud, sand and gravel present in each sample. Each jar containing the total sample (approximately 20 gm of dried sediment, accurately weighed) was filled with distilled water and left until the sample was hydrated and sediment grains were easily separated. The samples were then flushed (with water) through 2 mm and 63 μm sieves to separate into the different fractions. The sand and gravel fractions were put in the oven overnight to dry. The mud fraction was centrifuged, and then placed in a freeze drier overnight. Each fraction was then weighed and their percentages calculated.

Water Content, Porosity, and Bulk Sediment Densities:
Wet sample weights were determined by weighing the samples as soon as possible after sub-sampling the gravity cores, to minimise evaporation and water loss. All the samples were dried in a 50°C oven overnight and then re-weighed to measure the dry weight of the sample. The weight of water present in each sample was determined by difference between wet and dry weights. The volume of wet sediment used in the calculations below was 7 cm^3.

The porosity, water content and bulk sediment density of each sample was determined from the following equations:

Porosity (% by volume) = 100 x ([weight of water/density of seawater] ÷ volume of wet sediment)

Wet Bulk Density (g/cm^3) = weight of wet sediment ÷ volume of wet sediment

Dry Bulk Density (g/cm^3) = weight of dry sediment ÷ volume of wet sediment

Water Content (% by mass) = 100 x (weight of water ÷ weight of wet sediment)

Magnetic Susceptibility:
The magnetic susceptibility (μGauss) of each 7 cm^3 subsample was determined using a Digico Bulk Susceptibility Bridge at the AGSO Black Mountain Laboratory. The procedure used for determining magnetic susceptibility is set out in the Digico Bulk Susceptibility Bridge User Manual, using the SUSB2 data acquisition program running under PALDAS, (Digico Bulk Susceptibility Bridge User Manual, 1992).

RESULTS

The physical and chemical properties for the three cores analysed from survey 102 are presented in table form below: data for 102GC09 are summarised in Table 3; data for 102GC14 are summarised in Table 4; and data for 102GC17 are summarised in Table 5.

TABLE 3. Physical properties and bulk chemical composition for 102GC09.

Depth in Core (m)	Porosity (volume%)	Water Content (mass%)	Wet Bulk Density (g/cm^3)	Dry Bulk Density (g/cm^3)	$CaCO_3$ (%)	Magnetic Susceptibility (μGauss)	Gravel (%)	Sand (%)	Mud (%)
0-3	57.77	33.22	1.79	1.20	80	4.04			
0.6-9	55.14	33.03	1.72	1.15	84	3.81			
0.12-15	54.83	33.00	1.71	1.15	82	4.07		39	61
18-21	54.76	32.82	1.72	1.15	84	3.43			
24-27	55.59	32.93	1.74	1.17	82	3.67			
30-33	54.52	32.95	1.70	1.14	83	3.76		30	70
36-39	53.92	31.86	1.74	1.19	84	-4.14			
42-45	53.09	30.61	1.79	1.24	87	-5.11			
48-51	51.59	29.85	1.78	1.25	86	-6.41		28	72
54-57	51.07	29.85	1.76	1.24	86	-4.90			
60-63	50.68	29.98	1.74	1.22	87	-5.84			
66-69	52.76	31.35	1.73	1.19	95	-5.86			
72-75	50.94	29.53	1.78	1.25	88	-4.80			
79-82	53.58	31.82	1.73	1.18	85	-6.56			
85-88	52.87	31.57	1.72	1.18	86	-4.30			
91-94	55.52	32.51	1.76	1.19	87	-6.36			
97-100	54.05	31.97	1.74	1.18	88	-6.57			
103-106	54.97	32.62	1.74	1.17	88	-7.15			
109-112	54.50	32.83	1.71	1.15	88	-7.37			
115-118	54.83	33.04	1.71	1.14	81	-6.56		12	88
121-124	55.95	34.29	1.68	1.10	86	-6.96			

127-130	55.74	34.52	1.66	1.09	84	-7.03		
133-136	56.39	34.81	1.67	1.09	88	-7.70		
139-142	57.95	35.24	1.69	1.10	86	-5.08		
145-148	57.15	34.61	1.70	1.11	84	-6.13	14	86
151-154	55.15	33.28	1.71	1.14	87	-5.23		
157-160	55.80	33.57	1.71	1.14	86	-5.80		
163-166	54.82	33.37	1.69	1.13	86	-6.73		
169-172	53.48	32.31	1.70	1.15	84	-3.86		
176-179	55.07	32.36	1.75	1.19	85	-4.69		
182-185	54.53	32.24	1.74	1.18	86	-4.18		
188-191	55.03	31.38	1.81	1.24	82	-6.03		
194-197	54.18	31.61	1.77	1.21	88	-5.62		
200-203	53.66	31.78	1.74	1.19	85	-5.42		
206-209	53.59	31.21	1.77	1.22	87	-5.34		
212-215	53.94	31.66	1.75	1.20	83	-6.05		
218-221	54.60	31.94	1.76	1.20	77	-5.67		
224-227	52.35	31.60	1.71	1.17	85	-5.52		
230-233	53.36	31.90	1.72	1.17	89	-5.97		
236-239	53.99	32.14	1.73	1.17	83	-4.23		
242-245	53.87	31.64	1.75	1.20	86	0.68		
248-251	51.73	30.29	1.76	1.23	87	-4.40		
254-257	54.06	31.36	1.78	1.22	86	-4.55		
260-263	53.56	31.23	1.77	1.21	87	-4.77		
266-269	55.95	33.32	1.73	1.15	85	-3.44		
272-275	54.64	32.96	1.71	1.14	85	-5.55		
279-282	55.11	31.77	1.79	1.22	84	-4.98		
285-288	53.69	31.63	1.75	1.19	89	-4.85		
291-294	54.56	32.53	1.73	1.17	84	-3.57		
297-300	52.61	30.32	1.79	1.24	87	-1.97		
303-306	53.54	30.45	1.81	1.26	88	-4.18		
309-312	52.93	30.95	1.76	1.22	87	-4.78		
315-318	53.98	30.74	1.81	1.25	85	-4.47		
321-324	52.72	30.48	1.78	1.24	84	-5.03		
327-330	52.97	30.35	1.80	1.25	85	-4.99		
333-336	52.75	31.87	1.70	1.16	83	-5.41		
339-342	52.41	30.68	1.76	1.22	84	-4.15		
345-348	51.72	29.90	1.78	1.25	82	-6.85		
351-354	52.96	30.59	1.78	1.24	83	-4.54		
357-360	54.05	31.38	1.77	1.22	85	-5.35		
363-366	53.09	31.21	1.75	1.21	83	-4.70		
369-372	53.73	32.24	1.72	1.16	86	-4.00		
376-379	56.71	31.45	1.86	1.27	86	-3.84		
382-385	55.58	31.48	1.82	1.25	84	-3.08		
388-391	53.89	30.61	1.81	1.26	83	-3.03		
394-397	51.91	29.31	1.82	1.29	87	-3.72		
400-403	52.61	30.27	1.79	1.25	85	-2.24		
406-409	52.09	29.46	1.82	1.28	86	-2.27		
412-415	52.82	29.05	1.87	1.33	85	-3.73		
418-421	51.04	29.44	1.79	1.26	86	-1.64		
424-427	51.62	30.22	1.76	1.23	87	-3.92		
430-433	55.37	31.08	1.83	1.26	88	-2.31		
436-439	53.88	31.53	1.76	1.20	87	-3.20		
442-445	56.60	32.01	1.82	1.24	84	-1.68		
448-451	54.05	31.91	1.74	1.19	89	-1.97		

454-457	57.29	32.60	1.81	1.22	85	-0.47			
460-463	53.25	30.80	1.78	1.23	83	2.40			
466-469	55.43	33.20	1.72	1.15	80	0.97			

TABLE 4. Physical properties and bulk chemical composition for 102GC14.

Depth in Core (m)	Porosity (volume%)	Water Content (mass%)	Wet Bulk Density (g/cm^3)	Dry Bulk Density (g/cm^3)	$CaCO_3$ (%)	Magnetic Susceptibility (μGauss)	Gravel (%)	Sand (%)	Mud (%)
0-3	61.07	40.81	1.54	0.91	89	35.82			
6-9	58.40	39.29	1.53	0.93	90	37.99		27	73
12-15	57.73	38.24	1.55	0.96	90	44.09		33	67
18-21	58.75	36.88	1.64	1.04	90	57.51		33	67
26-29	56.32	37.27	1.56	0.98	89	13.09			
32-35	58.58	35.98	1.68	1.07	88	79.29			
38-41	56.61	35.24	1.65	1.07	89	54.59			
44-47	58.83	36.07	1.68	1.07	87	37.95			
50-53	57.48	36.59	1.62	1.03	88	32.94			
56-59	60.09	36.92	1.68	1.06	87	26.81			
62-65	58.98	37.84	1.60	1.00	87	3.20		34	66
68-71	61.05	37.26	1.69	1.06	88	37.44			
71-74	59.69	37.65	1.63	1.02	88	27.00			
77-80	58.46	36.45	1.65	1.05	87	27.93			
83-86	58.24	37.03	1.62	1.02	86	27.03			
89-92	59.88	38.51	1.60	0.98	86	20.06			
95-98	58.24	36.23	1.66	1.06	85	24.42			
98-101	60.72	37.43	1.67	1.05	86	7.08		36	64
104-107	61.08	37.97	1.66	1.03	85	41.30			
110-113	58.94	36.34	1.67	1.06	85	13.87			
116-119	58.79	36.25	1.67	1.06	84	58.63			
122-125	58.32	35.86	1.67	1.07	89	2.61			
126-129	57.04	35.30	1.66	1.08	90	3.44			
132-135	58.49	36.41	1.65	1.05	90	1.49			
138-141	59.05	36.83	1.65	1.04	87	12.15			
144-147	56.72	35.42	1.65	1.06	88	7.52			
150-153	57.49	36.26	1.63	1.04	87	38.57			
156-159	56.56	34.66	1.68	1.10	87	27.19			
162-165	53.92	33.34	1.67	1.11	87	19.12			
168-171	55.87	33.92	1.70	1.12	91	36.70			
174-177	55.92	35.25	1.63	1.06	92	15.83			
180-183	56.25	34.40	1.68	1.10	92	39.77			
186-189	54.68	33.82	1.66	1.10	91	30.31			
192-195	56.05	34.20	1.69	1.11	93	-0.88			
198-201	54.72	33.86	1.66	1.10	93	-1.36			
204-207	54.93	33.91	1.67	1.10	93	-2.91			
210-213	53.98	33.24	1.67	1.12	90	24.26			
216-219	53.14	32.00	1.71	1.16	89	31.36			
222-225	53.00	32.87	1.66	1.11	91	33.81			
229-232	56.53	35.02	1.66	1.08	91	33.67			
235-238	58.05	34.97	1.71	1.11	92	31.43			
241-244	57.42	35.68	1.66	1.07	92	21.82			
247-250	57.12	36.08	1.63	1.04	91	8.13			
253-256	58.31	36.09	1.66	1.06	93	-0.16			

259-262	57.09	36.13	1.63	1.04	95	-2.61
265-268	57.19	36.28	1.62	1.03	94	11.10
271-274	58.03	35.47	1.68	1.09	94	12.41
277-280	57.54	35.34	1.68	1.08	95	13.52
283-286	54.35	34.49	1.62	1.06	92	19.38
289-292	63.19	36.84	1.77	1.12	93	20.96
295-298	53.74	33.56	1.65	1.10	91	24.48
301-304	56.20	32.89	1.76	1.18	88	20.66
307-310	56.40	33.81	1.72	1.14	91	21.18
313-316	59.05	38.01	1.60	0.99	90	36.57
319-322	55.47	35.54	1.61	1.04	90	49.77

TABLE 5. Physical properties and bulk chemical composition for 102GC17.

Depth in Core (m)	Porosity (volume%)	Water Content (mass%)	Wet Bulk Density (g/cm^3)	Dry Bulk Density (g/cm^3)	$CaCO_3$ (%)	Magnetic Susceptibility (μGauss)	Gravel (%)	Sand (%)	Mud (%)
3-5	56.72	35.56	1.64	1.06	89	69.58		31	69
8-10	56.10	35.10	1.65	1.07	90	74.60			
14-17	51.15	31.97	1.65	1.12	91	123.14			
20-23	40.21	28.12	1.47	1.06	88	105.54			
26-29	47.36	30.13	1.62	1.13	88	135.05		50	50
32-35	54.64	32.72	1.72	1.16	85	139.54			
38-41	47.99	29.15	1.70	1.20	89	54.27			
41-44	46.06	27.44	1.73	1.25	93	15.53		25	75
46-49	46.81	28.34	1.70	1.22	92	50.76			
54-57	49.52	27.66	1.84	1.33	88	33.26			
58-61	53.20	31.26	1.75	1.20	91	25.62			
66-69	53.95	31.27	1.78	1.22	91	64.19			
72-75	51.74	30.02	1.78	1.24	92	19.82			
78-81	55.88	31.91	1.80	1.23	88	28.53			
84-87	53.59	31.06	1.78	1.23	88	16.00			
95-98	54.12	29.61	1.88	1.33	91	4.00			
98-101	51.07	35.52	1.48	0.95	89	2.74			
107-110	56.34	33.99	1.71	1.13	89	7.75			
113-116	57.23	34.65	1.70	1.11	88	4.69			
119-122	56.40	34.65	1.68	1.10	87	9.50			
125-128	57.01	35.14	1.67	1.08	87	20.15			
131-134	56.89	33.28	1.76	1.17	87	50.31			
137-140	58.03	34.25	1.75	1.15	87	101.40		30	70
143-146	60.68	37.39	1.67	1.05	82	48.89			
154-157	57.38	34.48	1.71	1.12	89	91.26			
161-164	56.64	34.44	1.69	1.11	88	111.80		34	66
167-170	57.88	35.12	1.70	1.10	88	107.64			
173-176	55.11	34.09	1.66	1.10	88	92.57			
179-182	55.49	33.26	1.72	1.15	87	133.90			
185-188	52.14	32.39	1.66	1.12	89	92.84			
191-194	53.73	31.06	1.78	1.23	90	89.81			
194-197	48.68	27.81	1.80	1.30	91	4.08			
200-203	50.52	28.54	1.82	1.30	91	8.64			
206-209	49.52	27.57	1.85	1.34	92	5.13			
214-217	50.74	28.51	1.83	1.31	91	8.06			
220-223	56.65	36.32	1.61	1.02	91	43.30			

226-229	56.83	35.78	1.64	1.05	91	78.42
232-235	55.66	34.48	1.66	1.09	88	117.28
241-244	54.63	33.54	1.68	1.11	88	103.27
247-250	50.63	29.39	1.77	1.25	89	38.00
250-253	53.19	31.60	1.73	1.19	92	29.88

The down-core variations in $\%CaCO_3$ for 102GC09 (water depth 769 m), are shown in Figure 15. Calcium carbonate varies between 75-95% (by mass), and porosity varies between 0.45-0.7% (Table 3). The down-core variations in total magnetic susceptibility are shown in Figure 16, and a combined plot of $CaCO_3$ and magnetic susceptibility is shown in Figure 17. Although glacial/interglacial signals cannot be definitively determined from these data, the data do provide some preliminary clues to these intervals. These data will be used to determine $CaCO_3$ mass accumulation rates and to assist in choosing sample for oxygen isotopic analysis.

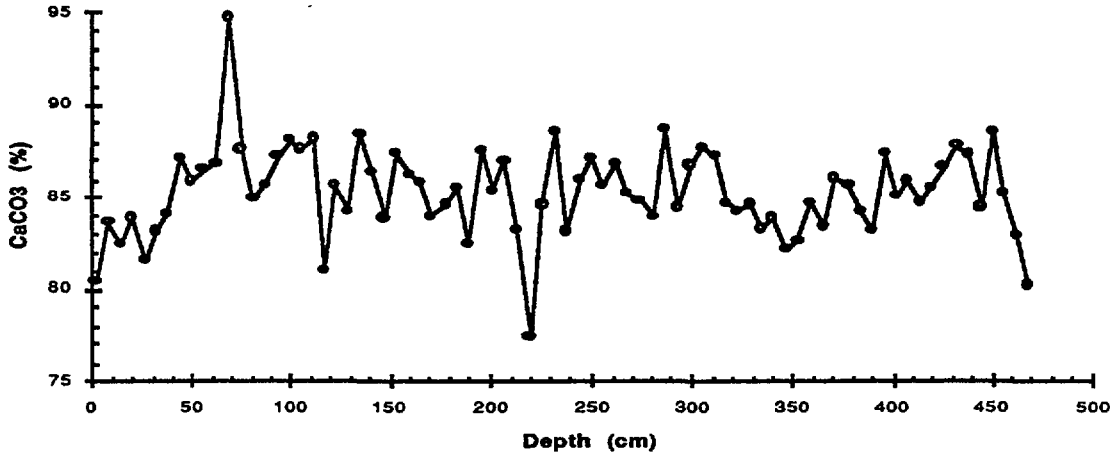

FIGURE 15. Plot of $CaCO_3$ (%) against depth (cm) for 102GC09.

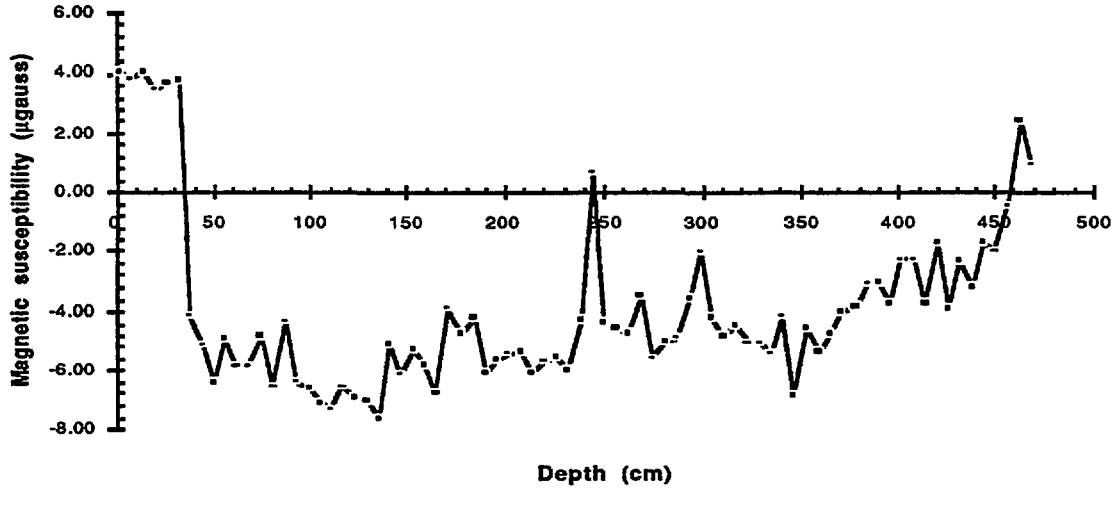

FIGURE 16. Plot of magnetic susceptibility (μgauss) against depth (cm) for 102GC09.

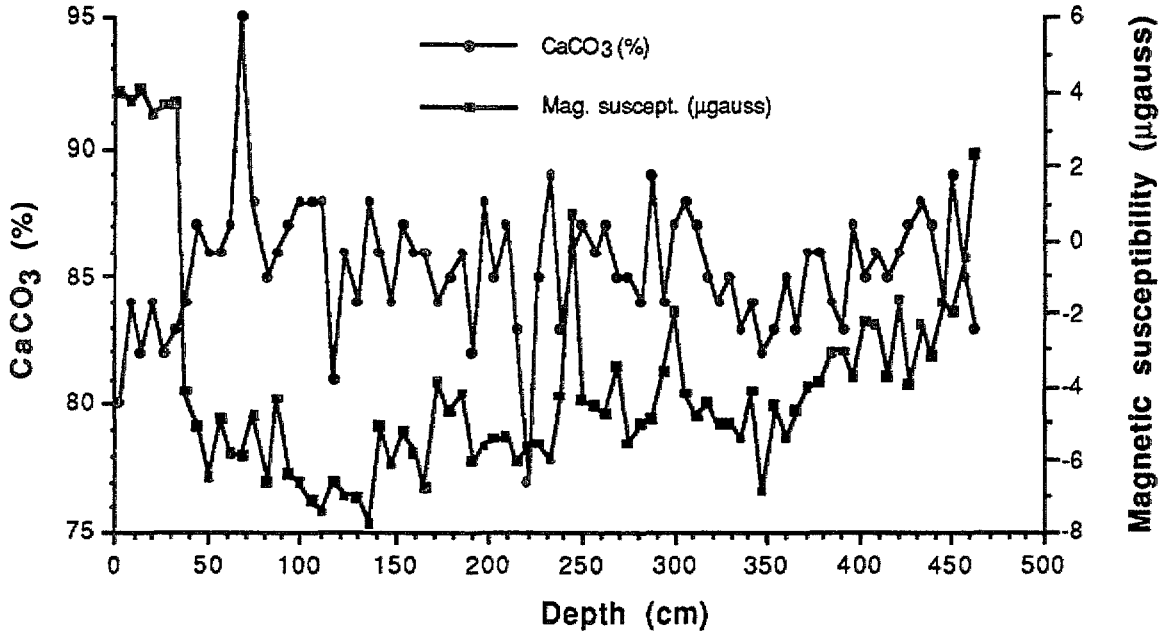

FIGURE 17. Plot of $CaCO_3$ (%) and magnetic susceptibility (μgauss) against depth (cm) for 102GC09.

Percent calcium carbonate vs depth (cm) for sediments from 102GC14 (water depth 1502 m) is shown in Fig. 18. The %$CaCO_3$ in these sediments ranges between 84-95%. Figure 19 illustrates magnetic susceptibility (μGauss) vs depth (cm) for core 102GC14. The summary plot for 102GC14 (Fig. 20) shows a combination of the %$CaCO_3$ in the sediments and their magnetic susceptibilities (μGauss). These data show down-core variations probably related to glacial/interglacial variations, but these results do not define glacial/interglacial periods definitely. As noted above, these data will be used to choose samples for oxygen isotopic analyses to define glacial/interglacial periods, and subsequently to determine mass accumulations rates of sediments.

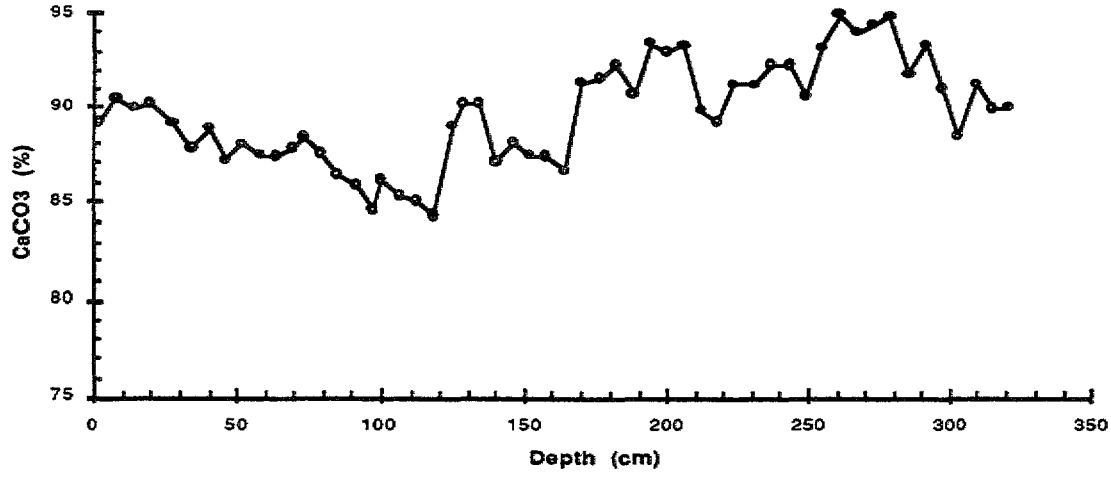

FIGURE 18. Plot of $CaCO_3$ (%) against depth (cm) for 102GC14.

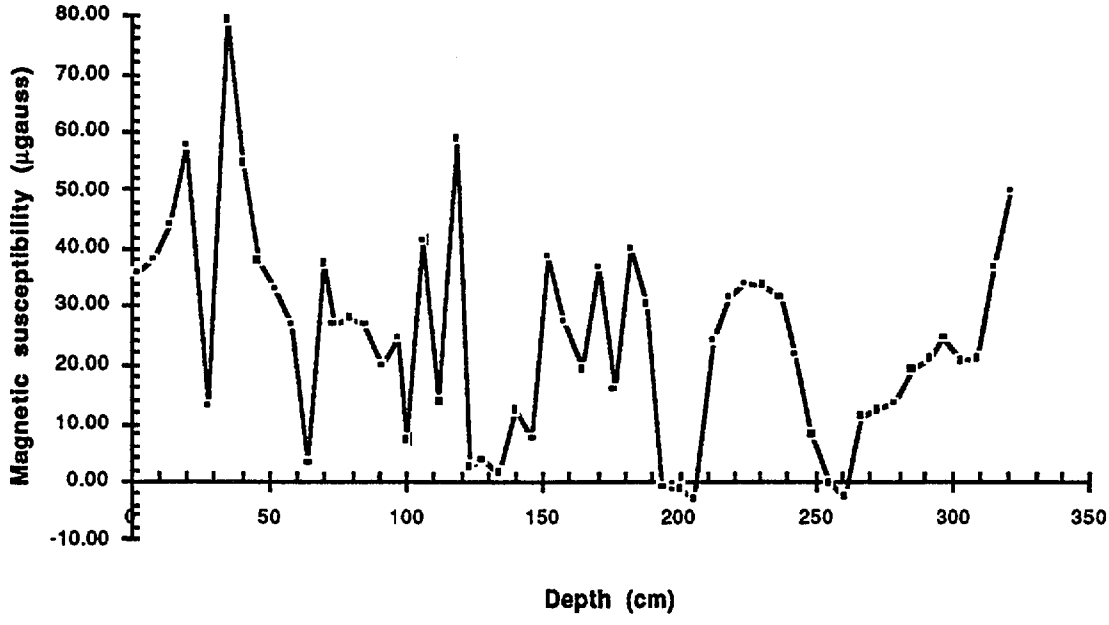

FIGURE 19. Plot of magnetic susceptibility (μgauss) against depth (cm) for 102GC14.

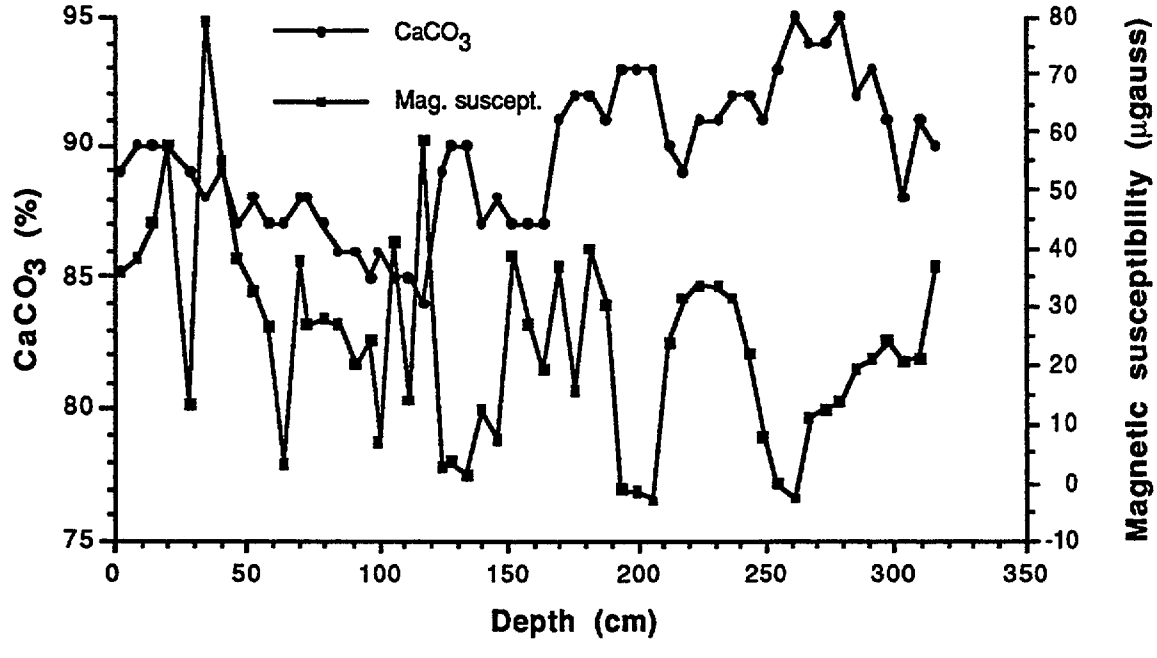

FIGURE 20. Plot of $CaCO_3$ (%) and magnetic susceptibility (μgauss) against depth (cm) for 102GC14.

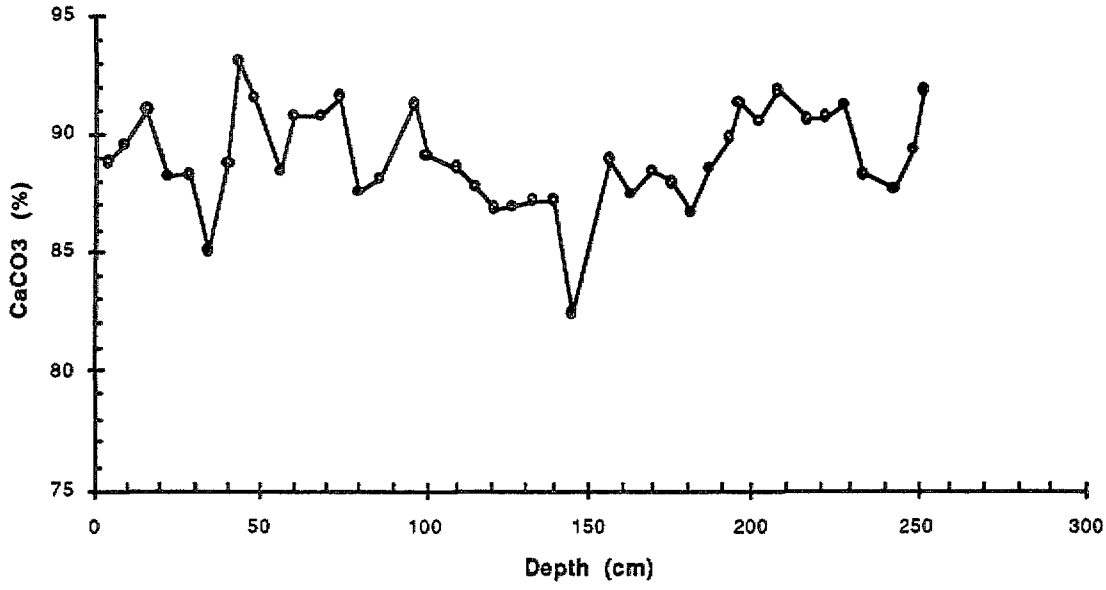

FIGURE 21. Plot of $CaCO_3$ (%) against depth (cm) for 102GC17.

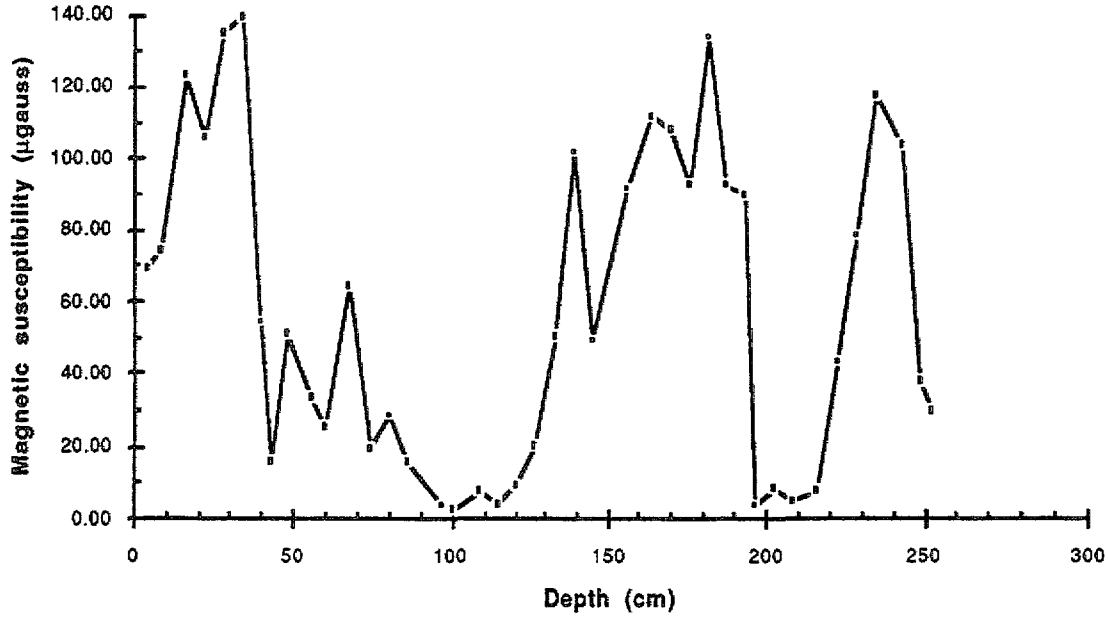

FIGURE 22. Plot of magnetic susceptibility (μgauss) against depth (cm) for 102GC17.

Percent calcium carbonate vs depth for marine sediments 102GC17 (water depth 3001 m) is shown in Fig. 21. The $CaCO_3$ present in these sediments ranges between 85-93%. The plot of magnetic susceptibility (μGauss) vs depth (cm) (Fig. 22) shows a great deal of variation down-core, probably related to changes in terrigenous input. The relationship between $\%CaCO_3$ and magnetic susceptibility

(μGauss) for 102GC17 is summarised in Fig. 23. This relationship is an inverse one, and should help identify the Last Glacial Maximum event. These data will be used to select samples for isotopic analyses, to precisely define glacial/interglacial transitions, and subsequently to determine mass accumulation rates.

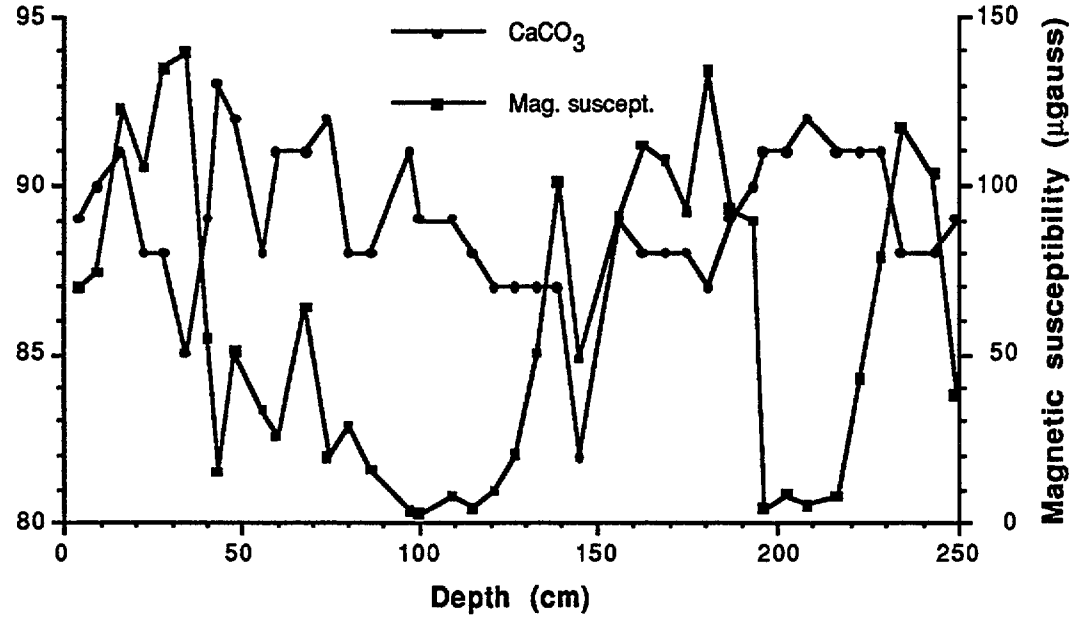

FIGURE 23. Plot of $CaCO_3$ (%) and magnetic susceptibility (μgauss) against depth (cm) for 102GC17.

SUMMARY

These preliminary results show the margin sediments are rich in calcium carbonate, indicating that biogenic input dominates over terrigenous input in this part of the continental margin. Porosity, bulk densities, and grainsize contents are typical of sediments dominated by *in situ* biogenic debris. Detailed downcore profiles of calcium carbonate content and total magnetic susceptibility show significant variations in these cores, indicative of variations in both biogenic and terrigenous inputs and hence of glacial/interglacial variations in the supply of terrigenous and biogenic sediments. These results are preliminary and will be used to select samples for carbon and isotopic analysis to define glacial and interglacial periods.

6.4 AREA D: GEOCHEMICAL SIGNATURES OF SOUTHERN OCEAN MAGMATISM

Dredging of ocean crust basalts from south of Australia provides the unique potential to address significant questions concerning the composition and organisation of mantle reservoirs supplying ridge basalts during continental break-up and seafloor spreading. In particular, it has been proposed that the area south

of the Great Australian Bight contains the only known boundary between mantle convection cells, and that the region should record whether the major change in seafloor spreading rates at about 45 Ma was associated with compositional variation of erupted basalts.

6.4.1 GEOCHEMICAL AND ISOTOPIC SIGNATURES OF SOUTHERN OCEAN MAGMATISM R. Lanyon and A.J. Crawford (Department of Geology, University of Tasmania).

BACKGROUND AND AIMS:
Dredging of oceanic crust during the Southern Margins cruise 102 of the *Rig Seismic* included four sites (102DR09, 102DR10, 102DR11, and 102DR13) south of the western Great Australian Bight (Fig. 24). Dredge site locations were chosen in an attempt to derive information about the Australian-Antarctic Discordance (AAD), a unique feature of the global mid-ocean ridge system, in order to ultimately enhance our understanding of the orientation and longevity of mantle reservoirs supplying the Southeast Indian Ridge (SEIR) during the opening of the Southern Ocean. The discordance is an approximately 500 km wide, anomalously deep, morphologically and geophysically complex region of the SEIR, south of the western Great Australian Bight between 120°E and 128°E at a latitude of 48°S to 51°S (e.g. Weissel and Hayes, 1971, 1974). It is thought to be a unique mid-ocean ridge feature associated with postulated downward convective flow within the upper mantle producing depression of lithospheric isotherms beneath this region; it has therefore been termed a mantle "cold-spot" (Hayes and Conolly, 1972; Menard, 1973; Weissel and Hayes, 1974).

Previous isotopic studies of zero-age basalts within and adjacent to the AAD indicate the presence of a unique and abrupt isotopic boundary located within a 40 km wide zone of the eastern AAD (Klein et al., 1988; Pyle et al., in press). Within this region, Pb, Sr and Nd isotopic values of the basalts change from those of typical Indian Ocean MORB in the west to values typical of Pacific and north Atlantic MORB to the east. The former is characterised predominantly by more radiogenic $^{207}Pb/^{204}Pb$ and $^{208}Pb/^{204}Pb$ at a given $^{206}Pb/^{204}Pb$ value, as well as more radiogenic $^{87}Sr/^{86}Sr$ and lower $^{143}Nd/^{144}Nd$ values compared to Pacific and north Atlantic MORB. It is therefore inferred that this isotopic boundary represents the site of convergence of two mantle convective cells, each a separate mantle reservoir. Two hypotheses can be proposed to explain the longevity of this isotopic boundary at its present position beneath the AAD:

1. The first hypothesis suggests that the geophysical and morphological features of the AAD are intimately associated with the existence of the isotopic boundary, possibly supporting a model of direct convergence, whereby an eastern convective regime continually feeds Pacific Ocean mantle to the AAD from the east while a western convective domain continually feeds Indian Ocean mantle to the AAD from the west (Klein et al., 1988). The isotopic boundary may therefore represent the site where the limbs of two convective regimes, each a separate mantle reservoir, converge and descend into the mantle. This idea of a stationary Indian-Pacific

mantle cell boundary beneath the AAD is supported by the fact that the discordance forms the central and most pronounced area of a 2000 km wide morphotectonic depression which extends from the southern half of Australia through the Southern Ocean to Wilkes Land, Antarctica, and appears to have been in existence at least since the commencement of Australian-Antarctic rifting (Veevers, 1982).

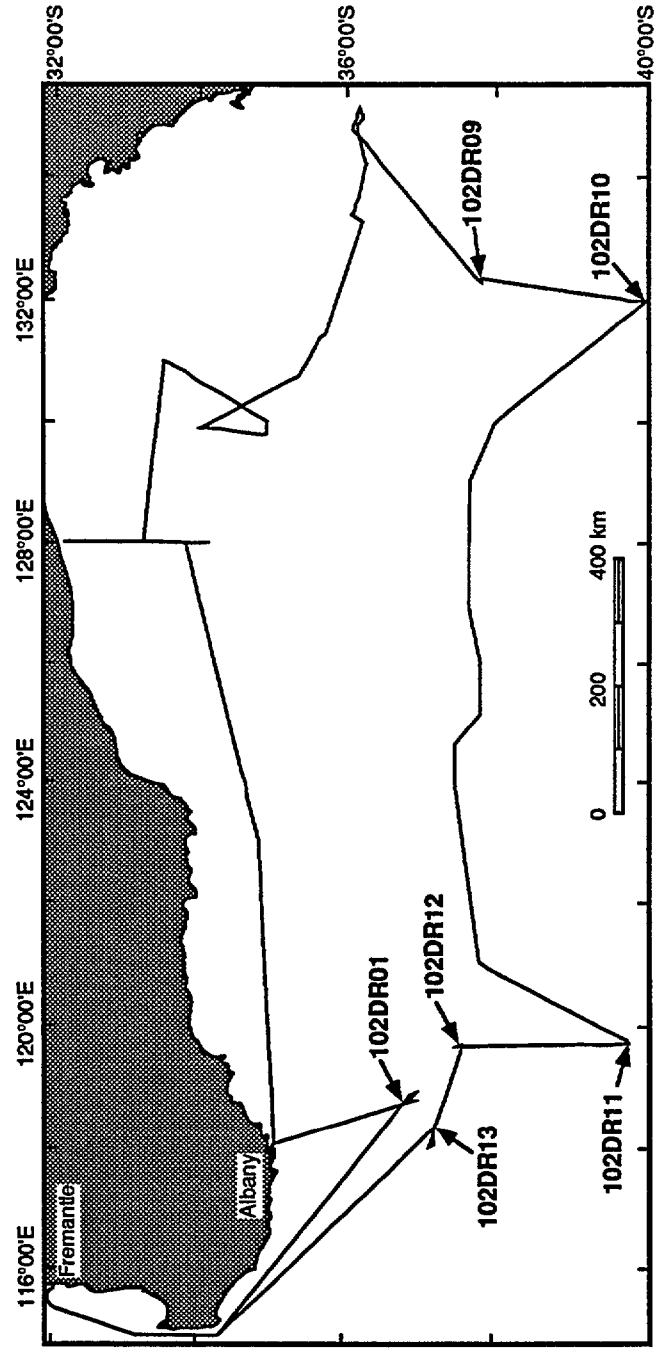

FIGURE 24. Location of Area D dredge sites in the Great Australian Bight.

2. The second hypothesis involves a proposed westward migration of Pacific Ocean mantle as a direct result of Australian-Antarctic rifting and the opening of the Southern Ocean, with the present "front" of invading Pacific mantle being located at the isotope boundary in the AAD. This stems from the idea that if convection within the Pacific Ocean mantle was bounded by deep continental roots, the opening of the Southern Ocean may have produced one of the few unobstructed pathways for communication between Pacific and Indian Ocean mantle convective regimes. The morphology of the large scale residual negative depth anomaly, dominating the discordance area (Marks et al., 1990), supports this idea. This depth anomaly, which appears to have persisted for at least the last 30 Ma, is arcuate in shape, roughly symmetrical about the Southeast Indian Ridge, and oblique to the spreading direction. Two prominent lows associated with 15 Ma-old crust on either side of the ridge indicate that although the source has varied in strength, it has remained positioned at the ridge axis for at least this length of time. The arcuate shape of the depth anomaly suggests a westward migration of the source along the ridge axis with time. This could therefore indicate that, as the South Tasman Rise separated from Antarctica somewhere between ~42 to 36 Ma, a wedge-shaped "front" of Pacific mantle pushed its way westwards into the Southern Ocean. This proposed westward migration of the isotope boundary is supported by the work of Pyle et al. (in press), who found that basaltic glasses from ~3 to 4 m.y. old seafloor south of the eastern ridge segment within the discordance have Indian Ocean Pb, Sr, and Nd isotopic signatures, whereas lavas dredged from the ridge axis directly to the north have Pacific MORB isotopic values. Their conclusion, that the isotopic boundary has migrated ~100 km westward during the last 3 to 4 Ma, requires a Pacific mantle migration rate of ~25 mm/year. This hypothesis of steady westward Pacific mantle flow implies that the isotopic boundary only recently arrived beneath the AAD, and is not directly related to the long-standing geophysical and morphological features of this region.

We intend to analyse a total of 17 rocks, including samples from each of the four dredge sites, for whole rock major and trace element geochemistry, 13 of which will also be analysed for Pb, Sr and Nd isotopes at the Research School of Earth Sciences, A.N.U. This analytical work is aimed at answering two main questions concerning this unique region of the Southern Ocean:

1. How long has the Pacific-Indian Ocean isotopic boundary persisted at its current location beneath the AAD? If the isotopic boundary has been migrating progressively westwards since the South Tasman Rise separated from Antarctica, rocks dredged on either side of the AAD would be expected to have Indian Ocean MORB isotopic signatures. However, if the isotope boundary has always maintained its current position, rocks from the eastern dredge sites (102DR09 and 102DR10) would yield a Pacific/Atlantic Ocean MORB signature whereas rocks from the western sites (102DR11 and 102DR13) would have an Indian Ocean MORB isotopic signature.

2. Was the dramatic increase in seafloor spreading rate between Australia and Antarctica at ~43 Ma accompanied by any changes in the isotopic composition of

the basalts erupted at the spreading centre? Two of the Southern Ocean dredge sites (102DR10 and 102DR11) were located on oceanic crust less than 38 Ma old (ie. south of anomaly 13) on either side of the discordance. The two northern dredges (102DR09 and 102DR13) were originally intended to be located within crust older than ~45 Ma (ie. north of anomaly 19), but the Diamantina Fracture Zone impeded on our siting of the western site, pushing it further south than originally planned. The latitudinal locations of the four dredge sites were chosen in order to attempt a comparison between the geochemical and isotopic composition of basalts erupted prior to ~45 Ma, during a period of ultra-slow seafloor spreading between Australia and Antarctica (<10 mm/year - full rate), with those erupted at the southern sites after the dramatic increase in seafloor spreading to ~60 mm/year at ~43 Ma, coincident with changes in spreading direction on the Southwest and Central Indian Ridges, and the change in spreading direction of the Pacific plate. Although it is already possible to study the compositions of MORB erupted during both rapid and relatively slow rates of seafloor spreading along different ridge axes, for example the fast-spreading South Pacific Rise (~120 mm/year) and the slow-spreading Mid-Atlantic Ridge respectively, the Southeast Indian Ridge provides us with an opportunity to study the effects of different spreading rates on basalts erupted through time from a single spreading centre.

GEOLOGICAL RESULTS:
The following description of rocks recovered from Area D is predominantly based on shipboard hand specimen descriptions, augmented by petrographic descriptions from thin sections prepared on board ship. Additional short petrographic descriptions are included for samples chosen for whole-rock geochemistry and/or radiogenic isotope analyses.

102DR01:
Latitude: 36°51.45'S
Longitude: 118°46.19'E
Water Depth: 5090 m
All samples have the prefix 102DR01

Total dredge recovery consisted of manganese nodules which have been subdivided into three main types:

1. The most abundant type (~90 to 95%) comprises spherical nodules, 7-12 cm in diameter, with dull black to dark-brown, uneven, "nobbly" outer surfaces. Cream to brown coloured friable clay material tends to infill irregularities and form a thin uneven layer on the outer surface of many nodules. Smoother surface textures, where present, appears to have resulted from some degree of exfoliation.

In terms of their internal structure, these nodules can be further subdivided into three groups:
1A) In cross-section most nodules have no obvious central nucleus. Reddish-brown to black microcrystalline Fe-Mn oxide material forms a dendritic pattern radiating out from the approximate centre of the nodule. Unconsolidated clay

material is disseminated through the nodule, particularly infilling the gaps between the ends of the dendrites which themselves produce an outer irregular nodule surface.

1B) A small number differ from type A in that they have a visible central nucleus comprising either a shell fragment (found in only two nodules) or, more usually, a mm-sized "clump" of clay material. Fine alternating laminations of soft brown to black Fe-Mn oxide material, <1 mm to 1 mm thick, form concentrically ringed bands up to ~0.5 cm around the nucleus. In a very few nodules, two to three of these ringed nuclei are themselves ringed by a band of concentrically laminated Fe-Mn material. Where the layering includes unlithified clay material, the latter tends to form more irregular and often discontinuous layers.

1C) A minor number of nodules with no discernible nucleus also lack dendritic structures. In cross-section, these nodules have a speckled appearance with mm-sized "nobbly" spheroids of black Fe-Mn oxide material surrounded by cream-brown clay.

The majority of these spherical nodules have an outer dark-brown to black, cm-wide, finely laminated crust of microcrystalline Fe-Mn oxides. Laminations may be either regular and concentric or convoluted and interspersed with minor amounts of clay material. This outer band appears to be the result of reactivation of deposition on the external surface of an already formed nodule, the latter being characterised by either an irregular"nobbly" layer (surrounding an internal dendroidal structure) internal to the laminated outer case, or an inner dark laminated band representing a previous outer nodule crust.

2. Approximately five percent of the nodules recovered are larger, up to 25 cm across, and more irregular in shape. These "mixed" nodules are generally composed of a number of type 1 nodules which appear to have completed their growth prior to incorporation into the larger structures. Evidence of later manganese dendritic growth and layering around the smaller type 1 nodules indicates that the latter may have acted as nuclei for irregular secondary Mn growth. Unlithified clay material is dispersed throughout the resulting structure, possibly acting as a "cementing" agent in places. These manganese and clay amalgamations sometimes have outer thinly-laminated crusts up to 1 cm thick. Several generations of growth are therefore implied.

3. Small black botryoidal manganese nodules, whose individual spheroids measure up to 2 cm in diameter, are only a very minor component.

The pipe dredge component is comprised of light cream to brown foraminifer-nannofossil clayey ooze. It contains fine to coarse grained, subangular to subrounded, Fe-stained quartz sand; phosphatic grains; sponge spicules; foraminifer and echinoid debris, and organic debris.

102DRO9:
Latitude: 37°46.87'S - 37°48.78'S
Longitude: 132°19.98'E - 132°17.59'E
Water Depth: 5550 - 4940 m
All samples have the prefix 102DRO9

1. Ten percent of recovery comprises manganese nodules, with diameters of 4 to 10 cm, similar to some of those described from dredge 01. They are therefore classified here as for the first dredge, with only major differences described.

1A) This is the most common type present. Approximately 50% of these nodules have an irregular dark Mn ring, probably representing a reactivation surface, enclosing a central dendritic Mn pattern. More Mn dendrites radiate out from this surface and are themselves enclosed by an outer hard "nobbly" shell of Mn and Fe material up to 0.5 to 1 cm thick. Outer surfaces are generally smoother than for the previous dredge.

1B) Spherical Mn nodules have nuclei of unconsolidated cream to brown clay material generally less than 1 cm in diameter. Nuclei are usually not ringed (as in 102DR01), many having only one thin outer ring of Mn surrounded by radiating dendrites. A small number of these nodules are irregular to elongate in shape, measuring ~4x1 cm.

One nodule is possibly a smaller version of a type 2 nodule, comprising two spherical type 1B) nodules joined by a common 0.5 cm wide Mn crust. No type 1C) or 3) nodules were recovered.

2. Thirty percent of the haul is made up of Mn-rich mudstones. These rocks vary greatly in shape; over 25% are tabular or elongate, ~50% are irregular in shape, and the remainder are subrounded. They range in size from approximately 18x12 cm down to 7x1.5 cm, with an average size of 8x5 cm. Most have an outer Mn coating up to several cm thick which is rough and porous, while yet others are coated with friable yellow (10YR8/6) mud. Internally, they are composed of black Mn-rich material and yellow unaltered mud. The larger rocks have yellow mud on both their upper and lower surfaces and a centre of Mn-rich material, while a small proportion of the smaller rocks display the opposite relationship. While most of the rocks exhibit irregular layering of these two materials, a minor proportion have a "dendritic" pattern of yellow mud radiating from the lower or central part of the rock. The mineralogy is predominantly soft, porous manganese plus up to thirty percent ?authigenic, non-calcareous mud.

3. 50% of the dredge haul consists of large rounded and tabular boulders (10 to 36 cm long x 15 cm thick) of laminated pelloidal grainstone/packstone composed of olive (5Y5/4) and brown (7.5YR5/6) pelloids in a very pale brown (10YR8/4) matrix. Concentrically-zoned angular to subrounded clasts, up to 1.6 cm in diameter, others of which are tabular and elongate, have mostly nucleated around intraclasts of pinkish siliceous ooze and occasionally around basalt grains.

Concentric zonation around nuclei is defined by the alternation of light green and darker red-brown authigenic minerals. Inter-granular pores are filled with a fine-grained green authigenic mineral and pinkish-cream siliceous ooze. Disseminated flecks of fine to coarse grained Mn material are scattered throughout the rock, and thin dendritic stylolitic seams of Mn (0.1 to 0.3 cm thick) are not uncommon. Manganese also occurs as a 0.1 to 2.5 cm thick, laminated crust on outer rock surfaces, commonly bored by small (0.1 to 0.5 cm diameter) meandering horizontal to subvertical Mn-encrusted tubes. Bedding is defined by subhorizontal alternations of pelloid-rich and matrix-rich laminations and by both grain size variations and compositional changes within the grainstone layers. Grainstone laminae are continuous to discontinuous and range in thickness from 0.2 to 3 cm. More matrix-rich packstone layers show a decrease in layering with "pockets" of pelloidal debris interspersed and floating in a fine-grained matrix. Sedimentary structures include normal grading, burrow mottling, and possible imbrication. Fractures up to 12 cm deep are infilled with matrix-rich packstone.

Interpretation: The presence of authigenic precipitates, pelloidal intraclasts, size-sorted and winnowed accumulations, filtered pelagic oozes, sedimentary cementation, fracturing and fracture infill as well as boring and Mn encrustation indicates a complex depositional history and an environment subject to episodically fluctuating bottom current conditions and generally low sedimentation rates. The calcareous-poor composition is probably a function of depth, being deposited below the CCD.

4. Ten percent of recovery comprises basalt which can be subdivided into three main types:

4A) (5%) One fine-grained, slightly vesicular (<5%), grey rock, ~10x7x6 cm, has a thin outer coating of Mn and clay material up to 0.3 cm thick. This basalt has a slightly glomeroporphyritic texture with 1 to 2% plagioclase phenocrysts, up to 2 mm long, forming glomerocrysts (clots). The groundmass is composed predominantly of - oriented plagioclase laths with an average length of 0.2 mm. Occasional clots of groundmass plagioclase appear to form radiating structures. The remainder of the groundmass comprises stubby clinopyroxene (probably augite) crystals (<0.1 to 1 mm long), finely disseminated and skeletal Fe-oxides, and possibly minor subhedral olivines (<0.1 mm). A subophitic texture is evident in some areas of groundmass with clinopyroxene crystals partially enclosing plagioclase laths. Clay (?smectite) occurs as thin layers lining and infilling subspherical to spherical vesicles, as well as forming irregular to "subhedral"-shaped "clumps", possibly after olivine.

Petrographic Description: 102DR09-4A:
This is a fine-grained, slightly vesicular, plagioclase-phyric dolerite with scattered phenocrysts and glomerocrysts of plagioclase up to 2 mm across. Anhedral to subhedral clinopyroxene crystals are either intergranular to, or subophitically enclose, plagioclase laths ~0.1 to 0.2 mm long. Clots of smectite and skeletal to finely disseminated Fe-oxides are abundant and intergranular to plagioclase.

4B) (60%) Vesicular (5 to 10%), light grey, porphyritic basalt contains phenocrysts of both plagioclase (laths up to 1 mm long) and subhedral to euhedral olivine (up to ~0.4 mm in diameter), often forming glomerocrysts. The groundmass is composed predominantly of plagioclase laths, subhedral clinopyroxene crystals, and Fe-oxides with an average grain size of 0.05 to 0.1 mm. Vesicles are generally spherical, <1 mm to 2 mm in diameter, and occasionally lined with a thin layer of clay material (probably smectite). Fresh rock tends to be surrounded by 1 to 2 cm wide rims of slightly darker weathered material rich in smectite. Where fractures through the rocks connect outer surfaces, several "cores" of fresh basalt, completely enclosed by weathered rims, may occur within one sample. Outer rinds of Mn and clay material range from ~1 mm to 3 cm in thickness.

Petrographic Description: 102DR09-4B1:
This is a slightly vesicular, sparsely glomeroporphyritic, quenched basalt. Subhedral to euhedral phenocrysts of clinopyroxene (up to ~0.5 mm) and elongate plagioclase crystals (up to 0.8 mm) may occur individually or form glomerocrysts, scattered throughout a fine-grained (<0.01 to 0.1 mm) groundmass of plagioclase, clinopyroxene, skeletal Fe-oxides and clay. Groundmass plagioclase laths are often subophitically enclosed by anhedral to subhedral clinopyroxene crystals. Small spherical vesicles are infilled with smectite.

Petrographic Description: 102DR09-4B2:
This plagioclase-phyric, slightly vesicular quenched basalt has phenocrysts of plagioclase up to ~1.5 mm long, occasionally forming monomineralic glomerocrysts. The groundmass is dominated by plagioclase laths, ~0.3 mm long, many of which are columnar and infilled with clinopyroxene, forming an intrafasciculate texture. Groundmass clinopyroxene may also be interstitial to, or subophitically enclose, plagioclase. Abundant fine, skeletal Fe-oxides, up to 0.01 mm long, are also interstitial to plagioclase.

Petrographic Description: 102DR09-4B4:
This is a quenched, plagioclase-phyric basalt comprising randomly-orientated plagioclase crystals, 0.02 to 0.2 mm long, which are often columnar and infilled with finer groundmass material including clinopyroxene, finely disseminated to skeletal Fe-oxides and alteration material. Glomerocrysts of clinopyroxene and/or plagioclase (up to 2 mm) and phenocrysts of plagioclase (up to ~1.8 mm) are relatively rare. Vesicles are lined or infilled with smectite.

Petrographic Description: 102DR09-4B5:
This is a relatively fresh, plagioclase-clinopyroxene-phyric, vesicular basalt comprising rare plagioclase phenocrysts (~0.5 mm) and glomerocrysts of plagioclase and clinopyroxene. The groundmass consists of 0.01 to 0.02 mm subhedral clinopyroxene crystals, plagioclase laths up to 0.1 mm long, and finely disseminated Fe-oxides.

4C) (35%) Light grey basaltic rocks with obvious reddish-brown "globular" Fe-staining on cut surfaces have 0.5 to 1 cm thick weathered outer rims of Fe and Mn material. This rock type is dominated by bundles of radiating plagioclase laths, ~0.5 to 1.2 mm in length, with interstitial Fe-oxides and Fe-stained material. The latter also infills hollows in columnar plagioclase crystals. Abundant smectite lines and infills spherical vesicles (5 to 10%) up to ~0.3 mm in diameter. "Clumps" of smectite and ?calcite possibly replace olivine phenocrysts (up to 0.5 mm diameter). The predominance of alteration material in this rock precludes the positive identification of any other minerals that may be present.

Petrographic Description: 102DR09-4C:
This altered, slightly vesicular quenched basalt is dominated by spherulitic bunches of diverging plagioclase and altered clinopyroxene needles up to ~1.5 mm in length. Interstices are occupied by finely divided Fe-oxides and smectite. Olivine phenocrysts, up to 0.5 mm, are completely altered to Fe-stained smectite and calcite. Fe-stained, elongate to feather-like structures may represent altered quenched olivines, although they often cross-cut the spherulites and may therefore be secondary features. Spherical vesicles are lined or infilled with smectite.

The pipe dredge component comprises greyish brown (10YR5/2) and light grey (10YR7/2) siliceous ooze containing quartz silt, Mn flakes, organic material, rare foraminifer debris and sponge spicules, silt- to mud-sized siliceous grains, possible mica flakes, red-brown clay aggregates, and minor nannofossil debris.

102DR10:
Latitude: 39°55.28'S - 39°55.34'5S
Longitude: 131°58.59'E - 131°58.61'E
Water Depth: 5567 - 5241 m
All samples have the prefix 102DR10

1. Seventy-five percent of the dredge haul consists of coarse-grained igneous rock. Although most of this rock type is very weathered, one less weathered boulder was recovered. Cut surfaces are a bluish-green colour and the rock consists predominantly of coarse grained plagioclase and clinopyroxene (?augite). Interlocking plagioclase crystals, up to 5 mm in length, are often very ragged and cracked in appearance. In places, only the skeletal remains of plagioclase crystals are visible due to radiate intergrowths of plagioclase and clinopyroxene. Large clots of plagioclase are quite common. Coarse clinopyroxene grains are generally only recognisable by an occasional unaltered core surrounded by very fine grained alteration products pseudomorphing the crystal shape. Alteration material does include some orange-brown Fe staining (more prevalent in the very altered rocks), although it consists predominantly of very fibrous, highly birefringent, green mineral/s - ?serpentine and/or chlorite. Thin veins of more coarsely fibrous green material cut through many plagioclase crystals. Skeletal opaques are a common feature.

One 3 to 4 mm wide elongate area of the rock, dominated by much finer grained,

more irregularly shaped plagioclase grains (<0.1 to 0.6 mm) and fine fibrous material, has a very "broken-up" appearance due to the variability of crystal size and shape and the often angular appearance of the plagioclase crystals. Occasional ?late-stage felsic veining is a rare feature (found in only one rock).

These rocks are conditionally described as (?serpentinised) gabbro, based on their observed mineralogy and grainsize.

Petrographic Description: 102DR10-1B:
This olivine-clinopyroxene-plagioclase gabbro has a coarse consertal texture and an average grainsize of ~3 to 5 mm. Cracked, anhedral olivines, rimmed with clusters of fine Fe-oxides, have varying degrees of alteration, predominantly manifested by Fe-staining along crystal partings. The remainder of the rock comprises anhedral clinopyroxene crystals, displaying varying degrees of uralitisation, plagioclase laths with irregular interlocking boundaries, and coarse-grained Fe-oxides.

Petrographic Description: 102DR10-1C:
This is a greenschist metagabbro comprising coarse-grained, ~4 to 5 mm, interlocking clinopyroxene, plagioclase, and Fe-oxide crystals. Although clinopyroxene crystals are altered to varying degrees by a combination of chlorite and fibrous green amphibole, fresh crystal cores are still visible. Twinning is quite a common feature of the anhedral to subhedral clinopyroxene crystals.

2. 10% of recovery consists of variously sized and shaped, poorly-sorted, conglomeritic rocks with thick "nobbly" cases of thinly laminated dark-brown to black Mn and Fe material. Angular bluish clasts of 102DR10-1 and finer grained igneous rock (102DR10-3), 1 to 40 mm across, bound together by fine yellow (10YR8/6) friable clay, have an outer irregular Mn coating up to 2 cm thick. The outer coat has itself incorporated fine angular igneous clasts, 1 to 5 mm across, and finely disseminated yellow clay. The proportions of igneous material and clay are variable; some rocks having very few clasts are composed almost totally of yellow clay flecked with fine grained manganese.

The angularity of the clasts and the lack of sorting tends to indicate that very little reworking occurred prior to the deposition of clay material and manganese.This is supported by the fact that the clasts are identical to the other rock types recovered from this dredge, indicating that little, if any, sediment transport occurred. As a number of small clasts have been incorporated into the Mn layers, some bottom current activity seems likely and possibly more than one phase of Mn deposition may have occurred.

3. 15% of recovery consists of fine-grained igneous rocks, most of which are mafic (except 102DR10-3D), and which are probably altered basalts. These rocks can be subdivided into five main categories of approximately similar proportions:

3A) Light greenish-grey, mafic, porphyritic rock is composed predominantly of

plagioclase phenocrysts (up to 50% of rock) occurring as both irregularly-shaped crystals and elongate laths up to 4 mm in length. Some plagioclase grains display oscillatory zoning, and many clot together to form glomerocrysts. Subhedral clinopyroxene (probably augite) phenocrysts, up to 2 mm across, and euhedral to subhedral olivines, up to 0.8 mm, partially enclose plagioclase laths in places thereby displaying a subophitic texture. One example of radiate intergrowth of plagioclase and clinopyroxene is visible in thin section. Clinopyroxene and olivine are often closely associated.

The groundmass is composed predominantly of alteration material including chlorite and a grey ?clay mineral (similar in appearance to sericite), both of which have a somewhat fibrous appearance and provide the general colour of the rock. Some of the plagioclase laths and smaller olivine crystals appear to be rimmed by the alteration minerals. Small plagioclase crystals plus variably shaped opaques (<0.1 to 1 mm across) and finely disseminated opaques are also present in the groundmass.

Petrographic Description: 102DRI0-3A:
This rock is a greenschist, plagioclase-phyric, porphyritic dolerite. Plagioclase phenocrysts (up to 3 mm) range from anhedral, zoned crystals to elongate laths with partly resorbed rims and may form scattered glomerocrysts ~2 to 3 mm across. The groundmass is dominated by 0.2 to 0.3 mm long plagioclase laths, many of which form hollow, columnar crystals infilled with pyroxene. The latter is often partially altered to fibrous amphibole and may subophitically enclose plagioclase. Fe-oxides are also scattered throughout the groundmass.

3B) Fine grained, porphyritic, greenish-grey rock has a finely speckled appearance in hand specimen due to variously shaped and scattered individual crystals and clots of an opaque mineral up to 1.5 mm across. Glomerocrysts composed of individual tabular plagioclase crystals, up to 1.2 mm long, are responsible for the porphyritic texture of the rock. Undulose extinction, oscillatory zoning, and ?sericitic alteration are features of at least some plagioclase crystals. Possible micro-antiperthitic texture present in some of the feldspars.

The groundmass is composed predominantly of flaky alteration material including ?sericite and chlorite. Chlorite may be secondary to olivine and/or pyroxene as it often appears to pseudomorph subhedral to euhedral crystal forms, and sometimes rims ragged clinopyroxene crystals.

3C) This is another fine grained, grey, mafic porphyritic rock. Phenocryst phases include plagioclase, clinopyroxene and olivine. Plagioclase phenocrysts occur as both laths and more ragged crystals up to 4 mm long. Some display oscillatory zoning, and many have elongate cracks infilled with groundmass-type alteration material. Clinopyroxene (?augite) phenocrysts are generally subhedral, up to 3 mm across, and commonly twinned. Both plagioclase and clinopyroxene phenocrysts have inclusions of smaller plagioclase laths and are commonly closely associated, forming glomerocrysts up to 5 mm in size. More than one

generation of plagioclase formation is therefore implied. Olivine is a less common phase, occurring as scattered 0.4 to 0.9 mm crystals with brownish (?iddingsite) alteration infilling cracks. Plagioclase laths are also embedded in rare subspherical cracked patches of fine grained ?carbonate rimmed with fibrous clay (possibly smectite). These patches may be secondary to olivine.

The groundmass is composed predominantly of plagioclase laths (0.5 to 0.9 mm long), opaques (<0.1 to 0.2 mm), and greenish fibrous alteration material, probably chlorite and clay. Clumps of this secondary material often appear to surround crystalline cores of ?groundmass clinopyroxene.

3D) This fine grained, greenish-grey rock is composed predominantly of quartz and chlorite. Patches of quartz may be several mm across, comprising individual grains displaying undulose extinction, triple junctions, and interlocking serrated grain boundaries. The quartz appears to have been recrystallised. Chlorite occurs in two distinct forms: as large single flakes ~0.8 mm across, possibly pseudomorphing an earlier mineral phase; and as much finer grained material. Patches of reddish-brown Fe-staining and opaque mineral grains, up to 0.9 mm across, are also common features of this rock.

3E) This fine grained grey mafic rock is very similar to 102DR10-3C in both its texture and mineralogy, although glomerocrysts are less abundant in this rock whereas individual phenocrysts appear to be more common. This is possibly another version of 102DR10-3C.

Petrographic Description: 102DRl0-3E:
This porphyritic rock has a groundmass of plagioclase laths (0.1-0.3 mm long, subophitically enclosed by clinopyroxene (the majority of which is altered to amphibole), and fine Fe-oxides. Plagioclase phenocrysts, 3 to 4 mm long, are zoned and partly resorbed. Anhedral to euhedral clinopyroxene phenocrysts, up to 1.5 mm, are often twinned and may have rims of amphibole. Completely altered olivine phenocrysts, up to ~1.5 mm, and glomerocrysts of plagioclase, clinopyroxene and altered olivine are also scattered through the rock.

Petrographic Description: 102DR10-4:
This is a hornblende-bearing gabbro, very similar to sample 102DR10-1C but with hornblende occurring either as discrete crystals or as inclusions within altered clinopyroxenes.

The pipe dredge component consists of brown (10YR5/4) siliceous ooze containing abundant siliceous fragments, quartz grains, red-brown clay aggregates, Mn flakes and minor organics.

102DR11:
Latitude: 39°45.92'S - 39°46.75'S
Longitude: 119°46.02'E - 119°44.70'E
Water Depth: 5240 - 5050 m
All samples have the prefix 102DR11

1. 90% of recovery consists of manganese nodules. 80% of these nodules are spherical with outer dark-brown to black, dull, uneven "nobbly" Mn- and Fe-rich cases. Nodule diameters range from 7 to 19 cm, although there are two main size subdivisions - 7 to 9 cm diameters and 15 to 16 cm diameters. They have soft, yellow (10YR8/6), Mn-flecked clay nuclei which vary greatly in both size (up to 12 cm across) and shape. Nuclei are generally surrounded by thinly laminated and convoluted manganese layers which sometimes incorporate disseminations and patches of yellow clay and form outer irregular crusts up to several cms thick.

Approximately 10% of nodules are subspherical, up to 26 cm across, and comprise "clumps" of yellow clay interspersed with dark Mn material, some of which forms a slightly dendritic pattern. Most are then surrounded by an outer, irregularly laminated Mn crust, several cms thick, although one rock has only half its outer surface coated with manganese.

5% of the nodules are more irregular in shape, with very irregularly shaped to elongate nuclei, possibly shell fragments or shell cross-sections up to 6x0.5 cm, surrounded by laminated manganese and disseminated friable yellow clay. One subspherical nodule has an irregularly shaped white central nucleus ~6 cm across, which does not react with dilute HCl and appears too soft to be silica - possibly dolomite.

Two to five percent lack any visible nuclei and are similar to the "speckled" type 1C) nodules of dredge 102DR01. These nodules are distinctive, as compared to the previously recovered nodules from this cruise, in that dendritic Mn patterns are generally absent or at best only very weakly defined (in the occasional larger subspherical sample). Most of the manganese has been deposited as thinly laminated layers and crusts.

2. Ten percent of the recovered material consists of two types of basalt:

2A) (70%) One type consists of elongate- to irregular-shaped boulders and pebbles with a thin coating of dark Mn and Fe-stained material. One rock has several cores of fresh material with 0.5 to 1 cm thick, darker grey weathered rims corresponding to cracks through the rock (similar to the weathering pattern observed in 102DR09-4B). This is a fine grained, grey, glomeroporphyritic basalt containing glomerocrysts (up to 2 mm across) of plagioclase, augite, and olivine set in a groundmass of finely disseminated opaques and brown devitrified glassy material. Average grainsizes vary for the different minerals: plagioclase laths range from 0.1 to 1 mm in length while subhedral pyroxene and olivine crystals average 0.2 to 0.3 mm. Within individual glomerocrysts, plagioclase laths appear to radiate

outwards but elsewhere in the rock these crystals are randomly orientated. A minor amount of plagioclase is represented by less elongate, more stubby and ragged crystals with oscillatory zoning and occasional inclusions of augite. This basalt is only slightly vesicular with spherical unfilled vesicles up to 1 mm in diameter comprising ~5% of the rock.

Petrographic Description: 102DR11-2A:
This is a plagioclase-clinopyroxene-phyric, quenched basalt comprising "clots" of clinopyroxene and plagioclase within a groundmass of devitrified glass and finely divided opaques. Randomly orientated plagioclase laths, 0.2 to 0.3 mm long, may be subophitically enclosed by euhedral to subhedral, 0.01 to 0.05 mm clinopyroxene crystals within the scattered mineral clots.

Petrographic Description: 102DR11-2A(iii):
This sample has a hypocrystalline, quenched texture. It comprises aggregates, up to ~3 mm, of olivine, clinopyroxene and plagioclase within a groundmass of devitrified glass and finely divided opaques. Plagioclase laths, ~0.2 to 1 mm long, may be columnar and infilled with groundmass material and/or subophitically enclosed by clinopyroxene. Clinopyroxene and altered olivine crystals are generally anhedral to subhedral with an average grainsize of 0.2 to 0.3 mm.

Petrographic Description: 102DR11-2A(iv):
This is a vesicular rock with a very similar quenched texture to sample 102DR11-2A.

2B) (30%) The remainder of the basalt recovered comprises one angular rock with a dark-brown, soft, outer coating of Mn up to 0.5 cm thick. This porphyritic, brownish-grey basalt is more altered than the previous sample, with abundant orange-brown Fe-staining and fine yellow clay (?smectite) material. Plagioclase phenocrysts up to 3 mm long, some of which form clots, have a fairly ragged appearance due to their irregular shapes and inclusions/veins of groundmass material. Many also display oscillatory zoning. Cracked patches of orange-brown Fe-stained material, 1 to 1.5 mm across, preserve the remnants of a highly birefringent ?carbonate mineral and are possibly replacing olivine phenocrysts. The groundmass is composed predominantly of alteration products (as described earlier); randomly oriented plagioclase laths with an average length of 0.4 mm, many of which are hollow and infilled with groundmass; finely disseminated opaques; and fine grained, low birefringent ?clinopyroxene which appears to have a branching feather-like crystal structure. Some of these branching crystals are also curved.

Petrographic Description: 102DR11-2B:
This is a porphyritic plagioclase-phyric basalt with phenocrysts of plagioclase and altered olivine. Plagioclase exhibits a continuous range in grainsize from ~0.01 to 8 mm. 0.01 to 0.03 mm crystals are often columnar and hollow, whereas larger grains are characterised by partly resorbed rims and inclusions of groundmass material. Olivine phenocrysts, ~0.05 to 0.25 mm, are altered to Fe-stained smectite. The groundmass comprises very fine-grained Fe-oxides and quenched needles of

plagioclase and clinopyroxene forming an intrafasciculate texture.

The pipe dredge component consists of Mn-flecked, siliceous, dark greyish-brown (10YR4/2) mud and yellow (10YR8/6) clay.

102DR12:
Latitude: 37°28.80'S - 37°35.89'S
Longitude: 119°40.00'E - 119°39.19'E
Water Depth: 5300 - 3961 m
All samples have the prefix 102DR12

Total recovery consists of spherical Mn nodules with diameters ranging from 7 to 12 cm. All have cm wide outer Mn cases although these are generally noticeably smoother than those of previous dredges, possibly due to reworking following formation. Type 1A) (classifications according to dredge 102DR01) nodules are the most common type, although there are several type 1B) nodules with cm-sized, irregularly-shaped clay nuclei. All have dendrites of manganese radiating outwards from the core, except for one speckled type 1C) nodule. In two cases, three to four spherical type 1A) nodules are joined by a common outer Mn case.

102DR13:
Latitude: 37°14.617'S - 37°10.00'S
Longitude: 118°09.35'E - 118°09.35'E
Water Depth: 4480 - 4600 m
All samples have the prefix 102DR13

1. 5% of recovery consists of one large irregular shaped boulder, 19x32x10 cm, with a thin outer coat of manganese 2 to 3 mm thick. This rock is primarily a medium grained, dark grey igneous rock composed predominantly of interlocking plagioclase and altered pyroxene crystals with an average grainsize of 0.6 to 3 mm. Abundant fine grained alteration is visible. This is similar (although not as coarse grained) to 102DR13-6 and it appears to be a gabbroic rock.

A 2 to 5 cm wide "band" (?dyke) of very fine grained, greenish-grey basalt, with sharp but irregular contacts, crosscuts this boulder. This second rock type has a fairly even texture with an average grainsize of <0.1 to 0.1 mm. Mineralogy comprises elongate plagioclase crystals, scattered opaques, and fine pyroxenes, many of which have greenish alteration.

2. 10% of the dredge haul is made up of a coarse, porphyritic, mafic rock type with plagioclase phenocrysts generally comprising 30 to 40% of the rock (up to 60% in some cases). Plagioclase phenocrysts, ranging in size from 0.1 to 1 cm, vary greatly in shape; most are fairly ragged and cracked with rounded grain edges and have a large degree of highly birefringent clay alteration (probably sericite). Inclusions within the phenocrysts comprise smaller plagioclase crystals, groundmass material, and chloritic alteration products.

The fine grained grey groundmass consists of randomly oriented plagioclase laths averaging 0.3 to 0.6 mm in length; opaques and abundant ragged mica flakes displaying green to brown pleochroism (average grainsize of 0.2 to 0.3 mm) which does not appear to be chlorite. The latter may be secondary to pyroxene.

Thin veins of fine grained chlorite, feldspar and a clay mineral, <1 mm to 1 mm thick, traverse the rock, cutting through both the groundmass and the phenocrysts. These veins are a late stage feature. Pink K-feldspar veins tend to cross-cut all features of some rocks and are probably an even later stage phenomenon.

3. 25-30% of recovery consists of variously sized (up to 14x22x13 cm), greenish-grey basalt with abundant late stage felsic veining. The intensity of veining varies from one rock to another, and is extremely pronounced in some samples. On average, the veins are 0.5 cm thick. This is a fairly equigranular rock composed predominantly of plagioclase laths; clinopyroxene altering to chlorite, and another flaky, green pleochroic, ?micaceous mineral; and scattered opaques. Remnant clinopyroxene cores are occasionally visible enclosed by alteration material. Average grainsize is 0.4 to 0.8 mm plus abundant fine flaky alteration products. This rock type has an overall "ragged" appearance in thin section with thin chloritic veining also visible.

Petrographic Description: 102DR13-3D:
This aphyric dolerite comprises plagioclase laths, ~0.l to 0.4 mm long, subophitically enclosed by anhedral clinopyroxene crystals with an average grainsize of ~0.4 mm, and scattered Fe-oxides. Pyroxene is partially altered to chlorite and amphibole.

Petrographic Description: 102DR13-3(iii):
This rock has a very similar texture to sample 13-3D but is slightly coarser-grained and less altered.

4. 5% of the dredge haul is very fine grained grey basalt, lacking felsic veining, which has here been subdivided into the following two types:

4A) Equigranular basalt composed predominantly of randomly oriented plagioclase laths, opaques, and green flaky alteration material, at least some of which is chlorite. The average grainsize is 0.2 to 0.3 mm. Occasional fine grained chloritic veins, with an average width <1 mm, traverse the rock.

4B) This is also a fine grained, relatively unveined basalt but it has a very ragged texture which is somewhat similar, although finer grained, than that of 102DR13-3. This texture is primarily the result of the abundance of the same flaky green ?micaceous mineral (as seen in the previous slides). The average grainsize of this rock is 0.2 to 0.4 mm. Patches of chlorite (distinguishable from the other micaceous mineral by its anomalous interference colours and lack of pleochroism) appears to be secondary to pyroxene, pseudomorphing subhedral crystal shapes in many cases. Occasional "phenocrysts", up to 4 mm across, have a subhedral crystal

shape but are now so altered as to be comprised of patches of various alteration minerals; the original mineralogy is unrecognisable.

5. Two irregularly-shaped Mn- and clay-rich boulders, up to 24x20 cm, make up approximately 10% of recovery. These rocks have alternating bands, 5 to 6 cm wide, of: (i) finely convoluted, laminated, dark-brown to black Mn-Fe material flecked with yellow (10YR8/6) clay and clay patches up to 2 mm; and (ii) dendritically-patterned Mn with disseminated unconsolidated yellow clay, The outer surfaces of these rocks are irregular but are not surrounded by a complete Mn crust of homogeneous thickness (as the manganese nodules from previous dredges are).

6. 10% of recovery consists of two angular boulders, up to 10x23x32 cm, of bluish-green, coarse grained gabbro (similar to 102DR10-1). This rock type consists primarily of finely sericitised, angular, interlocking plagioclase crystals averaging 1 to 4 mm. Some larger crystals have smaller plagioclase inclusions. The rest of the rock consists of a colourless, high relief alteration material, most of which is fine, fibrous and highly birefringent. While some of this mineral is disseminated through the rock, the remainder replaces individual, large, ragged-looking crystals which were probably originally pyroxene and measure up to ~6 mm across. Patches of fine grained, colourless alteration material (low birefringence) are also quite extensive, interspersed with patches of the previously described alteration material, and possibly pseudomorphing crystal shapes in places. There are some possible remnants of clinopyroxene grains visible in amongst all the alteration material.

7. 5% of recovery is made up of fine grained, "speckled", grey basaltic rocks, most of which are fairly tabular. A large proportion of these rocks display extensive orange-brown Fe-alteration plus a small amount of thin felsic veining <1 mm thick. This rock has a fairly even texture. The dominant mineralogy comprises random plagioclase laths, 0.5 to 0.7 mm long, many of which have fine inclusions of groundmass material; abundant subhedral clinopyroxene, 0.3 to 0.4 mm in diameter, some of which are twinned and display evidence of chloritic alteration (which often rims the crystals); altered olivines; and scattered opaques. Some of the slightly larger clinopyroxene crystals partially enclose plagioclase laths producing a subophitic texture.

8. 25-30% of recovery consists of miscellaneous altered rocks which have not been examined in any detail here. The most prevalent type of alteration appears to be hydrothermal, producing purple and yellow veined rocks with outer patchy Mn crusts. Others have extensive felsic alteration and chloritisation. One small soft rock is composed of patches and veins of chlorite, yellow clay and a white fibrous clay mineral - ?kaolinite.

The pipe dredge component comprises dark-brown (7.5YR4/4) siliceous clay and abundant angular grey basaltic pebbles and fragments. The clay contains silt-sized quartz grains, a fine grained orange vitreous mineral, and fine black organic fragments.

SUMMARY:
Although the basalts recovered from each dredge have here been subdivided on the basis of any observed petrographic variations, in terms of their texture, grainsize and mineralogy, they are probably mostly tholeiitic in composition. However, further petrographic and geochemical work is necessary before this can be confirmed. Dredge 102DR10 and 102DR13 basalts are very altered (?serpentinised and chloritised) with respect to those recovered from the other dredges. This is obviously not an age-related phenomenon. The presence of gabbro at both of these sites may be indicative of faulting from depth and late-stage hydrothermal activity is also indicated.

In order to fulfil the previously outlined aims of this dredging program, additional geochemical (major, trace and rare earth elements) and isotopic (Pb, Sr and Nd) analyses need to be performed.

In terms of the first aim, if the proposed isotopic boundary within the AAD has always been located in its present position, dredge 102DR13 basalts would be expected to yield an Indian Ocean isotopic signature while those from 102DR09 should have Pacific Ocean values. However, if the Pacific Ocean convection cell has "nosed" its way into its present position following Australian-Antarctic rifting, both 102DR13 and 102DR09 rocks should possess Indian Ocean isotopic signatures.

The second main aim can also be fulfilled by performing additional geochemical and isotopic analyses. By comparing the data for the younger (102DR10 and 102DR11) and older (102DR09 and 102DR13) crustal basalts, the existence of any relationship between spreading rate variations and magma chemistry can be established. The fact that gabbros have been dredged from both pre- and post-45 Ma crust means that deeper crustal material can also be compared.

Although dredges 102DR01 and 102DR12 were unsuccessful in terms of providing any information about Southern Ocean magmatism, they do confirm the wide extent of Mn deposition on the Southern Ocean seafloor. The material recovered during these dredges may be used in the future to further knowledge about the prevailing conditions and rates of accumulation of seafloor minerals.

6.5 BIOSTRATIGRAPHY OF CRUISE 102 SAMPLES

The results of biostratigraphic analyses of cruise 102 samples are presented as a general report covering all samples (Section 6.5.1 below), and a more detailed analysis of the paleoenvironmental significance of the foraminiferal succession in two cruise 102 cores (102GC08 and 102GC17) and a single cruise 66 core (66GC03), collected from higher on the Ceduna Terrace (see Section 6.5.2 below).

6.5.1 MICROFOSSIL BIOSTRATIGRAPHY -- BMR CRUISE 102 IN THE GREAT AUSTRALIAN BIGHT

S. Shafik (AGSO), N.F. Alley (South Australian Department of Mines and Energy), and B. McGowran (Department of Geology and Geophysics, University of Adelaide)

ABSTRACT

Microfossils from samples obtained on board the *R/V Rig Seismic* during BMR Cruise 102 date the sequence sampled from the Ceduna Terrace in the Great Australian Bight as Late Cretaceous to early Tertiary. Palynofloras suggestive of the early Campanian to late Maastrichtian *Nothofagidites senectus* to *Forcipites longus* Zones, and the late Maastrichtian *Manumiella druggii* Zone were identified in mostly organic-rich siltstones, claystones and mud samples recovered in several dredges and at the bottom of two gravity cores. The sampled unit is probably the Potoroo Formation. Calcareous nannofossil and foraminiferal assemblages extracted from several carbonate samples indicate a sequence ranging in age from Middle Eocene through to Late Oligocene. The sampled sequence consists of the Wilson Bluff Limestone (or equivalent) and younger Oligocene carbonates not known onshore in the Eucla Basin.

The Maastrichtian clastic samples lack calcareous nannofossils and foraminifers, although these fossils were identified previously in lithologically similar coeval samples from sites to the west, between the Eyre and Ceduna Terraces. The marine influence of the Maastrichtian ingression into the nascent Southern Ocean (the Ceduna Transgression of McGowran, 1991) may have rapidly diminished away from its source in the west. The Middle to Late Oligocene assemblages lack the low-latitude nannofossils, *Sphenolithus distentus* and *S. ciperoensis*, recorded previously from carbonates dredged during BMR Cruise 66. This suggests that the excursions of these species into southern Australia were probably short-lived, and occur for only a part of their stratigraphic ranges in the tropics.

INTRODUCTION

The aim of this study is to date sediments recovered during BMR Cruise 102 which sampled the continental shelf and the Ceduna Terrace in the Great Australian Bight. Successful dredging in the Great Australian Bight, mainly the Ceduna Terrace area, during BMR Cruise 66 (Davies and others, 1989), provided the basis for several recent studies which contributed significantly to our knowledge of the Mesozoic to early Tertiary sedimentary record there. Studies of the Maastrichtian to early Tertiary parts of the record are by Shafik (1990), who documented its calcareous nannofossil assemblages, and McGowran (1991) who investigated the foraminifers. The Mesozoic succession has been dealt with recently by Alley and Clarke (1992). Among the more significant results derived from these studies was the discovery of marine Maastrichtian and Oligocene sediments, which are not known in the onshore Eucla Basin.

The nannofossil assemblages pointed to Middle-Late Oligocene warming, based on the presence of the low-latitude key species *Sphenolithus distentus* and *S. ciperoensis*. Whether the warming was a short event, a series of short events, or simply encompassed the whole Middle to Late Oligocene interval, could not be determined fully because of lack of adequate sampling. Only through a speculative analogy with the Otway Basin in southeastern Australia could the presence of *Sphenolithus ciperoensis* in the Great Australian Bight succession be interpreted to be due to a 'short' warm episode; the other key species, *S. distentus*, has not yet been found in the Otway Basin.

Important sampling targets attempted during BMR Cruise 102 were the Mesozoic clastics and the Cainozoic carbonates, but results given below suggest that dredging was not as comprehensive as that achieved during BMR 66.

PALYNOLOGICAL RESULTS

Nine samples were processed and their palynofloras were examined. Age determinations are based on correlation with the palynofloral zones of Helby and others (1987). Attempts are made to correlate the palynofloras with both microplankton and spore/pollen zones, and assemblages with insufficient dinoflagellates are assigned to spore/pollen zones only. Where correlation with a single zone cannot be achieved, a range of possible zones is given. Table 6 summarises the palynological results.

Campanian - Maastrichtian

***Nothofagidites senectus* to *Forcipites longus* Zones** Subsamples 102DR03-1, 102DR03-pipeB and 102DR07-J contain consistent occurrences of *Gambierina rudata*, which makes its first appearance in the upper part of the early Campanian *Nothofagidites senectus* Zone, along with very rare *N. senectus*, the nominate species for the latter zone. *Tubulifloridites (*al. *Tricolporites) lilliei* and *Forcipites (*al. *Tricolpites) longus*, the first appearances of which are used to define the bases of the two succeeding middle Campanian to late Maastrichtian zones (Helby and others, 1987), are absent from these samples. However, *Ornamentifera sentosa* is consistently present. This species is known to have its highest occurrence at the top of the *F. longus* Zone.

Extremely rare specimens of *Tricolporites apoxyexinus* are present in subsamples 102DR03-1 and 102DR07-J. The stratigraphic occurrences of this species are shown to be consistent in the lower part of the Santonian *Tricolporites apoxyexinus* Zone and inconsistent higher up to the top of the Middle Campanian to early Maastrichtian *T. lilliei* Zone (Helby and others, 1987). One specimen of *Triporopollenites sectilis*, a species known to be restricted to the *T. lilliei-F. longus* zonal interval, was found in subsample 102DR03-pipeB.

Thus, bearing in mind that some very rare specimens may have been recycled from older sediments, the most confident conclusion which can be reached is that

from older sediments, the most confident conclusion which can be reached is that the palynofloras may range in age from the upper *N. senectus* to *F. longus* Zones. Such a conclusion is supported by the presence of rare *Beaupreaidites orbiculatus* which is believed to range in age from *N. senectus* to *F. longus* Zones in the Otway Basin (see Dettmann and Jarzen, 1988).

Table 6. Summary of palynological results.

Sample	Palynological zone	Age	Environment
102DR03-1	*Nothofagidites senectus* to *Forcipites longus*	Campanian-Maastrichtian	Marine
102DR03-pipe B	upper *Nothofagidites senectus* to *Forcipites longus*	Campanian-Maastrichtian	Marine
102DR05-1	*Forcipites longus*; upper *Manumiella druggii*	late Maastrichtian	Marginal/ restr. marine
102DR05-2	*Forcipites longus*; upper *Manumiella druggii*	late Maastrichtian	Marine
102DR05-pipe1	*Forcipites longus*; upper *Manumiella druggii*	late Maastrichtian	Marine
102DR07-K	upper *Forcipites longus*	latest Maastrichtian	Marine
102DR07-J	*Nothofagidites senectus* to *Forcipites longus*	Campanian-Maastrichtian	Paralic
102GC26-CC	*Forcipites longus*; upper *Manumiella druggii*	late Maastrichtian	Marginal/ restr. marine
102GC27-CC	upper *Forcipites longus*	late Maastrichtian	Marine

Maastrichtian

***Forcipites* (al. *Tricolpites*)*longus* Zone**. The samples assigned to the *F. longus* Zone (Table 6) may contain consistent occurrences of one or all three species known to be restricted to the interval, namely *Forcipites longus*, *Grapnelispora evansii* and *Quadraplanus brossus* (see Helby and others, 1987). Other species present include *Tetracolporites verrucosus* which ranges from the base of the *Forcipites longus* Zone into the early Tertiary, and *Tubulifloridites lilliei*, *Nothofagidites senectus*, *Tricolporites confessus* and *Ornamentifera sentosa* which disappear at the top of, or within, the *F. longus* Zone. The palynoflora of subsample 102DR07-K is assigned to the upper part of the *F. longus* Zone because of the

presence of *Stereisporites* (*Tripunctisporis*) sp. which is known to first appear late in the *F. longus* Zone.

The age of the palynofloras of 102DR05-1, 102DR05-2, 102DR05-pipeA and 102GC27-CC is late Maastrichtian. Subsample 102DR07-K is latest Maastrichtian in age, based on assignment to the upper *F. longus* Zone.

***Manumiella druggii* Zone**. The base of the *M. druggii* Zone is defined by lowest occurrences of the nominate species, and its top by the lowest occurrence of *Trithyrodinium evitii*. Samples assigned to this zone (Table 6) contain consistent or common *M. druggii* and/or *M. conorata* which is restricted to upper part of the zone. *Trithyrodinium evitii* was not found in the samples. The age is late Maastrichtian (see Helby and others, 1987).

Environment of Deposition

Abundance and diversity of the microplankton species in 102DR05-1, 102DR07-J and 102GC26-CC are generally low, and the low-diversity assemblage in 102GC26-CC is dominated by a single species. This evidence indicates deposition in relatively marginal marine, or restricted marine, environments. The lithologies of these samples, being organic-rich, greyish-brown siltstone/claystone (102DR05-1), semi-consolidated, dark brown mudstone (102DR07-J or 102GC26-CC) support this conclusion. These samples are non-calcareous and lack calcareous nannofossils and foraminifers.

Microplankton species in 102DR03-1, 102DR03-pipeB, 102DR05-pipe1, 102DR05-2, 102DR07-K and 102GC27-CC are relatively more frequent and more diversified than the other samples, suggesting deposition in deeper or more open marine conditions. Lithologically, these samples are similar to 102DR05-1, 102DR07-J and 102GC26-CC. They are dark grey clay with minor silt-sized quartz (102DR03-1), very dark greyish-brown mud (102DR03-pipeB), unconsolidated, greyish-brown, organic-rich mud (102DR05-pipeA), very dark grey to black claystone with minor quartz (102DR05-2), semi-consolidated dark brown mudstone (102DR07-K and 102GC27-CC). They lack calcareous nannofossils and foraminifers.

The age and conditions of deposition suggest that the sediments analysed are correlative with the Potoroo Formation and were deposited during the Maastrichtian ingression into the nascent Southern Ocean (Ceduna Transgression of McGowran, 1991). The palynofloras are similar to those determined from the Potoroo Formation dredged from several submarine canyons in the Bight and Duntroon Basins during BMR Cruise 66 (see Alley and Clarke, 1992).

Maastrichtian Marine Ingression: The sediments recovered during BMR Cruise 66, which were assigned to the late Maastrichtian spore/pollen *Forcipites* (al. *Tricolpites*) *longus* Zone and the microplankton *Manumiella druggii* Zone by Alley and Clarke (1992), were dredged from two main areas in the Great Australian Bight (from a submarine canyon between the Eyre and Ceduna Terraces, and,

from about 500 km to the southeast, in several canyons in the Duntroon Basin). The sediments from the area between the Eyre and Ceduna Terraces were found to also contain late Maastrichtian calcareous nannofossils (see Shafik, 1990) and foraminifers (see McGowran, 1991), but the sediments from the Duntroon Basin lacked these calcareous microfossils. The co-occurrence of nannofossils, foraminifers and dinoflagellates between the Eyre and Ceduna Terraces indicates open marine conditions in the west. The presence of dinoflagellates, without the association of nannofossils and foraminifers, in the Duntroon Basin samples suggests marginal marine or restricted marine conditions in the east. This suggests that the marine influence of the Maastrichtian ingression into the nascent Southern Ocean (the Ceduna Transgression of McGowran, 1991) rapidly diminished away from its source in the west. This conclusion is supported by the lack of calcareous microfossils from the upper Maastrichtian sediments obtained during BMR Cruise 102 which came from either the Duntroon Basin or from an area on the Ceduna Terrace between the two areas sampled during BMR Cruise 66.

Recycled Palynomorphs: Recycled pollen, spores and microplankton are present in all of the palynofloras. These are dominantly Early Cretaceous in age, with lesser frequencies of Early Permian, Jurassic and perhaps early Late Cretaceous palynomorphs. These may provide evidence for the provenance of the Maastrichtian sediments deposited in this part of the Australian-Antarctic rift zone.

NANNOFOSSIL AND FORAMINIFERAL RESULTS

Pre-Quaternary sediments bearing calcareous microfossils are confined to carbonates obtained in dredge haul 102DR07 and vibrocore 102VC11. Dredge haul 102DR07 was collected from the outer margin of the Ceduna Terrace (Lat. 36°08.23' S, Long. 134°53.69'E) at a depth of 4380 m and vibrocore 102VC11 was from the continental shelf in the western Great Australian Bight (Lat. 32°10.00'S, Long. 128°01.52'E) at a depth of 22.2 m. Lithological summary and age determinations based on recovered nannofossil and foraminifer assemblages are given in Table 7.

Eocene Assemblages

Middle Eocene assemblage A. Subsample 102DR07-A was found to contain abundant, moderately preserved, and highly diversified nannofossils. The assemblage includes frequent *Blackites spinulus*, rare *Campylosphaera dela* (displaced from older Eocene), rare *Chiasmolithus expansus*, frequent *C. grandis*, rare *C. solitus*, rare *Clausicoccus cribellum*, frequent to common *Coccolithus eopelagicus*, frequent to common *C. formosus*, common to abundant *Cyclicargolithus floridanus*, common to abundant *C. reticulatus* (two distinct sizes: the larger size, probably an oceanic variety, has a relatively smaller central opening; the smaller size, with relatively large central opening, is usually dominant in hemipelagic sediments), rare *Daktylethra punctulata*, rare *Discoaster barbadiensis*, rare *D. binodosus*, rare *D. deflandrei*, rare *D. saipanensis*, rare to

frequent *D. tanii* nodifer, frequent *Helicosphaera compacta*, *H. heezenii*, rare *H. lophota*, rare *H. seminulum*, rare *Holodiscolithus macroporus*, frequent *Lanternithus minutus*, rare *Markalius inversus*, frequent to common *Neococcolithes dubius*, frequent *Pontosphaera multipora*, rare *Prediscosphaera cretacea* (reworked from Cretaceous source), rare *Pseudotriquetrorhabdulus inversus* (reworked from older Eocene), frequent *Reticulofenestra hampdenensis*, rare *R. scrippsae*, common *R. umbilicus*, frequent *Sphenolithus moriformis*, rare *S. pseudoradians*, rare *Syracosphaera labrosa*, rare *Transversopontis pulcher*, frequent *T. zigzag*, rare *Vekshinella dorfii* (reworked from Cretaceous source), rare *Watznaueria barbnesae* (reworked from Cretaceous source), *Zygrhablithus bijugatus bijugatus*, and frequent *Z. bijugatus crassus*.

The nannoflora of subsample 102DR07-A is assigned to the biostratigraphic datum interval bracketed by the lowest occurrences of *Cyclicargolithus reticulatus* and *Reticulofenestra scissura*, which correlates with a position high in the planktonic foraminiferal P12 Zone (see Shafik, 1983, 1990), at about the middle of NP16 Zone of Martini (1971) or near the base of CP14 Zone of Okada and Bukry (1980). This is based on the presence of *C. reticulatus*, *Chiasmolithus grandis* and other Eocene species (such as *Chiasmolithus solitus*, *Discoaster barbadiensis* and *Neococcolithes dubius*) and the absence of *Reticulofenestra scissura*. The age is Middle Eocene, about 43.5 Ma (Shafik, 1990; see also Truswell and others, 1991).

A similar nannoflora (the 66DR14A(5) *Cyclicargolithus reticulatus* Assemblage in Shafik, 1990), lacking reworked Cretaceous forms, has recently been recorded from the Ceduna Terrace at Canyon J (Spencer Canyon of Jongsma and others, 1991).

The foraminiferal assemblage recovered from subsample 102DR07-A includes *Globigerinatheka index*, *Acarinna primitiva*, *Acarinina* spp., *Subbotina linaperta* and *Pseudohastigerina micra*, suggesting a late Middle Eocene age.

Middle Eocene assemblage B. Subsample 102DR07-B yielded a moderately-preserved nannofossil assemblage which includes rare *Blackites perlongus*, rare *B. spinulus*, rare *B. tenuis*, extremely rare *Calcidiscus protoannulus*, extremely rare *Campylosphaera dela* (displaced from older Eocene), rare *Chiasmolithus expansus*, rare *C. grandis*, rare *C. solitus*, extremely rare *C. titus*, rare *Clausicoccus cribellum*, frequent to common *Coccolithus eopelagicus*, frequent to common *C. formosus*, common to abundant *Cyclicargolithus floridanus*, common to abundant *C. reticulatus* (two distinct sizes), frequent *Daktylethra punctulata*, rare *Discoaster barbadiensis*, rare *D. saipanensis*, rare to frequent *D. tanii nodifer*, frequent *Helicosphaera compacta*, rare *H. heezenii*, rare *H. seminulum*, frequent to common *Lanternithus minutus*, extremely rare *Markalius astroporus*, frequent to common *Neococcolithes dubius*, rare *Pontosphaera multipora*, frequent *Reticulofenestra hampdenensis*, rare *R. scissura*, rare *R. scrippsae*, common *R. umbilicus*, rare *Sphenolithus spiniger*, rare *Transversopontis pulcher*, frequent *T. zigzag*, frequent to common *Zygrhablithus bijugatus bijugatus*, and frequent *Z. bijugatus crassus*.

The nannoflora of subsample 102DR07-B is assigned to the biostratigraphic datum interval bracketed by the lowest occurrence of *Reticulofenestra scissura* and the highest occurrence of *Daktylethra punctulata* which correlates within the planktonic foraminiferal P13 Zone (see Shafik, 1983). This assignment is based on the presence of *Chiasmolithus grandis, C. solitus, Cyclicargolithus reticulatus, Daktylethra punctulata* and *R. scissura*. The age is Middle Eocene, about 43 Ma (Shafik, 1990; see also Truswell and others, 1991).

In terms of Martini's (1971) or Okada and Bukry's (1980) zonations, the nannoflora of subsample 102DR07-B can be placed within the upper part of NP16 Zone or within CP14a Subzone respectively.

The nannoflora of subsample 102DR07-B correlates well with another from the Lacepede Formation of the Otway Basin. The latter represents a marine ingression in the western Otway Basin, following an ingression connected with the onset of the Middle Eocene marine transgression (the Wilson Bluff Transgression of McGowran and Beecroft, 1986) over the onshore Eucla Basin (see Shafik, 1983, 1985).

The nannoflora of subsample 102DR07-B evidently came from a widespread stratigraphic horizon on the Ceduna Terrace, since similar nannoflora were recorded previously from two widely-spaced canyons on the outer Ceduna Terrace (see Shafik, 1990: the 66DR08B and 66DR14A(6) *Reticulofenestra scissura* Assemblages at Canyons F (small un-named canyon of Jongsma and others, 1991) and J (Spencer Canyon of Jongsma and others, 1991), respectively; another similar nannoflora was identified from subsample 102DR07-G.

The foraminiferal assemblage recovered from subsample 102DR07-B is well preserved. Its composition is similar to that recovered from subsample 102DR07-A. The age is late Middle Eocene.

Table 7. Summary of nannofossil and foraminiferal results.

Sample	Comments	Age/correlation	Environment
102DR07-A	Chalk; abundant diversified nannofossils, with rare reworked Cretaceous spp; planktonic foraminifers include *Acarinina, primitiva, Acarinina* spp., *Subbotina linaperta, Globigerinatheka index* and *Pseudohastigerina micra.*	Middle Eocene; equivalent to Wilson Bluff Limestone.	Open marine, neritic.
102DR07-B	Chalk; abundant diversified nannofossils without reworked components; planktonic foraminiferal assemblage as for preceding.	Middle Eocene; equivalent to Wilson Bluff Limestone.	Open marine, neritic.
102VC11, base	Echinoidal-bryozoan facies; poor nannoflora; neritic benthic assemblage (*Cibicides, Gyroidinoides*, etc.); small rare nondescript planktonic foraminifers.	Late Eocene; Wilson Bluff Limestone.	Good access to open sea; neritic.
102DR07-I	Chert and chalk with poorly preserved nannoflora, and common but undeterminable globigerinids	Early Oligocene; probable equivalent to Gambier Lst (upper member).	Open marine, neritic.
102DR07-C and D	Sticky chalk, abundant biogenic silica (opal-A); nannofloras with reworked Eo/ Oligocene species; poor foraminiferal assemblages containing *Subbotina angiporoides, Globorotaloides testarugosa,* small forms of *gemma-juvenilis* group; contaminated by Neogene foraminifers.	Early Oligocene (foraminifers); Middle to Late Oligocene (nannos).	Open marine, neritic.
102DR07-E and F	Sticky chalk, opal-A abundant; nannofloras with reworked Eocene/ Oligocene species; very poor foraminifers including *Turborotalia* cf. *opima*, and uncertain large globigerinids.	Middle to Late Oligocene	Open marine, neritic.
102DR03-B	Brown micaceous mudstone; no indigenous calcareous microfossils found.	undetermined	Paralic or restr. marine.
102DR03-1	Brown micaceous mudstone; no indigenous calcareous microfossils found.	undetermined	Paralic or restr. marine.

Wilson Bluff Limestone (Late Eocene) assemblage. A poorly-preserved, (recrystallised and hence limited) nannofossil assemblage was identified from a white dolomitic limestone at the base of core 102VC11 (between 70 and 76 cm levels); lithologically the sample is very similar to the Wilson Bluff Limestone. The assemblage includes common *Coccolithus eopelagicus*, rare to frequent *C. formosus, Coccolithus* sp. cf. *C. pelagicus*, abundant *Cyclicargolithus floridanus*,

frequent *Discoaster saipanensis*, rare (heavily calcified) *D. tanii*, rare (heavily calcified) *Isthmolithus recurvus*, rare *Markalius inversus*, rare *Reticulofenestra scissura*, frequent *R. scrippsae*, frequent *R. umbilicus*, and rare to frequent *Zygrhablithus bijugatus crassus*.

The nannofossil assemblage is assigned to the broad biostratigraphic datum interval between the lowest occurrence of *Isthmolithus recurvus* and the highest occurrence of *Discoaster saipanensis*, based on the presence of these two index species. This biostratigraphic interval equates with the combined Late Eocene NP19/NP20 Zones of Martini (1971) or the CP15b Subzone of Okada and Bukry (1980). It is difficult to judge whether the absence of the index species *Chiasmolithus oamaruensis* and *Cyclicargolithus reticulatus* from the assemblage is due to diagenetic or ecological factors, and the assemblage could be younger than the extinction datum of *C. reticulatus*.

The nannofossil assemblage probably belongs to the narrow latest Eocene interval between the highest occurrences of *Cyclicargolithus reticulatus* and *Discoaster saipanensis*, on account of the absence of *C. reticulatus*. This suggests placement high within the combined NP19/20 Zones or CP15 Zone. This biostratigraphic interval correlates with the planktonic foraminiferal late P16 Zone (Shafik, 1981); the age is latest Eocene, about 37.4-37 Ma (as indicated by Berggren and others, 1985 for the later part of P16; see also Truswell and others, 1991).

The nannofossil assemblage at the base of core 102VC11 is younger than the base of the Wilson Bluff Limestone in the onshore Eucla Basin (e.g. in Eyre-1 well). The Middle Eocene assemblages from 102DR07 (discussed above) correlate with assemblages from the lower part of the Wilson Bluff Limestone in onshore sections (e.g. in Eyre-1 well).

There is a lack of reworked Cretaceous nannofossils in the Middle Eocene assemblage from subsample 102DR07-B, and in the younger Eocene assemblage from sample 102VC11-base. Reworking of Cretaceous sediments in the Eocene of the southern margin therefore seems to be limited to the narrow Middle Eocene biostratigraphic datum interval, bracketed by the lowest occurrences of *Cyclicargolithus reticulatus* and *Reticulofenestra scissura*.

A neritic benthic foraminiferal assemblage was recovered from sample 102VC11-base. It includes the genera *Cibicides* and *Gyroidinoides*. A small rare nondescript plankton is noted.

Eocene Depositional Environment: The Middle Eocene nannofossil assemblage A includes *Daktylethra punctulata, Lanternithus minutus, Pontosphaera multipora, Transversopontis pulcher, Zygrhablithus bijugatus*, and others which indicate a neritic (shelf) paleoenvironment (see Shafik, 1990). Displaced nannofossils of mainly Late Cretaceous age (such as *Prediscosphaera cretacea*) were incorporated during the deposition. These were brought to the Ceduna Terrace,

presumably mainly from areas to the west, by short-lived bottom currents (see Shafik, 1985).

A shelf/neritic environment is also indicated by several neritic nannofossil species such as *Daktylethra punctulata, Lanternithus minutus* and *Zygrhablithus bijugatus* in the Middle Eocene nannofossil assemblage B.

The Upper Eocene Wilson Bluff Limestone at the base of 102VC11 represents echinoid-bryozoan facies deposited on the shelf.

Oligocene Assemblages

Early Oligocene assemblage. Subsample 102DR07-I yielded a poorly-preserved nannofossil assemblage, with most species showing signs of recrystallisation or addition of secondary calcite. Species identified include frequent *Coccolithus eopelagicus*, common *Coccolithus* sp. cf. *C. pelagicus*, rare *Corannulus germanicus*, abundant *Cyclicargolithus floridanus* (some specimens mimic the Eocene *C. reticulatus*), rare *Isthmolithus recurvus*, rare to frequent *Reticulofenestra orangensis*, common *R. scissura*, frequent *R. scrippsae*, common *R. umbilicus*, and rare to frequent *Zygrhablithus bijugatus bijugatus.*

Species identification has been hampered by poor preservation and thus biostratigraphic and age assignment are tentative. The nannofossil assemblage is assigned to the biostratigraphic datum interval bracketed by the highest occurrences of *Coccolithus formosus* and *Reticulofenestra umbilicus*, which coincides with NP22 Zone of Martini (1971) and CP16c of Okada and Bukry (1980). The tentative age is Early Oligocene, around 35 Ma according to calibrations by Berggren and others (1985) (see also Truswell and others, 1991).

Undetermined globigerinids were common in subsample 102DR07-I, suggesting an Early Oligocene age. The lithology (chert and chalk) of this sample and its age suggest a probable correlation with the upper member of the Gambier Limestone in the Gambier Basin.

Middle to Late Oligocene assemblages. Nannofossil assemblages identified from the carbonates of subsamples 102DR07-C, 102DR07-D, 102DR07-E, 102DR07-F and 102DR07-H are similar. The main elements of these assemblages include *Blackites* spp. (including *B. perlongus, B. spinulus* and *B. tenuis*), *Chiasmolithus altus* (either some specimens mimic *C. expansus, C. grandis, C. oamaruensis* and *C. solitus*, or these species do rarely occur, suggesting displacements from Eocene provenance), *Coccolithus eopelagicus, Coccolithus* sp. cf. *C. pelagicus, Cyclicargolithus floridanus* (often represented by two sizes), *Discoaster deflandrei, D. tanii nodifer, Helicosphaera bramlettei, H. recta, Reticulofenestra orangensis, R. scissura, R. scrippsae, R. umbilicus* (reworked from Eocene or older Oligocene levels), occasional *Sphenolithus moriformis, S. predistentus, Transversopontis* spp. (probably reworked from Eocene or older Oligocene levels) and *Zygrhablithus bijugatus.*

Both *Helicosphaera bramlettei* and *H. recta* are always very rare. In contrast, *Reticulofenestra umbilicus* and *R. scissura* are common in all assemblages. *Chiasmolithus altus*, usually abundant to common, is rare in subsample 102DR007-H. Very rare specimens of a *Sphenolithus* resembling the key species *S. distentus* were noted in subsample 102DR007-F.

The collective nannofossil assemblage listed above contains species whose stratigraphic ranges do not usually overlap. The key species *Helicosphaera recta* is among the younger species. Its stratigraphic range is known to span the Middle to Late Oligocene NP24 and NP25 Zones (see Martini, 1971; Perch-Nielsen, 1985) which equate with CP19 Zone of Okada and Bukry (1980); the highest occurrence of *H. recta* has been used widely as a good approximation of the top of the Oligocene. The index species of the NP24 and NP25 Zones, namely *Sphenolithus distentus* and *S. ciperoensis*, were not found in the material examined from dredge haul 102DR07, although they have been recorded previously from other dredges collected from the Ceduna Terrace (see Shafik, 1990).

The occurrence of *Helicosphaera recta* in the assemblages from dredge haul 102DR07, though rare, suggests that their age is Middle to Late Oligocene (NP24 and NP25 Zones, within the bracket 30-23.6 Ma according to data in Berggren and others (1985). The presence of *Helicosphaera bramlettei* supports this age determination.

Subsamples 102DR07-E and 102DR07-F were found to contain opal-A as spicules, radiolarians and diatoms, and foraminifers including *Turborotalia* cf. *T. opima* and uncertain large globigerinids. The age is Oligocene, probably Late Oligocene. Subsamples 102DR07-C and 102DR07-D were found to contain opal-A also, but their poorly preserved foraminifers included evidence suggestive of Early Oligocene age. Because the associated nannofossil assemblages include reworked Eocene/Oligocene species (such as *Reticulofenestra umbilicus*), the Early Oligocene foraminifers in subsamples 102DR07-C and 102DR07-D may be reworked as well.

Oligocene Depositional Environments: The overall composition of the Early Oligocene assemblage (102DR07-I) suggests deposition on the shelf in a cool-water regime. This conclusion is based on the presence of *Isthmolithus recurvus* and *Zygrhablithus bijugatus*; poor preservation may have removed the evidence of other species. Nevertheless, *Corannulus germanicus* may suggest some warm influence.

The abundance of *Chiasmolithus altus* and the scarcity of discoasters in the Middle to Late Oligocene assemblages suggest deposition in a cool-water regime. The Middle to Late Oligocene *Sphenolithus distentus* and *S. ciperoensis* are known to be warm-water species, and their absence agrees with the abundance of the cool-water indicator *Chiasmolithus altus*. The hemipelagic taxa *Transversopontis* spp. and *Zygrhablithus bijugatus* suggest deposition on the shelf, but their presence

could be (partly or wholly) allochthonous, a result of reworking.

DISCUSSION

Evidence indicating cool to cold surface waters in the Southern Ocean during the Oligocene is undeniable (Shafik, 1992 and references therein), and is supported by the results in this study. The warm-water species, *Sphenolithus distentus* and *S. ciperoensis* have been recorded from the Ceduna Terrace in dredges obtained during BMR Cruise 66 (Shafik, 1990) and the latter species has also been recorded in southeastern Australia, in the Otway Basin and west of Tasmania (Shafik, 1987). Shafik (1990) suggested that the presence of *S. ciperoensis* in the Oligocene of southern Australia represents a short warm episode. Similarly, the excursion of *S. distentus* into southern Australia was short, but, unlike *S. ciperoensis*, it did not reach the Otway Basin in the east. Shafik (1990, 1992) suggested that a warm surface current, analogous with the Leeuwin Current, brought the warm-water sphenoliths into southern Australia during the Middle and Late Oligocene. This current, the proto-Leeuwin Current, like its modern counterpart, was intermittent and varied in intensity over time. Its effect was more widespread during a short period in the Late Oligocene (*S. ciperoensis*) than earlier in the Oligocene (*S. distentus*).

The scenario of the proto-Leeuwin Current bringing *Sphenolithus distentus* and *S. ciperoensis* to southern Australia would mean that the lowest appearance level of either of these species in the southern Australian record is most likely to be isochronous. This is important because the stratigraphic range of *S. distentus* in the Ceduna Terrace Oligocene, or of *S. ciperoensis* in the Ceduna Terrace and the Otway Basin sequences, does not necessarily equate with the stratigraphic ranges of these species in low-latitude sections such as those used in the development of the zonations of Martini (1971) or Bukry (1973; 1975 which are the basis for Okada and Bukry's 1980 scheme). The temporal ranges of the species in the southern Australian sequences probably represent only parts of their ranges in the low-latitude sections. The local stratigraphic and geographic ranges of species depended on the duration and overall intensity of the intermittent proto-Leeuwin Current during the Oligocene, be this duration instantaneous in terms of geological time.

Reworking during the Middle to Late Oligocene

The key species *Helicosphaera recta* and *Reticulofenestra umbilicus* do not usually occur together. The highest occurrence of *R. umbilicus* has been widely used to define the top of the Lower Oligocene, and the vertical range of *H. recta* is known elsewhere to span the Middle and Upper Oligocene. Indeed a biostratigraphic gap, represented in continuous stratigraphic sections by NP23 Zone, separates the highest occurrence of *R. umbilicus* and the lowest occurrence of *H. recta* (see Martini, 1971). The co-occurrence of these two species in the Middle-Upper Oligocene carbonates of dredge haul 102DR07 indicates reworking; older sediments (probably Eocene or Lower Oligocene and containing *R.*

umbilicus) were included during deposition of the Middle to late Oligocene *H. recta*. Evidence of similar reworking has been recorded previously in Middle and Late Oligocene assemblages from the Ceduna Terrace (see Shafik, 1990), from chalk and limestone collected during BMR Cruise 66. Shafik (1992) indicated that reworking of Lower Oligocene/Eocene sediments from around Australia during the Middle and Late Oligocene has been extensive. He recorded its evidence in the Perth and Carnarvon Basins as well. Shafik (1992) suggested that the reworking resulted from a large scale erosion of nannofossil-bearing sediments from lower or intermediate oceanic section (such as the Naturaliste Plateau) during an interval of changing gateways around Australia. During the Middle to Late Oligocene interval two important events occurred: the complete separation of Australia and Antarctica (at about 35 Ma) clearing the way for deep waters south of Tasmania, and the collision of Australia with a subduction zone in its north (at about 30 Ma) eventually closing the seaway in the north of Australia which connected the Indian and Pacific Oceans.

The Early Oligocene foraminifers recorded from subsamples 102DR07-C and 102DR07-D (see Table 7) could be displaced, a result of reworking of Eocene/Oligocene sediments during the Middle to Late Oligocene.

Lower Tertiary Correlations

The Eocene carbonates identified from the Ceduna Terrace (Davies and others, 1989; this study) correlate well with the Wilson Bluff Limestone known from the onshore Eucla Basin (see Lowry, 1970). Sediments equivalent to the Oligocene recorded on the Ceduna Terrace (Shafik, 1990, 1992; McGowran, 1991; present study) are not known from the onshore Eucla Basin (see Lowry, 1970; Hocking, 1990). They occur further east on the Australian southern margin, in the Otway Basin (see McGowran, 1973).

6.5.2 LATE QUATERNARY FORAMINIFERAL SUCCESSIONS IN CORES FROM THE GREAT AUSTRALIAN BIGHT AND THEIR ENVIRONMENTAL SIGNIFICANCE

D. Almond (Department of Geology and Geophysics, University of Adelaide)

INTRODUCTION

Recent interest in Quatemary foraminiferal biostratigraphy in Australian waters has seen the successful development of a biostratigraphy for lower latitudes (Chaproniere, 1991). This study will describe the foraminiferal succession in the Great Australian Bight on the temperate margin of the continent and describe how this relates to changes in the environment.

The materials used were taken from three cores recovered during BMR cruises 66 and 102. Their locations and depth of retrieval are displayed in Table 8 and in Figure 25.

Table 8. Core location and water depth for detailed foraminifer study.

core	latitude	longitude	depth (m)
102GC08	33°35. 01'S	128°01.51'E	912
66GC03	33°51. 07'S	132° 05.31'E	600
102GC17	34°53.45'S	130° 03.33'E	3002

MATERIALS AND METHODS

Core 102GC08 was the longest core studied, being 489 cm long, and is a nannofossil foraminifer ooze with, as minor constituents, echinoid fragments, pteropods, mollusc fragments, and sponge spicules. Minor turbidites occur at 407 cm and 425 cm. The colour variation in the core is from white to grey (Fig. 26).

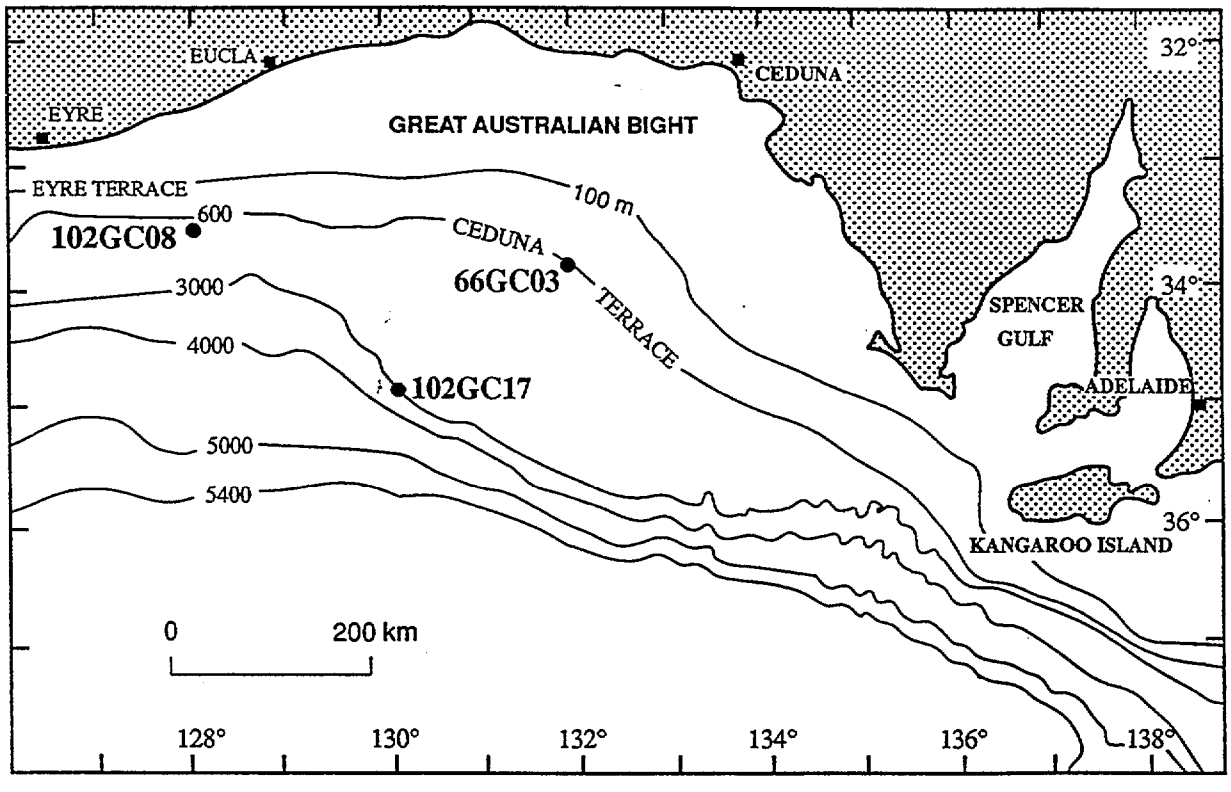

FIGURE 25. Location of the three gravity cores from AGSO cruises 66 and 102 used for the detailed environmental study.

Core 66GC03 is 346 cm long and is made up of a significant fraction of marine detritus: sponge spicules, mollusc and echinoid fragments, pteropod shells, and small calcareous detrital fragments. The core is white near the top and grades into grey towards the base (Fig. 27).

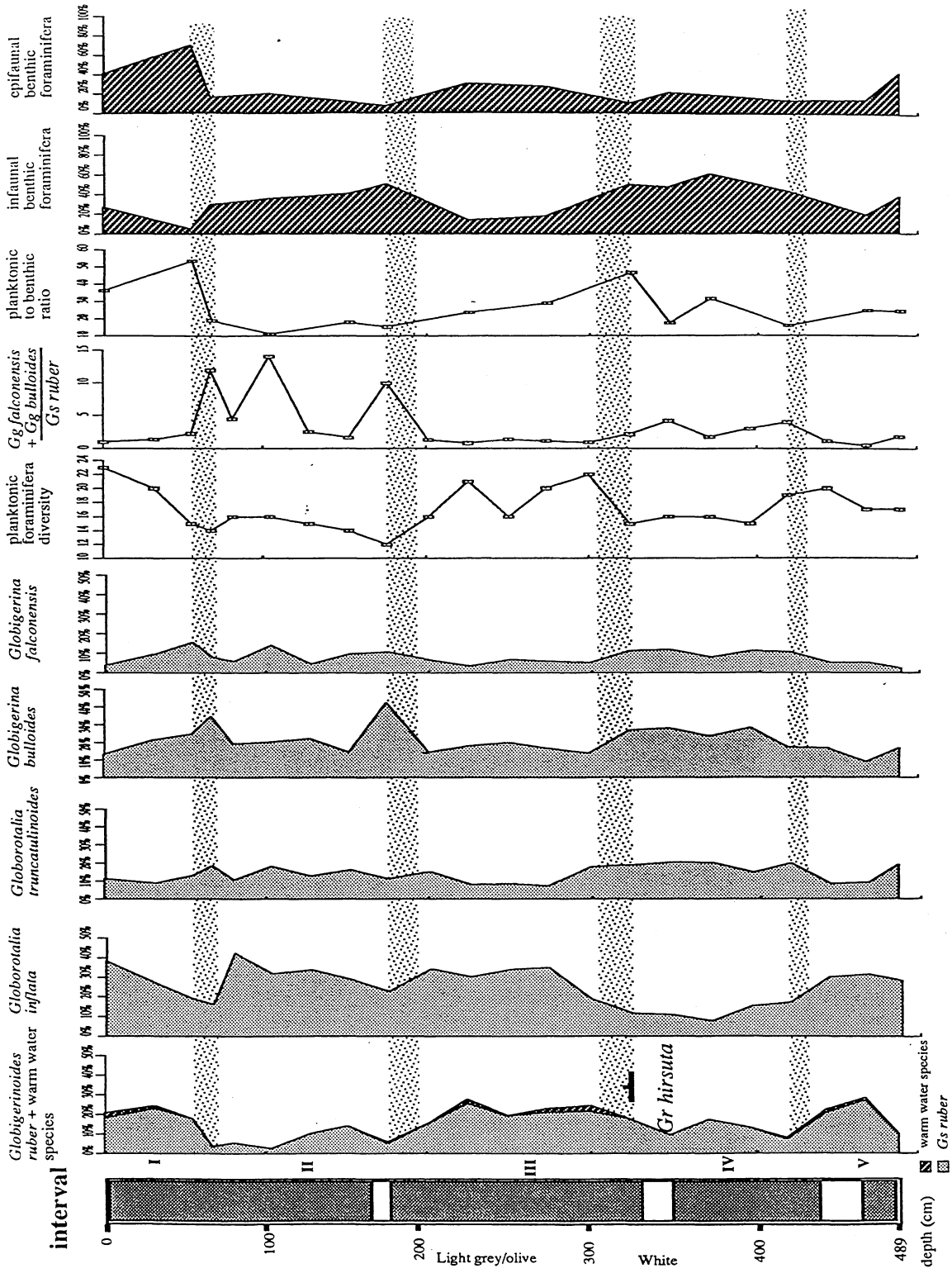

FIGURE 26. Schematic log and foraminifer abundance data for 102GC08.

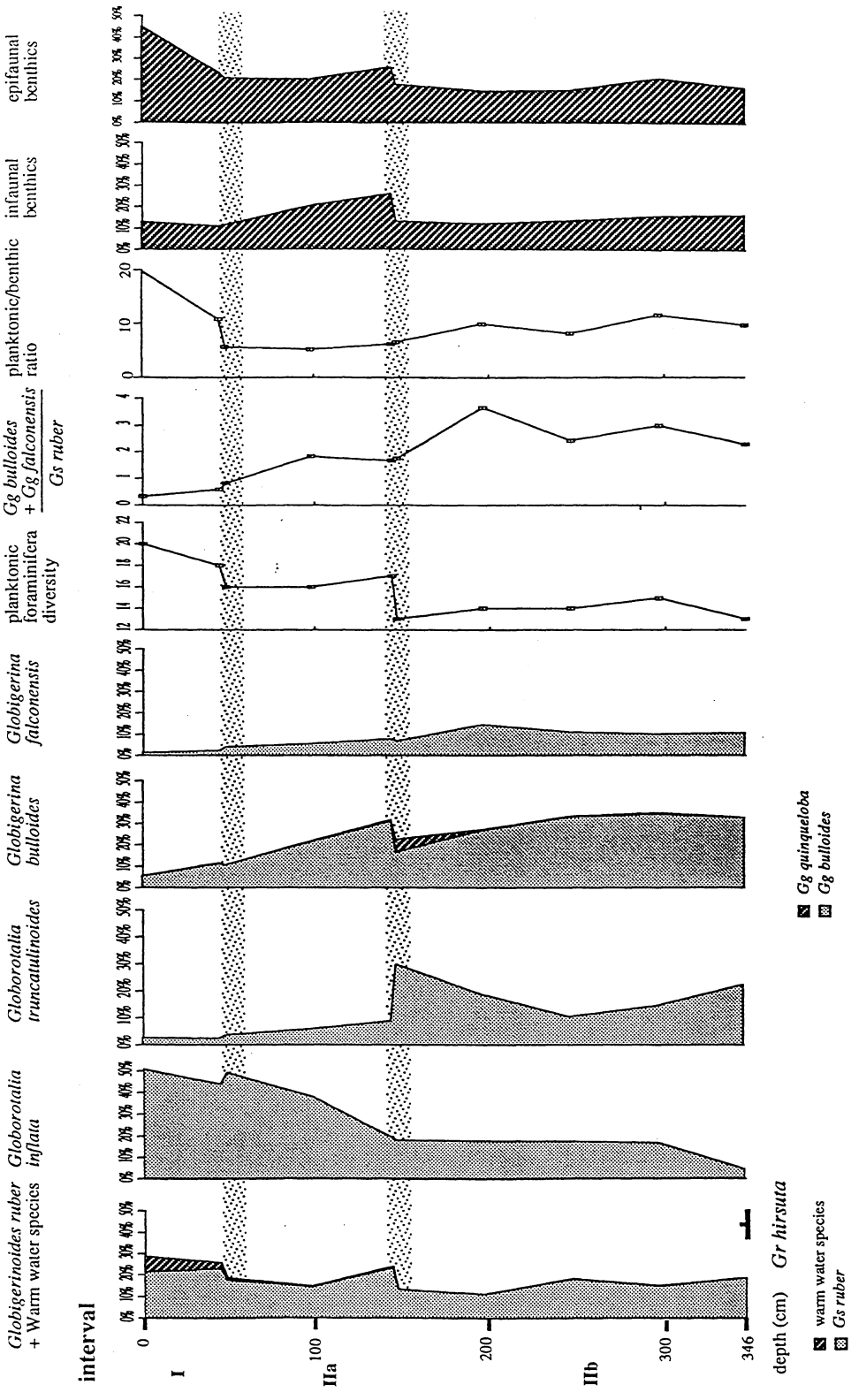

FIGURE 27. Schematic log and foraminifer abundance data for 66GC03.

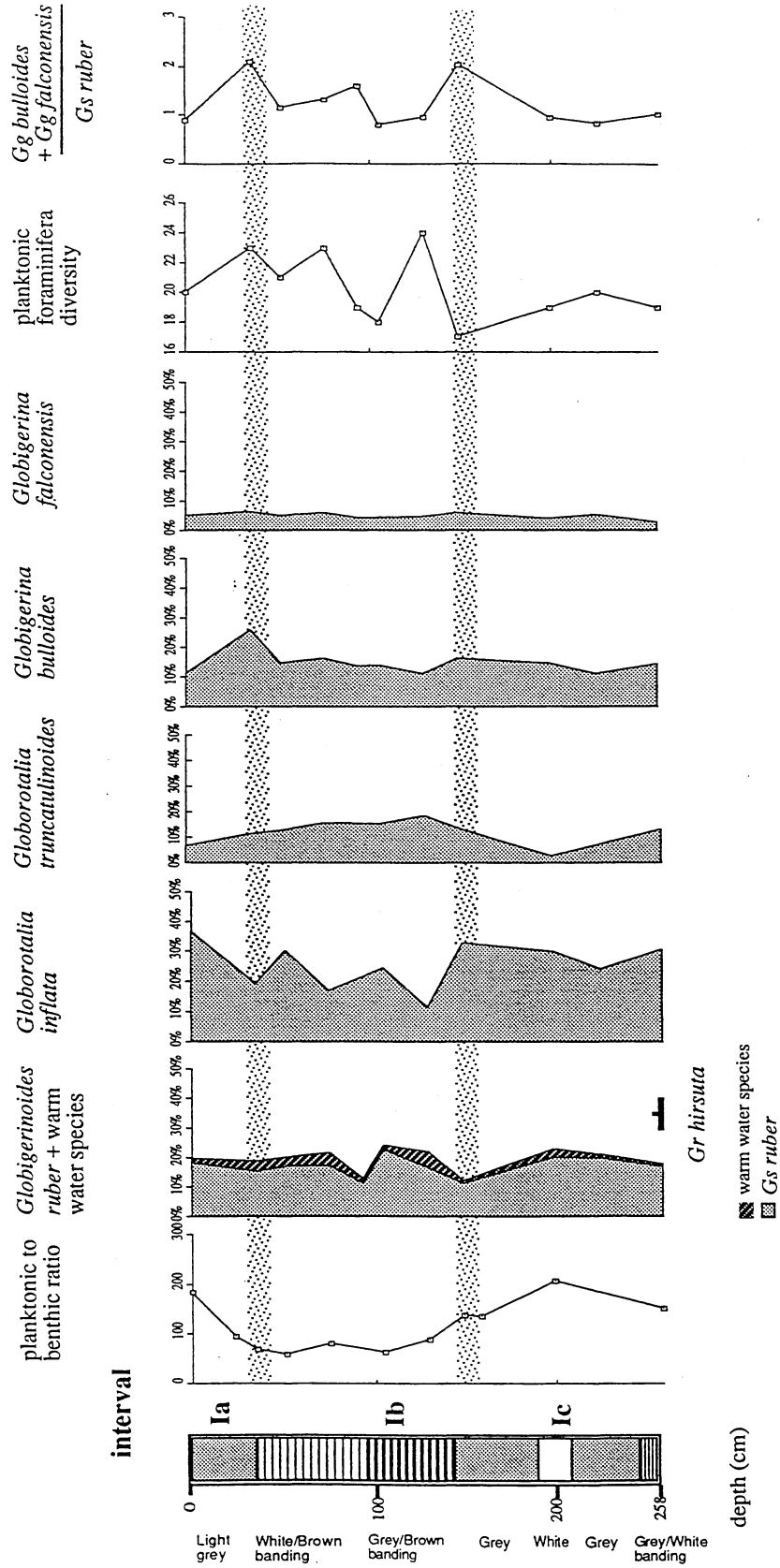

FIGURE 28. Schematic log and foraminifer abundance data for 102GC17.

Core 102GC17 consists of a foraminifer nannofossil ooze, is 258 cm long and lacks the detrital grains that occur in the others. The grain size of foraminifers is relatively large. Colour banding distinguishes this core: alternations are between white/brown, grey/brown, and white and grey intervals (Fig. 28). Burrow mottling occurs at 40-97 cm, 170 cm, l90 cm, and at 220 cm. Bioturbation is evident at 120-140 cm.

Cores were sampled at the AGSO laboratories in Canberra by extracting a 2 cm wide block of ooze. These samples were taken at 10 cm intervals and were boiled in a detergent and bicarbonate solution until disaggregation was complete. The resultant mixture was sieved and washed using a standard 63μm sieve and the wet foraminifers were oven-dried.

For the analysis of planktonic foraminifers, approximately 300 specimens were picked using the method outlined by Kennett and Vella (1975). 150 were taken from the fraction greater than 250 μm and 150 were taken from the fraction less than 250 μm but greater than 150 μm. They were sorted into individual species and the percentages of the total planktonic assemblage were compiled. The coiling ratios of *Globorotalia truncatulinoides* were checked in five samples of core 102GC08 and were found to be entirely sinistrally coiled. The reasons for coiling differences are complicated (Hemleben and others, 1989, Kennett, 1976) and this line of investigation was pursued no further. Each sample was searched for all species to determine the diversity of planktonic foraminifers. The planktonic: benthic ratio was determined on counts of at least 250 specimens for core 66GC03, 700 for core 102GC08, and 1500 for core 102GC17. For the analysis of benthic foraminifers, around 50 benthic foraminifers were picked from cores 102GC08 and 66GC03. Benthic foraminifers from core 66GC03 were divided into three groups using the methods outlined by Corliss and Chen (1988) - infaunal morphotypes, epifaunal morphotypes, and indeterminant specimens. The percentages of infaunal and epifaunal types were calculated. For core 102GC08, the benthic foraminifers were identified and the same analysis was made.

Samples were picked and sorted every 50 cm intervals for 66GC03 and at 25 cm intervals for 102GC08. Samples in core 102GC17 were picked and sorted every 25 cm in the brown section and 50 cm elsewhere.

The sample for radiocarbon dating, taken at 67 cm in core 102GC08, was prepared by heating in a solution of detergent followed by sieving the greater than 150μm fraction.

FORAMINIFERAL SUCCESSION

The most abundant foraminifers present in the cores included species from all five latitudinal biogeographic regions of the world. Core 102GC08 shows the most comprehensive succession. This core may be divided on the basis of changes in both the planktonic and benthic foraminifers even though these changes are gradational. Five intervals, I to V downhole, have been established in this manner (Fig. 26). The oldest interval (interval V) has high abundances of *Gs ruber, Gr*

inflata and lower abundances of *Gr truncatulinoides*, *Gg bulloides* and *Gg falconensis*. Warm water species are also present in small numbers in this interval. Interval IV overlies interval V and differs: both *Gs ruber* and *Gr inflata* are less abundant whereas *Gr truncatulinoides*, *Gg bulloides* and *Gg falconensis* make up the bulk of the fauna. In addition, warm water species are not present and the diversity of planktonic species is comparatively low. Interval III has a similar faunal assemblage to interval V: warm water species are present, diversity is high, and *Gs ruber* and *Gr inflata* are abundant. *Gr truncatulinoides*, *Gg bulloides* and *Gg falconensis* are less numerous and the first occurrence of Gr *hirsuta* marks its beginning. The overlying interval, interval II, is similar to interval IV, although in contrast, Gs *ruber* is less abundant and *Gr inflata* is most abundant. Interval I at the top is like interval III in its high diversity, high abundances of *Gs ruber* and *Gr inflata* and low abundances of *Gr truncatulinoides, Gg bulloides* and *Gg falconensis.* A ratio of *(Gg bulloides + Gg falconensis) ÷Gs ruber* has been calculated and is high in interval IV, higher in interval II and low in intervals I, III, and V.

The benthic foraminiferal succession may be divided in a similar way. The ratios of planktonic to benthic foraminifers for intervals II and IV are lower than in intervals I, III and V. In broad terms, changes in the abundance of *Gs ruber* show a similar trend to changes in this ratio. Infaunal benthic foraminifers are most abundant during intervals II and IV and less abundant during intervals I, III and V whereas epifaunal benthic foraminifers vary in the opposite sense.

The succession in core 66GC03 (Fig. 27) can be correlated with that in core 102GC08. *Gr hirsuta* is present at the base and dates the core as interval III and/or younger. Most of the core is designated interval II and is divided into intervals IIa and IIb. It correlates with interval II in core 102GC08. Interval IIb has high abundances of *Gr truncatulinoides*, *Gg bulloides* and *Gg falconensis.* A sharp discontinuity occurs between IIb and IIa, at 150 cm. Above this, *Gr truncatulinoides* is rare, *Gg bulloides* and *Gg falconensis* decrease and *Gr inflata* is more abundant. The diversity, which was low in interval IIb, increases across the boundary. Infaunal and epifaunal benthic foraminifers are more abundant in interval IIa, whereas the planktonic:benthic ratio decreases. Interval I in this core, has high abundances of *Gs ruber* and *Gr inflata* and low abundances of *Gr truncatulinoides, Gg bulloides* and *Gg falconensis.* In addition, warm water species are present and diversity is highest. The planktonic:benthic ratio increases across the I / II boundary. Epifaunal benthic foraminifers are most abundant in interval I; infaunal forms are not. The *Gg bulloides + Gg falconensis ÷Gs ruber* ratio is lower in this core and has been plotted on a reduced scale. It decreases across the IIb / IIa boundary and again in interval I. Based on this accumulated evidence, I correlate interval I in the two cores.

Core 102GC17 is divided into three intervals: Ia and Ib and Ic (Fig. 28). There is a trend in the planktonic:benthic ratio which is similar to the trend through intervals I, II and III in core 102GC08. However, there is almost an order of magnitude difference between their values and it is questionable whether a reliable

correlation can be made on this basis. *Gg bulloides* and *Gg falconensis* show little variation and are less common in this core. *Gs ruber* is abundant in each interval and warm water species are always present. The *(Gg bulloides + Gg falconensis) ÷ Gs ruber* ratio has been plotted on a reduced scale and is very low. This suggests that all three intervals may be correlated with interval I of core 102GC08. However, diversity is low in intervals Ia and Ic but is higher in interval Ib. This suggests that intervals Ia, Ib, and Ic of core 102GC17 correlate with intervals II, III and IV in core 102GC08. This interpretation is not valid though because the base of core 102GC17 has specimens of *Gr hirsuta* which means that the base of interval Ic is younger than the beginning of interval III in core 102GC08. This thus excludes interval Ic as correlating with interval IV of core 102GC08. It is unclear how this core can be correlated with the other cores, but because of the presence of warm water species and a high abundance of *Gs ruber*, it possibly correlates with interval I or III, or perhaps with both and interval II is missing. Numerical dating would resolve this problem. *Gr inflata* is abundant in interval Ib and less abundant in interval Ia, and *Gr truncatulinoides* is not common in interval Ic.

In each core, less common species were observed and their abundance recorded. This data has been compiled into three tables. Tables 9, 10, and 11 present the changes for cores 102GC08, 66GC03, and 102GC17 respectively.

AGE DETERMINATION

The radiocarbon date puts the base of interval I for core 102GC08 at an age of 25,800 ± 1300 years. This number, however, is most likely older than the true age. This is because although small detrital grains were eliminated by sifting, the carbon analysis required a certain minimum weight. The decision was made therefore to date the fraction greater than 150 µm which contained less detrital grains but which were still present. The age therefore must be older than the real age, but despite this the age does indicate that interval I was deposited since the last glacial and not before.

INTERPRETATION AND CONCLUSIONS

Gs ruber is an oligotrophic species (Chaproniere, 1991) and *Gg bulloides* and *Gg falconensis* are eutrophic (Bé, 1977). The *(Gg bulloides + Gg falconensis) ÷ Gs ruber* ratio can therefore be used to determine changes in stratification of the water mass and in nutrient content. Diversity is also an indication of stratification and is higher in stratified water (Lipps, 1987). In core 102GC08, the diversity is high when the ratio is low in interval I and I conclude that, interval I, the present interglacial, was oligotrophic. Intervals III and V have similar ratios and diversities and are also oligotrophic. Interval II, which records the last glacial period, has a high ratio and indicates mixed, nutrient-rich water. The infaunal benthic foraminifers, which are more abundant where the organic content is high (Corliss and Chen, 1988), indicates high productivity during this time and also upwelling onto the shelf. The changes in the epifaunal benthic foraminifers confirm this, as they live where carbon content is low (Corliss and Chen, 1988) and they vary in the opposite sense to the infaunal assemblage. The changes in the water depth may be inferred from the planktonic:benthic ratio which is highest in deeper water (Boltovskoy and

TABLE 9. Foraminifer faunal list for core 102GC08.

species	0 cm	31	55	67	80	104	128	152	176	202	226	250	274	300	324	348	372	396	420	444	468	489
B digitata	O	O							O		O										O	
Ga glutinata	X	O	O	X	F	X	X		X	X	X	O	X	O	X	O	X	O	X		O	O
Ge aequilateralis	X	O			X	O				X	O	X	X	X		O	O	X	O	X	O	O
Ge obesa	X	X	O	O	X	O	O	X	X	O	X		X	X	X	O	X	X	X	X		X
Gg species	O	O	X	O	O	X	O	X	O	O	O	X	X	X	O	C	X	F	O	X		X
Gg quinqueloba		O	O	X			O		O					O		O					O	O
Gr crassaformis			O					O					O			O			X	X	X	
Gr hirsuta	X	X	X	C	F	C	F	C		X	X	X	X	C		O	O	X	O	O		X
Gr scitula	O	O		O	X	O	O			O	O	O	X	X	X	O	O	X	X	O	X	O
Gr species 1			X		X	O		O	O			O	O	O	O	O	O		O		O	O
Gr species 2	O	O	O	X	O	O	O	O		X	O	X		X	O	O	O	O	X	O	X	O
Gr tumida	O	O									O											
Gs tenellus	O			O					O		O		O	O					O	O	O	
Gs sacculifer	O										O		O	X						O	O	
Gs cf conglobatus	O																					
Gs conglobatus		O									O		O	X					O	O		
Gs quadrilobatus	O	O									O		O							O		
Gs trilobus		O										O	O	O	O							
N dutertrei	X		O		O	O		O		O		O	X	O	O	O	O	O	X	X	F	
N pachyderma	X	X	X	F	X	X	C	X	X	F	F	X	X	X	C	C	C	F	Δ	C	C	
N species														O		X	X	X			X	
O suturalis	O																					
O bilobata	O						O												O			
O universa	X	O		X	X	X	X	X	X	Y	O	O	X	X	O	O	F	X	F	X	X	X
S dehiscens											O			O								
T humilis															O							
0 = 0-1%																						
X = 1-3.5%																						
F = 3.5 - 5%																						
C = 5 - 10%																						
Δ = 10-12%																						
interval		II					IIII					IIIII					IIV				V	

TABLE 10. Foraminifer faunal list for core 66GC03.

species	0 cm	44	48	95	144	147	196	246	296	344
B digitata	O									
Ge aequilateralis	X	X	O	X	O				O	
Ge obesa	O	O	O	O	O	O	O	O	O	X
Ga glutinata	O	O	O	X	O	X	O	O	O	O
Gg quinqueloba		O		O	O	C	O	O	O	
Gg species	O		X	O	O		O	X	X	X
Gr crassaformis						O				
Gr hirsuta	O	X	X	X	X	X	C	F	O	X
Gr scitula	O		O		O		O	O	O	
Gr species 1						O		O		
Gr species 2	X	X	X	X	O				O	O
Gr tumida	O	O								
Gs quadrilobatus		O								
Gs sacculifer	O			O						
Gs tenellus	X	X	X		O			O	O	
Gs trilobus	O									
N dutertrei	X	X	O		O					X
N pachyderma	X	X	F	F	X	C	X	X	F	F
O bilobata		O		O			O			
O universa	O	X	X	X	O	O	X			O
O = 0-1%										
X = 1-3.5%										
C = 5-10%										
interval	I			IIa					IIIb	

Wright, 1976), and therefore relative highstands occurred during oligotrophic periods. The changes in temperatures and stratification may be due to the Leeuwin current which was apparently present during interglacial periods. Conditions were similar at the site of 66GC03, although in interval IIa the infaunal benthic foraminifers became less abundant and therefore productivity decreased but the diversity increased (more stratified water column) and oligotrophic conditions prevailed. This can be related to the development of the Great Australian Bight Current which was prevalent by interval I and flows at this locality in the modern ocean.

Core 102GC17 was in an area where stratification and temperatures were high, sometime since the beginning of the last interglacial. The Great Australian Bight

Current also flows over this location at present and would have flowed as a warm current during deposition of the core.

TABLE 11. Foraminifer faunal list for core 102GC17.

species	0 cm	36	52	76	105	129	148	199	258
Bella digitata	O	O	O						
Bolliella adamsi						O			
Ga glutinata	O	O	O	O	O	X	O	O	O
Ge aequilateralis	O	X	X	O	X	X	X	O	F
Ge obesa	X	O	X	O	O	X	X	O	X
Gg species	O	X	X	O		O	X	X	X
Gr crassaformis		X	X	X		X		X	O
Gr hirsuta	C	X	X	F	C	F	F	Δ	F
Gr scitula	O	X	X	X	X	X	O	O	O
Gr species 2	X	X		X		X		O	
Gs conglobatus		O	X	O	O	O	O	X	
Gs quadrilobatus	O	O	O	O	O	X			
Gs sacculifer	O		O	O	O	O	O		O
Gs tenellus	O	O	O	X		X			
Gs trilobus		O		O		O	O	O	O
O bilobata	O	O		O	O	O	O	O	O
O suturalis									O
O universa	F	X	X	X	F	X	X	X	F
N dutertrei	O	O	X	O		O			O
N species					O				
N pachyderma	X	X	X	F	X	F	X	X	X
S dehiscens		O	O	O	O	O		O	
O = 0-1%									
X = 1-3.5%									
C = 5-10%									
Δ = 10-12%									
interval	Ia			IIb					Ic

This study shows that climatic cycles are linked with the trophic continuum and productivity on the southern margin of Australia. Temperatures are linked to the flow of the Leeuwin Current, which flowed during interglacial periods, and the Great Australian Bight Current which began developing in the last glacial. Upwelling from the Southern Ocean brought cool water onto the shelf during glaciation and supplied nutrients to surface waters.

7. TECHNICAL SYSTEMS

The following descriptions of the characteristics and performance of the technical systems used onboard *RIG SEISMIC* during cruise 102 are based substantially on internal operational reports submitted by the senior scientist or technical officer in each section.

7.1 GEOLOGICAL SAMPLING SYSTEMS

DREDGING:

A total of 13 dredge stations were occupied during Cruise 102 (Appendix 1), of which 10 were successful. In each case, the dredge configuration consisted of a standard AGSO chain bag dredge, with a weak link connection (determined by water depth) to the wire rope spelter socket, and with two pipe dredges connected to the tail end of the chain bag. Pipe dredges were 300 mm in diameter and 750 mm in length, with one having a closed end to sample mud, and the other having a 30x10 mm grid to recover pebble- and cobble-sized material which would otherwise pass through the chain bag mesh. Dredges were deployed with 50-60 kg of weights attached 50 m up the wire rope, in an attempt to ensure that the mouth of the dredge was weighed down. In two cases, failure of the dredge to recover material could be attributed to the dredge not contacting the seafloor, as a result of the strong winds and rough following seas present during a number of attempted dredges.

GRAVITY CORING:

A total of 38 gravity cores were attempted during Cruise 102 (Appendix 1), of which 28 were successful. Core recovery ranged from 0.22 m to 5.20 m at successful sites. Penetration was achieved by accelerating the rate of wire-out to approximately 130 m/min from an estimated 150 m above the seafloor, after first allowing the corer to stabilise at that depth. Gravity corer configuration consisted of a 1 tonne, variable weight head, attached to lengths of steel core barrel enclosing a 90 mm core liner, with a core cutter and core catcher at the base. During coring operations in Areas B and C, 6 m and 10 m core barrel lengths were used. In Area A, where the intention was to penetrate indurated sediments, a 2 m barrel was used. Despite two instances of bent core barrels, the gravity coring configuration was highly successful. In two instances (102GC10 and 102GC12), failure of the corer to recover material could be attributed to the presence of relatively well-sorted, medium or coarse sand at the seafloor. This material is essentially impenetrable for a gravity corer. On one other occasion (102GC37), all fingers on the core catcher were sheared off, and no core was recovered.

VIBROCORING:

Fourteen vibrocores were attempted, at 10 sites on the Eucla Shelf (Appendix 1). Seven vibrocores were successful, recovering between 0.30 m and 1.37 m of sediment. Vibrocore configuration consisted of a 300 kg head attached to a 6 m length of 75 mm diameter aluminium pipe, within a three-legged frame. Deployment was from the ship's crane, with the co-axial armoured cable used for deploying the vibrocorer also carrying electric power to the vibrating head. Time

restrictions throughout this program prevented any extensive testing to determine optimum vibration time once the frame was on the seafloor, and it is possible that better results may have been achieved with longer vibration times.

GRAB SAMPLING:
Prior to vibrocoring at each site, a grab sample was taken to ensure that there was a suitable substrate for vibrocoring. Grab sampling equipment consisted of a 150 kg Van Veen grab, "cocked" prior to deployment, and triggered by contact with the seafloor. Deployment was with the hydrographic winch. This sampling system gave a good indication of substrate, and it is notable that the smallest grab recovery (102GR04) was at the site where it was virtually impossible to recover material with the vibrocorer (102GR06 and 102GR06A).

SEAFLOOR PHOTOGRAPHY:
During a transit across the Eucla Shelf following the sampling traverse, the seafloor camera system was deployed at 7 of the vibrocore sites (Appendix 1). This system consisted of a BENTHOS camera unit connected to a BENTHOS flash, mounted on a BMR-constructed steel frame. The intention originally was to use a bottom-contact switch to trigger the camera. However this unit was found to be non-operational, and the system therefore needed considerable wiring and electronic modification before it could be used. However because of the relatively shallow water depths in which the system was deployed (22-91 m), it was feasible to set the camera going, with a flash/shutter interval of approximately 10 seconds, as the unit was deployed from the ship. The system was lowered on the hydrographic winch to the seafloor, and then raised approximately 3 metres. The ship was then allowed to drift, with the ship's movement producing exposures at variable distances above the seafloor. This exercise was considered to be experimental, and the results were poor.

7.2 NAVIGATION AND DAS SYSTEM

The navigational and non-seismic data acquisition systems (DAS) performed exceptionally well on Cruise 102. Since the cruise covered such a wide area, one of the secondary objectives of the cruise was to acquire differential navigation correction data from two widely spaced shore stations, in order to determine what loss of accuracy occurred at increasing distance from the shore station.

Non-seismic data acquisition was based on a HP1000F computer system running on RTE/6-VM. This computer is interfaced to several sensors, including navigation, gravity, magnetics and water depth. Output is to magnetic tape, as well as to various printers and strip chart recorders to facilitate quality control. A secondary acquisition system was onboard for the express purpose of acquiring differential Global Positioning System (dGPS) data for comparison purposes. This was installed by Racal and was operated by their observer. The hardware consisted of a Hewlett Packard 9826 micro-computer, running HP Basic operating system, and "GNS Survey" navigation software. The primary navigation system on Cruise 102 was differential GPS, using a service and equipment supplied by Racal Pty Ltd.

The secondary system was stand-alone GPS using the Magnavox T-Set. The third system was dead reckoning (DR) using doppler sonars and gyrocompass with ties to Transit satellite position fixes using Magnavox satellite navigators. The dead reckoning system was used when both dGPS and GPS dropped out, for periods of only a few tens of minutes each day.

The results of processing of dGPS navigation data, which was acquired using shore stations at Perth and Broome, suggest that accuracy to better than 35 m was achieved using the Perth shore station (ranges of about 1000 km), and that the loss in accuracy when using Broome shore station (ranges of approximately 2000 km) was of the order of 7-10 m.

Neither echo sounder system gave satisfactory output continuously throughout the cruise. The digital water depths are of very poor quality in the deep water areas of interest, due to the sea states experienced. It has been necessary to revert to the analogue EPC records to manually digitise the bathymetry in the vital areas.

The magnetometer was not deployed for parts of the cruise due to the stop/start nature of the sampling operations. However, a total of 4600 km of magnetic data was recorded on the long transits between sites. Much of these data are plagued by spikes, whose frequency of occurrence varied considerably.

The gravity meter functioned satisfactorily without failure for the duration of the cruise. Gravity data were recorded for the entire cruse; a total of 6560 km on transits. No caging happened despite the moderate to severe sea conditions and high accelerations. The noise envelope in the high frequency component was up to 60 mms-2 in rough seas and 20-30 mms-2 in quiet seas.

7.3 SEISMIC ACQUISITION SYSTEM

The seismic acquisition system was the only system which failed completely during Cruise 102. This was particularly frustrating as the sea state was abnormally calm during the time when the seismic program was due to be undertaken, and the program was such an important component of the cruise scientific objectives.

During the transit to the first seismic line, the Micro-Vax system was thoroughly tested. One of the main objects of this testing was to set the acquisition parameters for the seismic survey. During all phases of testing the system worked faultlessly. Once the streamer and the waterguns were deployed, acquisition was started. Soon afterwards the system crashed. After many attempts the programs were recompiled and reinstalled. The system ran for about 10 hours in test mode and did not show any problems. When acquisition was resumed, the system failed again. At this stage the seismic program had to be abandoned. Throughout the remainder of the cruise, repeated unsuccessful attempts were made to get a stable seismic system up and operating reliably. Work on the system was hampered by rough weather, with rough seas leading to numerous bad connections and loose connectors. However the main source of problems seems to have been the QD-33

disk controller, which appears to have failed and corrupted the disk. In addition, an RS-232 cable which had the insulation scraped off and a DHQ-11 card which only half worked also probably caused some tape drive problems.

7.4 MECHANICAL AND ELECTRONIC SYSTEMS

In general, mechanical and electronic systems performed admirably, particularly considering the rough sea conditions encountered during much of the cruise.

Dredge and gravity core sampling operations used the main sampling winch, containing some 9500 m of 19 mm wire rope. During the cruise, a section of kinked wire rope with a damaged core led to the loss of a complete dredge and 1000 m of cable. Also the cable was re-terminated three times due to suspected faults. As a consequence, the working length was reduced to 7500 meters. As has been the case for most of the time since installation in 1985, the AWH Winch Controller using FESTO software did not operate correctly and it was often impossible to be certain when bottom contact occurred. In addition, spooling problems were experienced when retrieving the wire rope, particularly during rough seas.

Both the hydrographic winch (used for grab sampling and camera deployment) and the vibrocore winch operated satisfactorily.

Initially, the Benthos camera equipment was unserviceable due to failure of the trigger unit, poorly wired connections, and to flat and corroded batteries. After correcting these problems, it was possible to use the unit in automatic mode. However this meant that camera work was "hit and miss", with the distance of the camera above the sea floor being impossible to determine accurately.

8. CONCLUSIONS

RIG SEISMIC Cruise 102 sailed from Fremantle on the 12th June 1991, and docked in Fremantle on the 10th July 1991 after carrying out geological sampling operations at a range of sites across Australia's Southern Margin. The scientific objectives of the cruise were virtually all successfully completed, despite the cruise taking place in mid-winter in an area of ocean renowned for having the roughest seas of any part of the Australian margin. A total of 10 dredge sites, 28 gravity core sites, and 8 grab and vibrocore sites were successfully occupied. In addition, 4600 line km of magnetometer data and 6560 line km of bathymetric data were collected. This report presents preliminary scientific results for each of the components of the program; the results of on-going scientific analysis for many of the components will be reported separately.

The Southern Margin Sampling Program (121.27) was proposed as a multi-objective survey, designed to address a range of geological problems. The primary objectives of the survey emphasised (i) the further evaluation of the hydrocarbon prospectivity of the deep Ceduna Sub-basin segment of the Great Australian Bight Basin, to complement and expand on earlier *RIG SEISMIC* surveys; and (ii) the

development of a high energy, cool-water, carbonate depositional model based on the sedimentary characteristics of Cenozoic carbonate deposits on the Eucla Shelf-Eyre Terrace. Additional objectives involved seafloor sampling for Quaternary paleochemistry and mantle magmatism projects, and the collection of bathymetric data for AGSO's Offshore Resource Map Series.

Sampling results, with respect to the cruise objectives for each area, are as follows:

AREA A - to determine the biostratigraphy and sedimentary facies of the deep Ceduna Sub-basin sequence. During this segment of the survey, particularly poor weather conditions resulted in considerable difficulty in precise core and dredge operations. A total of 6 dredges (3 successful) and 17 gravity cores (12 successful) were attempted at 11 sites. The successful dredge hauls recovered an extensive suite of terrigenous siliciclastic rocks and, in one dredge, a range of calcareous (calcarenite, calcilutite, and semi-lithified foraminifer ooze) and dolomitic rocks. Nannofossil data show that the calcareous rocks are of Middle Eocene to mid-late Oligocene age, and palynological study shows that the terrigenous siliciclastic rocks are of Late Cretaceous (Campanian to latest Maastrichtian) age. Attempts to use a short-barrelled gravity corer to sample older sediments was only marginally successful; Quaternary cover prevented penetration through to Mesozoic targets in all but two cores, which recovered late Maastrichtian (*Manumiella druggii* Zone) mudstones. The Late Cretaceous ages for the terrigenous mudstones and siltstones show that these rocks are correlatives of the Potoroo Formation, and their faunas and sedimentary facies indicate that they represent deposition in paralic, marginal to restricted marine, and marine depositional environments. The Middle Eocene to mid-late Oligocene calcareous rocks are time equivalents of the Wilson Bluff Limestone of the Eyre, Eucla, and Bight Basins and of the Eucla Group limestones in Potoroo-1 and Platypus-1. Faunal and sedimentary facies data indicate that these carbonates were deposited in open marine, neritic environments.

Quaternary oozes recovered from gravity cores show that:
(1) Much if not all of the Ceduna Canyons transport system is currently dormant.
(2) Highstand deposition within the canyons is dominated by pelagic calcareous deposition. Up to several tens of cm of pinkish-brown, foraminifer nannofossil oozes have accumulated since the beginning of the Holocene transgression. In deeper water areas, the presence of the lysocline and CCD significantly reduces the thickness of this pelagic veneer.
(3) Regressive and lowstand deposition is represented by fine-grained, terrigenous deposition on canyon walls and mixed coarse-grained, calcareous/terrigenous deposition in more axial and canyon floor localities.
(4) Transgressive episodes record starved deposition, minor mixed terrigenous/ calcareous sedimentation, and authigenic mineral growth in canyon wall locations; and episodic downslope movement of shelf-derived, coarse-grained calcareous and terrigenous material in more axial locations.
(5) Highstand deposition is currently occurring under strongly oxidising conditions

in the bottom water depositional environment.

AREA B - to determine the sedimentary characteristics and develop an appropriate facies model for high energy, cool-water Cenozoic carbonate deposition on the Eucla Shelf-Eyre Terrace. A small program of high-resolution, single watergun seismic required to provide facies geometry data on which to base the sampling transect had to be abandoned as a result of failure of the seismic acquisition system. Nevertheless, a total of 10 successful gravity cores recovered some 32 m of core at the seaward end of the transect, while 7 successful vibrocores recovered between 0.30 and 1.37 m of sediment at the nearshore end of the transect. Preliminary sample analysis provides the following conclusions:

1) The Eyre shelf is variably veneered with a thin (<2.0 m) veneer of Holocene sediment which overlies Tertiary bedrock or ?Pleistocene carbonate. Much of the shallow shelf inboard of 60 m water depth is bedrock which is being scoured by waves, bored by endolithic organisms, and colonised by attached calcareous and non-calcareous benthos.

2) A thin mollusc and lithoclast lag deposit covers bedrock on the shallow shelf and a rhodolith pavement mantles the deep outer shelf.

3) The thin patchy cover of Holocene sediments consists of two facies. Palimpsest, quartzose, bioclastic sand composed of benthic foraminifers, coralline algae, bivalve fragments, lithoclasts and trace amounts of bryozoans together with, on average, 50% relict grains veneers the mid- to inner-shelf to depths of 80 m, some 90 km from shore. The deeper outer shelf is covered by fine, microbioclastic, muddy-sand rich in catenecellid bryozoans, pelagic foraminifers, ostracodes, and infaunal echinoid debris.

5) The presence of the large foraminifer *Marginopora*, both modern and relict, suggests that the overall environment of deposition is somewhat warmer than that to the east.

6) The shelf edge (~150-200 m water depth) is the site of prolific and diverse carbonate production in the form of bryozoans, bivalves, ahermatypic corals and sponges.

7) Detrital dolomite concentrations in modern shelf sediments are intimately related to exhumed Eocene dolomitic limestones on the inner shelf plain, which may act as a nucleation source and catalyst for modern marine dolomite formation.

8) The upper 2 m of sediment, over bedrock on the mid- to inner-shelf and above a rhodolith layer on the outer shelf, is all Holocene. The rhodolith layer is ~9 ka to 13 ka. The inner shelf package is younger, generally less than 3 ka.

9) Shelf sediments periodically move downslope as turbidity currents and grainflows, but shelf-derived deposition appears to be confined to upper slope (<1000 m) and deep canyon-accessed slope apron locations.

10) Mid to lower slope deposition is dominated by pelagic sedimentation (foraminifer-nannofossil oozes), with only minor terrigenous input. Bioturbation decreases down slope, with inversely-related preservation of colour banding. A yellow-brown, surface-oxidised layer increases in thickness downslope from <30 cm in upper slope cores to >100 cm at 3000 m depth, and reflects the increased effect of oxygenated bottom waters at greater depths.

11) There is a general zonation of ichnofacies downslope: <1000 m

homogenization by bioturbators; 1000-2500 m dominated by *Zoophycos*- and *Planolites*-style burrowing; 2500-4000 m burrow mottling and sulphide-filled burrows.
12) Cyclic repetition of oxic/anoxic colour banding is apparent in lower slope cycles and may be related to climatic fluctuations in Antarctic bottom water - pink Mn-oxide staining associated with interglacial periods and increased oxygenated bottom waters; grey sulphide-filled burrows associated with reduced circulation glacial episodes.

AREA C - to document the Late Quaternary paleochemistry of the southern margin, in order to evaluate the nature and extent of glacial/interglacial cyclicity as the control on sea-level variation, organic carbon fluxes, seafloor mineral accumulation, and continental weathering. A total of 6 successful gravity cores on a transect across the western end of the Ceduna Terrace recovered more than 18 m of Quaternary foraminifer nannofossil ooze in water depths between 1000 and 3500 m. A further gravity core attempt, into a coarser-grained sandy substrate at the nearshore end of the transect, was unsuccessful. Analytical work to date has consisted of the description of carbonate and magnetic susceptibility variations on three cores. The applicability of the transect cores to the Australian margin paleochemistry project must await further shore-based work; nevertheless the sedimentology of these cores provides valuable Quaternary environmental data. Increasingly well-preserved colour banding in the deeper cores, coinciding with decreased bioturbation, probably reflects climate-controlled cyclic oxygenation variations caused either by Antarctic bottom water fluctuations or by distal Leeuwin Current effects.

AREA D - to determine the geochemical characteristics of Southern Ocean magmatism between the continent-ocean boundary and magnetic anomaly 13 (approximately 38 Ma), in order to determine the changing composition, organisation, and longevity of mantle reservoirs supplying ridge basalts during the breakup of Gondwana and the rifting of Australia and Antarctica. Outstandingly successful dredging at four widely-spaced sites produced an extensive and varied assemblage of tholeiitic basalt and gabbroic rocks. Although seafloor and possible hydrothermal alteration is present in most rocks recovered, initial indications are that sufficient less-altered rock is available for detailed geochemical (major, trace and rare earth elements) and isotopic (Pb, Sr and Nd) analyses. In addition, two further dredges with oceanic crust targets recovered large quantities of manganese nodules and crusts. Although unsuccessful in their primary aim, these dredge hauls nevertheless provide valuable data on the nature and extent of Southern Ocean seafloor mineralisation.

AREA E - a request for bathymetric data to fill critical data gaps in AGSO's Offshore Resource Map Series EYRE and ESPERANCE sheets, then in the final stages of preparation, was received shortly before the cruise departed. More than 900 line km of apparently high quality bathymetric data were collected to fulfil this objective, and the data in the EYRE segment has since been published.

9. ACKNOWLEDGMENTS

We wish to acknowledge the skill and professionalism, in often arduous conditions, of the Master and crew of the *RIG SEISMIC*. Of particular importance to cruise harmony and morale, and accordingly the successful achievement of scientific objectives, was the exceptional culinary efforts of Henk Dekker and Warren Leary, assisted by Steve Staveley and Steve O'Rourke, who provided fine cuisine in even the roughest seas. Assistance toward defining and refining the Cruise 102 program was provided by Mr H.M.J. Stagg, Mr J.B. Willcox, and Dr D.T. Heggie, (all of the Marine Division, AGSO), Professor N.P. James (Queen's University, Ontario), and Dr A.J. Crawford (University of Tasmania).

10. REFERENCES

Alley, N.F., and Clarke, J.D.A., 1992. Stratigraphy and palynology of Mesozoic sediments from the Great Australian Bight area, southern Australia. *BMR Journal of Geology and Geophysics*,13 (2): 113-129.

Bé, A.W.H., 1977. An ecologic, zoogeographic and taxonomic review of Recent planktonic foraminifera. *In* Ramsay, A.T.S., (Ed.): Oceanic Micropalaeontology, Academic Press, London: 1-100.

Bein, J., and Taylor, M.L., 1981. The Eyre Sub-basin: recent exploration results. *The APEA Journal*, 21: 91-98.

Berggren, W.A., Kent, D.V., and Flynn, J.J., 1985. Jurassic to Paleogene: Part 2 Paleogene geochronology and chronostratigraphy. *In* Snelling, N.J. (ed.): The chronology of the geological record. The Geological Society, Memoir 10: 141-195.

Boeuf, M.G., and Doust, H., 1975. Structure and development of the southern margin of Australia. *The APEA Journal*, 15: 33-43.

Boltovskoy, E., and Wright, R., 1976. Recent Foraminifera. Dr. W. Junk b.v., publishers.

Bone, Y., James, N.P., von der Borch, C.C., and Gostin, V., 1991. Modern cool-water siliciclastic/carbonate sediments, Lacepede Shelf, South Australia [Abstract]. *American Association of Petroleum Geologists Bulletin*, 75: 545.

Bukry, D., 1973. Low-latitude coccolith biostratigraphic zonation. *In* Edgar, N.T., Saunders, J.B., and others: Initial Reports of the Deep Sea Drilling Project, 15, Washington (U.S. Government Printing Office): 685-703.

Bukry, D., 1975. Coccolith and silicoflagellate stratigraphy, Northwestern Pacific Ocean, Deep Sea Drilling Project Leg 32. *In* Larson, R.L., Moberly, R., and others: Initial Reports of the Deep Sea Drilling Project, 32, Washington (U.S. Government Printing Office): 677-701.

Cande, S.C., and Mutter, J.C., 1982. A revised identification of the oldest sea-floor spreading anomalies between Australia and Antarctica. *Earth and Planetary Science Letters*, 58: 151-160.

Chaproniere, G.C.H., 1991. Pleistocene to Holocene planktic foraminiferal biostratigraphy of the Coral Sea, offshore Queensland, Australia. *BMR Journal of Australian Geology and Geophysics*, 12: 195-221.

Collins, L.B., 1988. Sediments and history of the Rottnest Shelf, southwest Australia: a swell-dominated, non-tropical carbonate margin. *Sedimentary Geology*, 60: 15-50.

Conolly, J.R., Flavelle, A., and Dietz, R.S., 1970. Continental margin of the Great Australian Bight. *Marine Geology*, 8: 31-58.

Conolly, J.R., and von der Borch, C.C., 1967. Sedimentation and physiography of the sea floor south of Australia. *Sedimentary Geology*, 1: 181-220.

Corliss, B.H., and Chen, C. 1988. Morphotype patterns of Norwegian Sea deep-sea benthic foraminifera and ecological implications. *Geology*, 16: 716-719.

Davies, H.L., Clarke, J.D.A., Stagg, H.M.J., Shafik, S., McGowran, B., Alley, N.F., and Willcox, J.B., 1989. Maastrichtian and younger sediments from the Great Australian Bight. *Bureau of Mineral Resources Australia, Report* 288: 40pp.

Davies, P.J., Symonds, P.A., Feary, D.A., and Pigram, C.J., 1988. Facies models in exploration - the carbonate platforms of North-east Australia. *The APEA Journal*, 28: 123-143.

Deighton, I., Falvey, D.A., and Taylor, D.J., 1976. Depositional environments and geotectonic framework - southern Australia continental margin. *The APEA Journal*, 16: 26-36.

Dettmann, M.E., and Jarzen, D.M., 1988. Angiosperm pollen from uppermost Cretaceous strata of southeastern Australia and Antarctic Peninsula. *Memoir of the Association of Australasian Palaeontologists*, 5: 217-237.

Dodd, C., 1986. The sedimentology of the Cretaceous Platypus Formation in well Duntroon-1, offshore South Australia. *South Australia Dept Mines and Energy Open File Envelope* 6228(1), (unpub.).

Falvey, D.A., 1974. The development of continental margins in plate tectonic theory. *The APEA Journal*, 14: 95-106.

Falvey, D.A., and Mutter, J.C., 1981. Regional plate tectonics and evolution of Australia's passive continental margins. *BMR Journal of Australian Geology and Geophysics*, 6: 1-29.

Feary, D.A., 1991. Southern Margin Sampling Program (Project 121.27). Research Cruise Proposal. *Bureau of Mineral Resources Australia, Record* 1991/21. 32 pp.

Feary, D.A., Davies, P.J., Pigram, C.J., and Symonds, P.A., 1991. Climatic evolution and control on carbonate deposition in northeast Australia. *Palaeogeography, Palaeoclimatology, and Palaeoecology (Global and Climatic Change Section)*, 89: 341-361.

Forbes, A., Martin, M.J., and Tadiar, E., 1984. Permit EPP-21, Duntroon embayment offshore South Australia, exploration report 1984. *Getty Oil Development Company Ltd, Petroleum Division Report*, (unpub.).

Fraser, A.R., and Tilbury, L.A., 1979. Structure and stratigraphy of the Ceduna Terrace region, Great Australian Bight. *The APEA Journal*, 19: 53-65.

Hayes, D.E., and Conolly, J.R., 1972. Morphology of the southeast Indian Ocean. *In* Hayes, D.E. (Ed.): Antarctic Oceanology 11: The Australian - New Zealand Sector. *Antarctic Research Series*, 19: 125-145; American Geophysical Union, Washington.

Heggie, D.T., and O'Brien, G.W., 1988. Hydrocarbon gas geochemistry in sediments of the offshore Otway and Gippsland Basins - preliminary post-cruise report. *Bureau of Mineral Resources Australia, Record* 1988/32. 149 pp.

Helby, R., Morgan, R., and Partridge, A.D., 1987. A palynological zonation of the Australian Mesozoic. *Association of Australasian Palaeontologists Memoir*, 4: 1-94.

Hemleben, Ch., Spindler, M., and Anderson, O.R., 1989. Modern Planktonic Foraminifera, Springer-Verlag.

Hill, A.J., 1989. Stratigraphy of the Bight and Duntroon Basins, South Australia. *South Australia Dept. Mines and Energy Report Book*, 89/81.

Hocking, R.M., 1990. Eucla Basin. *In* Geology and Mineral Resources of Western Australia. *Western Australia Geological Survey Memoir*, 3: 548-561.

James, N.P. 1983. Reefs. *In* Scholle, P.A., Bebout, D.G., and Moore, C.H. (Eds): Carbonate Depositional Environments. *American Association of Petroleum Geologists Memoir,* 33: 345-440.

James, N.P., and von der Borch, C.C., 1991. Carbonate shelf edge off South Australia: a prograding open-platform margin. *Geology*, 19: 1005-1008.

Jongsma, D., Johnston, C.R., Davies, H.L., and Jernakoff, P., 1991. Ceduna (1:1 000 000 scale Offshore Resource Map). *Bureau of Mineral Resources, Geology and Geophysics,* Canberra, Australia.

Jongsma, D., Johnston, C.R., and Davies, H.L., 1992. Eyre (1:1 000 000 scale Offshore Resource Map). *Bureau of Mineral Resources, Geology and Geophysics,* Canberra, Australia.

Kennett, J.P., 1976. Phenotypic variation in some Recent and Late Cenozoic planktonic foraminifera. *In* Hedley, R.J., and Adams, C.J., (Eds): Foraminifera vol. 2, Academic Press: 111-170.

Kennett, J.P., and Vella, P., 1975. Late Cenozoic planktonic foraminifera and paleoceanography at DSDP site 284 in the cool subtropical South Pacific. *In* Kennett, J.P., Houtz, R.E., and others: Initial Reports of the Deep Sea Drilling Project, 29, Washington (U.S. Government Printing Office): 769-799.

Klein, E.M., Langmuir, C.H., Zindler, A., Staudigel, H., and Hamelin, B., 1988. Isotope evidence of a mantle convection boundary at the Australian-Antarctic Discordance. *Nature*, 333: 623-629.

Hocking, R.M., 1990. Eucla Basin. *In* Geology and Mineral Resources of Western Australia. *Western Australia Geological Survey Memoir*, 3: 548-561.

Lipps, J.H., 1987. Extinction dynamics in pelagic ecosystems. *In* Elliott, D.K., (Ed.): Dynamics of extinction. John Wiley: 87-104.

Lowry, D.C., 1970. Geology of the Western Australian part of the Eucla Basin. *Geological Survey of Western Australia Bulletin*, 122.

Ludbrook, N.H., 1969. Tertiary Period. *In* L.W. Parkin (Ed.): Handbook of South Australian Geology. *Geological Survey of South Australia*: 172-203.

McCorkle, D.C., Veeh, H.H., and Heggie, D.T., 1990. Glacial-interglacial sedimentation and paleochemistry in the southeastern Indian Ocean. *Eos*, 71: 1382.

McGowran, B., 1973. Observation bore No. 2, Gambier Embayment of the Otway Basin: Tertiary micropalaeontology and stratigraphy. *Mineral Resources Review, South Australia*, 135: 43-55.

McGowran, B., 1991. Maastrichtian and early Cainozoic, southern Australia: planktonic foraminiferal biostratigraphy. *In* Williams, M.A.J., De Deckker, P., and Kershaw, A.P. (eds): The Cainozoic in Australia: a reappraisal of the evidence. *Geological Society of Australia Special Publication,* 18: 79-98.

McGowran, B., and Beecroft, A., 1986. Neritic, southern extratopical foraminifera and the terminal Eocene event. *Palaeogeography, Palaeoclimatology, and Palaeoecology*, 55:23-34.

Marks, K.M., Vogt, P.R., and Hall, S.A., 1990. Residual depth anomalies and the origin of the Australian-Antarctic Discordance. *Journal of Geophysical Research*, 95: 17325-17337.

Marshall J.F., and Davies, P.J., 1978. Skeletal carbonate variation on the continental shelf of eastern Australia. *BMR Journal of Australian Geology and Geophysics*, 3: 85-92.

Martini, E., 1971. Standard Tertiary and Quaternary calcareous nannoplankton zonation. *In* Farinacci, A. (ed.): Proceedings of the II Planktonic Conference, Roma 1970, Edizioni Tecnoscienza, Roma, 2: 739-785.

Menard, H.W., 1973. Depth anomalies and the bobbing motion of drifting islands. *Journal of Geophysical Research.*, 78: 5128-5137.

Morgan, R., 1986. Palynology of BP Duntroon-1, Duntroon Basin, South Australia. Report for BP Australia. *South Australia Dept. Mines and Energy Open File Envelope* 6228(5), (unpub.).

Nelson, C.S., 1988. An introductory perspective on non-tropical shelf carbonates. *Sedimentary Geology*, 60: 3-14.

Okada, H., and Bukry, D., 1980. Supplementary modification and introduction of code numbers to the low-latitude coccolith biostratigraphic zonation (Bukry, 1973; 1975). *Marine Micropaleontology*, 5: 321-325.

Perch-Nielsen, K., 1985. Cenozoic calcareous nannofossils. *In* Bolli, H.M., Saunders, J.B., and Perch-Nielsen, K. (Eds): Plankton Stratigraphy, Cambridge earth science series, Cambridge University Press, Cambridge: 427-554.

Powis, G., and Partridge, A.D., 1980. Palynological analysis of Jerboa-1, Eyre Basin, Western Australia. *In* P.U. Huebner: Well completion report, Jerboa-1. *Esso Australia Limited Report*, (unpub.).

Pyle D.G., Christie D.M., and Mahoney J.J., (in press). Resolving an isotopic boundary within the Australian-Antarctic Discordance. *Earth and Planetary Science Letters.*

Read, J.F., 1986. Carbonate platform facies models. *American Association of Petroleum Geologists Bulletin*, 69: 1-21.

Robertson, C.S., Cronk, D.K., Nicholas, E., Mayne, S.J., and Townsend, D.G., 1979. A review of petroleum exploration and prospects in the Great Australian Bight region. *Bureau of Mineral Resources Australia, Record* 1979/20 (unpub.).

Shafik, S., 1981. Nannofossil biostratigraphy of the Hantkenina (foraminiferid) interval in the upper Eocene of southeastern Australia. *BMR Journal of Australian Geology and Geophysics*, 6: 108-116.

Shafik, S., 1983. Calcareous nannofossil biostratigraphy: an assessment of foraminiferal and sedimentation events in the Eocene of the Otway Basin, southeastern Australia. *BMR Journal of Australian Geology and Geophysics*, 8: 1-17.

Shafik, S., 1985. Cretaceous coccoliths in the Middle Eocene of the western and southern margins of Australia. *BMR Journal of Australian Geology and Geophysics*, 9: 353-359.

Shafik, S., 1987. Tertiary nannofossils from offshore Otway Basin and off West Tasmania. *In Bureau of Mineral Resources, Australia, Record* 1987/11: 67-96.

Shafik, S., 1990. The Maastrichtian and early Tertiary record of the Great Australian Bight Basin and its onshore equivalents on the Australian southern margin. *BMR Journal of Geology and Geophysics*, 11: 437-497.

Shafik, S., 1992. Eocene and Oligocene calcareous nannofossils from the Great Australian Bight : evidence of significant reworking episodes and surface-water temperature changes. *BMR Journal of Geology and Geophysics*, 13: 131-142.

Stagg, H.M.J., Cockshell, C.D, Willcox, J.B., Hill, A.J., Needham, D.J.L., Thomas, B., O'Brien, G.W, and Hough, L.P., 1990. Basins of the Great Australian Bight region: geology and petroleum potential. *Bureau of Mineral Resources, Continental Margins Program Folio* 5.

Talwani, M., Mutter, J., Houtz, R., and Konig, M., 1979. The crustal structure and evolution of the area underlying the magnetic quiet zone on the margin south of Australia. *In* J.S. Watkins, L. Montadert, and P.W. Dickerson (Eds): Geological and geophysical investigations of continental margins. *American Association of Petroleum Geologists Memoir*, 29: 151-175.

Tilbury, L.A., and Fraser, A.R., 1981. Submarine valleys on the Ceduna Terrace. *BMR Journal of Australian Geology and Geophysics*, 6: 259-264.

Truswell, E.M., Chaproniere, G.C.H., and Shafik, S., (compilers), 1991. Australian Phanerozoic Timescales: 10. Cainozoic Biostratigraphic Chart and Explanatory Notes. *Bureau of Mineral Resources, Australia, Record* 1989/40.

Vail, P.R., Mitchum, R.M., Todd, R.G., Widmer, J.M., Thompson, S., Sangree, J.B., Bubb, J.N., and Hatlelid, W.G., 1977. Seismic stratigraphy and global changes of sea level. *In* C.E. Payton (Ed.): Seismic stratigraphy - application to hydrocarbon exploration. *American Association of Petroleum Geologists Memoir*, 26: 49-212.

Veevers, J.J., 1982. Australian-Antarctic depression from the mid-ocean ridge to adjacent continents. *Nature*, 295: 315-7.

Veevers, J.J., 1984. Phanerozoic earth history of Australia. Oxford University Press, Oxford, UK.

Veevers, J.J., 1986. Breakup of Australia and Antarctica estimated as mid-Cretaceous (95 $\pm$ 5 Ma) from magnetic and seismic data at the continental margin. *Earth and Planetary Science Letters*, 77: 91-99.

Veevers, J.J., 1988. Seafloor magnetic lineations off the Otway/west Tasmanian basins: ridge jumps and the subsidence history of southeast Australian margins. *Australian Journal of Earth Sciences*, 35: 451-462.

Veevers, J.J., and Evans, P.R., 1975. Late Palaeozoic and Mesozoic history of Australia. *In* K.S.W. Campbell (Ed.): Gondwana Geology. ANU Press, Canberra: 579-607.

Veevers, J.J., Stagg, H.M.J., Willcox, J.B., and Davies, H.L., 1990. Pattern of slow seafloor spreading (< 4mm/year) from breakup (96 Ma) to A20 (44.5 Ma) off the southern margin of Australia. *BMR Journal of Australian Geology and Geophysics*, 11: 499-507.

von der Borch, C.C., Conolly, J.R., and Dietz, R.S., 1970. Sedimentation and structure of the continental margin in the vicinity of the Otway Basin, southern Australia. *Marine Geology*, 8: 59-83.

von der Borch, C.C., and Hughes Clarke, J.E., 1993. Slope morphology adjacent to the cool-water carbonate shelf of South AustraliaL GLORIA and Seabeam imaging. *Australian Journal of Earth Sciences*, 40: 57-64.

von Sanden, A.T., and Barten, H.G., 1977. Stratigraphy and palynology of the Great Australian Bight. *Shell Development (Australia) Report*, 217 (unpub.).

Wass, R.E., Conolly, J.R., and Macintyre, R.J., 1970. Bryozoan carbonate sand continuous along southern Australia. *Marine Geology*, 9: 63-73.

Weissel, J.K. and Hayes, D.E., 1971. Asymmetric seafloor spreading south of Australia. *Nature,* 231: 518-522.

Weissel, J.K., and Hayes, D.E., 1972. Magnetic anomalies in the southeastern Indian Ocean. *In*: D.E. Hayes (Ed.): Antarctic Oceanology II: The Australian-New Zealand Sector. *Antarctic Research Series*, 19: 165-196.

Weissel, J.K., and Hayes, D.E., 1974. The Australia-Antarctic Discordance. *Journal of Geophysical Research*, 79: 2579-2587.

Whyte, R.K., 1978. Shell's offshore venture, in South Australia. *The APEA Journal*, 18: 44-51.

Willcox, J.B., 1978. The Great Australian Bight - a regional interpretation of gravity, magnetic, and seismic data from the Continental Margin Survey. *Bureau of Mineral Resources Australia Report*, 201.

Willcox, J.B., 1981. Petroleum prospectivity of Australian marginal plateaus. *In* Halbouty, M.T. (Ed.): Energy Resources of the Pacific Region. *American Association of Petroleum Geologists, Studies in Geology*, 12: 245-272.

Willcox, J.B., Stagg, H.M.J., Davies, H.L., and others, 1988. Rig Seismic research cruises 10 and 11: geology of the central Great Australian Bight region. *Bureau Mineral Resources Australia Report*, 286.

Wilson, J.L., 1975. Carbonate facies in geologic history. Springer-Verlag, Heidelberg, 471pp.

APPENDIX 1 - Geological Sampling Sites

DREDGE SITES

102DR01; 36°51.45'S 118°46.19'E to 36°55.59'S 118°45.30'E; WD range 4200-5150 m; recovered 3/4 chain bag and full pipe dredges of manganese nodules, and with 2 kg of mud in the closed pipe dredge. Quaternary age for pipe dredge material.

102DR02; 33°19.10'S 128°01.51'E to 33°55.59'S 128°01.49'E; WD range 260-180 m; chain bag and grid pipe dredges empty, closed pipe dredge full of medium to coarse sand. Quaternary age for pipe dredge material.

102DR03; 35°16.76'S 130°45.10'E; WD 4180m; approx. 4 kg of mudstone in chain bag and grid pipe dredges, mud and small mudstone fragments in closed pipe dredge. Late Cretaceous (Campanian to Maastrichtian) age for mudstone in chain bag and pipe dredge, and Quaternary age for other pipe dredge material.

102DR04; 35°45.00'S 131°30.00'; WD 4680 m; dredge, weights, and 800 m wire lost, despite there being only a single pull of 95 kN.

102DR05; 36°16.73'S 134°12.71'E to 36°16.22'S 134°14.90'E; WD 5206-4370 m; approx 20 kg mud and 20 kg rock recovered. Late Cretaceous (late Maastrichtian) age for mudstone in chain bag and pipe dredge, and Quaternary age for other pipe dredge material.

102DR06; 36°08.98'S 134°44.23'E to 36°09.04'S 134°46.13'E; WD 3815-3694 m; approx 50 g mud recovered; weather conditions, with rough following seas and strong wind, made effective dredging impossible. Quaternary age for pipe dredge material.

102DR07; 36°08.80'S 134°55.00'E to 36°08.34'S 134°50.74'E; WD3700-3500 m; approx 50 g mud and 250 kg rocks recovered. Wide range of ages - Late Cretaceous (Campanian to Maastrichtian and latest Maastrichtian) age for mudstone in chain bag; Middle Eocene, Early Oligocene, and Middle to Late Oligocene age for carbonates in chain bag; and Quaternary age for other pipe dredge material.

102DR08; 36°13.30'S 134°58.10'E to 36°13.30'S 135°02.50'E; WD 4550-3700 m; nil recovery; once again, weather made effective dredging impossible.

102DR09; 37°46.87'S 132°19.98'E to 37°48.78'S 132°18.00'E; WD 5550-4940 m; 20 kg mud and 250 kg rock recovered. Quaternary age for pipe dredge material.

102DR10; 39°55.28'S 131°59.59'E to 39°55.12'S 131°58.97'E; WD 5550-5241 m; 5 kg mud and 200 kg rock recovered. Quaternary age for pipe dredge material.

102DR11; 39°45.92'S 119°46.02'E to 39°46.75'S 119°44.70'E; WD 5240-5050 m; 50 g mud and 60 kg rocks recovered. Quaternary age for pipe dredge material.

102DR12; 37°28.80'S 119°40.00'E to 37°35.89'S 119°39.19'E; WD 5300-3961 m; approx 25 kg Mn nodules recovered. Quaternary age for pipe dredge material.

102DR13; 37°14.62'S 118°09.35'E to 37°10.00'S 118°09.35'E; WD 4480-3950 m; approx 5 kg mud and 150 kg rocks recovered. Quaternary age for pipe dredge material.

GRAVITY CORE SITES

CORE	RECOVERY	LATITUDE	LONGITUDE	WATER DEPTH	OLDEST AGE
102GC01	3.85 m	34°09.99'S	128°01.47'E	3615 m	Quaternary
102GC02	4.30 m	34°04.99'S	128°01.50'E	3114 m	Quaternary
102GC03	2.63 m	34°00.00'S	128°01.48'E	2755 m	Quaternary
102GC04	2.24 m	33°55.01'S	128°01.51'E	2282 m	Quaternary
102GC05	2.44 m	33°49.98'S	128°01.55'E	1787 m	Quaternary
102GC06	4.57 m	33°44.99'S	128°01.52'E	1427 m	Quaternary
102GC07	3.00 m	33°40.02'S	128°01.45'E	1178 m	Quaternary
102GC08	4.90 m	33°35.01'S	128°01.52'E	913 m	25,800 ± 1300 yrs B.P.
102GC09	4.80 m	33°30.00'S	128°01.51'E	769 m	Quaternary
102GC10	0.01 m	33°24.99'S	128°01.55'E	527 m	Quaternary
102GC11	0.22 m	33°25.01'S	128°01.51'E	529 m	
102GC12	0.00 m	31°31.43'S	131°00.51'E	498 m	
102GC13	5.17 m	33°49.46'S	130°48.21'E	1008 m	Quaternary

102GC14	3.26 m	34°22.49'S	130°25.07'E	1502 m	Quaternary
102GC15	3.10 m	34°35.23'S	130°15.65'E	2003 m	Quaternary
102GC16	2.83 m	34°45.17'S	130°08.46'E	2495 m	Quaternary
102GC17	2.58 m	34°53.45'S	130°03.33'E	3001 m	Quaternary
102GC18	2.13 m	34°57.32'S	130°00.43'E	3504 m	Quaternary
102GC19	0.38 m	34°55.45'S	129°47.20'E	3901 m	Quaternary
102GC20	0.00 m	34°55.44'S	129°47.20'E	3902 m	
102GC21	1.42 m	34°55.44'S	129°47.17'E	3900 m	Quaternary
102GC22	1.00 m	34°02.15'S	129°53.35'E	1458 m	Quaternary
102GC23	0.00 m	34°02.14'S	129°53.39'E	1465 m	
102GC24	0.01 m	34°02.21'S	129°53.36'E	1404 m	
102GC25	0.02 m	34°02.19'S	129°53.33'E	1453 m	
102GC26	0.53 m	35°22.56'S	130°44.43'E	4568 m	late Maastrichtian
102GC27	0.80 m	35°45.22'S	131°30.05'E	4536 m	late Maastrichtian
102GC28	0.00 m	36°13.67'S	133°17.43'E	4960 m	
102GC29	0.40 m	36°13.67'S	133°17.37'E	4930 m	
102GC30	2.63 m	36°04.59'S	133°24.18'E	3804 m	Quaternary
102GC31	0.00 m	36°05.88'S	133°22.15'E	3994 m	
102GC32	1.65 m	36°05.80'S	133°22.24'E	4014 m	Quaternary
102GC33	0.00 m	36°06.84'S	133°20.77'E	4630 m	
102GC34	0.98 m	36°06.87'S	133°20.78'E	4378 m	Quaternary
102GC35	0.52 m	36°16.58'S	134°11.09'E	5219 m	?Quaternary
102GC36	2.40 m	36°05.14'S	134°47.96'E	3320 m	Quaternary
102GC37	0.00 m	36°05.15'S	134°46.70'E	3792 m	
102GC38	3.62 m	37°15.89'S	118°21.13'E	5339 m	

VIBROCORE SITES

CORE	RECOVERY	LATITUDE	LONGITUDE	WATER DEPTH	OLDEST AGE
102VC01	0.00 m	33°19.57'S	128°01.49'E	277 m	
102VC02	0.30 m	33°16.49'S	128°01.53'E	184 m	9,250 ± 110 yrs B.P.
102VC03	0.40 m	33°16.48'S	128°01.53'E	184 m	9,990 ± 80 yrs B.P.
102VC04	1.37 m	33°15.03'S	128°01.50'E	152 m	13,000 ± 100 yrs B.P.
102VC05	1.04 m	33°04.98'S	128°01.52'E	113 m	9,910 ± 80 yrs B.P.
102VC06	0.00 m	32°55.00'S	128°01.53'E	80 m	
102VC06A	0.01 m	32°55.00'S	128°01.53'E	80 m	
102VC07	1.30 m	32°45.00'S	128°01.53'E	67 m	
102VC08	0.75 m	32°35.00'S	128°01.52'E	69 m	2,780 ± 110 yrs B.P.
102VC09	0.00 m	32°25.00'S	128°01.51'E	58 m	
102VC09A	0.00 m	32°24.99'S	128°01.51'E	58 m	
102VC10	0.00 m	32°15.02'S	128°01.54'E	31 m	
102VC10A	0.01 m	32°15.02'S	128°01.54'E	31 m	
102VC11	0.76 m	32°09.97'S	128°01.53'E	22 m	late Eocene

SEDIMENT GRAB SITES

STATION	RECOVERY	LATITUDE	LONGITUDE	WATER DEPTH
102GR01	1.00 kg	33°16.49'S	128°01.53'E	184 m
102GR02	1.00 kg	33°15.03'S	128°01.50'E	152 m
102GR03	2.00 kg	33°04.94'S	128°01.51'E	112 m
102GR04	0.06 kg	32°55.00'S	128°01.53'E	80 m
102GR05	4.00 kg	32°45.00'S	128°01.53'E	67 m
102GR06	4.00 kg	32°34.99'S	128°01.52'E	70 m
102GR07	1.00 kg	32°25.00'S	128°01.51'E	58 m
102GR08	1.00 kg	32°15.01'S	128°01.54'E	31 m
102GR09	1.00 kg	32°09.98'S	128°01.52'E	22 m

SEAFLOOR PHOTOGRAPHY SITES

STATION	LATITUDE	LONGITUDE	WATER DEPTH
102CM01	32°09.97'S	128°01.53'E	22 m
102CM02	32°15.00'S	128°01.53'E	31 m
102CM03	32°25.02'S	128°0155'E	39 m
102CM04	32°35.00'S	128°01.52'E	45 m
102CM05	32°45.05'S	128°01.52'E	49 m
102CM06	32°55.00'S	128°01.51'E	59 m
102CM07	33°04.99'S	128°01.51'E	91 m

APPENDIX 2 - "ORMS" Bathymetry Way Points

During the crossing of the Great Australian Bight from east to west, a series of bathymetric lines were run to fill data gaps in the BMR's Offshore Resource Map Series (ORMS) EYRE and ESPERANCE maps, at present in preparation. The way points for these lines were:

Start Line 1	38°00.0'S	130°00.0'E
Start Line 2	37°40.0'S	129°00.0'E
Start Line 3	37°40.0'S	127°00.0'E
Start Line 4	37°50.0'S	126°00.0'E
Start Line 5	37°50.0'S	125°10.0'E
Start Line 6	37°30.0'S	124°40.0'E
Start Line 7	37°30.0'S	124°00.0'E
End Line 7	37°50.0'S	121°00.0'E

APPENDIX 3 - Equipment Used During Cruise 102

GEOLOGICAL SAMPLING EQUIPMENT

- Deep-sea winch with 8300 m of 19 mm wire
- Hydrographic winch with 4000 m of 5 mm wire
- Vibrocorer with 6 m core barrel
- Gravity corer with 2-10 m core barrels
- Chain bag and pipe (closed and grid) dredges
- Van Veen grab
- Bottom sediment photographic camera and flash assembly
- Core splitting equipment

SEISMIC EQUIPMENT (this equipment was deployed and tested, but due to failure of the seismic acquisition system was not used)

- Digital seismic acquisition system designed and built by BMR; 16-bit floating point, SEG-Y output at 6250 bpi; 1 millisecond sampling
- A-300 Price compressor, providing 300 scfm at 2000 psi (62 litres/min. at 14 MPa)
- FJORD Instruments seismic receiving array: 12.5 m groups, 96 channels, 1200 m active streamer length
- Syntron RCL-3 cable levellers; individual remote control and depth read-out
- SSI-80 (80 cu.in.) waterguns

OTHER GEOPHYSICAL EQUIPMENT

- Geometrics G801/803 magnetometer
- Bodenseewerk Geosystem KSSS-31 marine gravity meter

NAVIGATION AND ECHO-SOUNDER EQUIPMENT

- Non-seismic data acquisition system built around Hewlett-Packard 1000 E-series minicomputer, with tape drives, disc drives, 12" and 36" plotters, line printers, and interactive terminals
- Racal Differential GPS system and Marisat datalink
- Magnavox T-Set stand-alone GPS receiver
- Magnavox MX1107RS (dual channel) and MX1142 (single channel) transit satellite receivers
- Magnavox MX610D and Raytheon DSN450 dual axis sonar dopplers; Ben paddle log
- Sperry, Arma-Brown, and Robertson gyro-compasses
- Raytheon deep-sea echo-sounder, 3.5kHz (2kW) 16-transducer sub-bottom profiler
- Raytheon deep-sea echo-sounder, 12kHz (2kW) precision echo-sounder

APPENDIX 4 - Cruise Operational Diary

Wednesday 12th June
[slight sea; moderate to heavy swell; overcast with occasional showers]
1030 - new people (except Ruth Lanyon) given safety tour by Claude Saroch (Safety Officer) and Lindsay Gillies (Mate).
1130 - advised that last stretch section on the 1200m streamer had been accidentally damaged by the dancing deck flap - repair deferred until later
1300 - Pre-departure Meeting
1325 - Safety Meeting - all staff + visitors present except Jon Stratton and Petar Vujovic (they will have separate meeting later)
1550 - Gangway raised - ship left at 1557
2055 - streamed magnetometer

Thursday 13th June
[moderate sea; moderate to heavy swell; cloudy with occasional showers]
1050 - whale sightings; 2 ?humpbacks.
1100 - safety muster - new people given briefing on foam smothering gear and Carley Float.
1330 - damaged stretch section swapped out

Friday 14th June
[slight to moderate sea; moderate swell; overcast with occasional squalls]
1140 - recovered magnetometer
1200 - arrived at way point to start EPC survey prior to Dredge 102DR01; DAS crashed, EPC's couldn't see bottom, and when they could, there was no feed to the winch room, flat bed plotter wouldn't work, and found that we couldn't use the stern camera to feed both winch room and bridge; winch tension meter also wouldn't work
1430 - arrived back at start point - delayed half hour by auto-pilot problems
1510 to 0030 - dredge 102DR01; 36°51.45'S 118°46.19'E to 36°55.59'S 118°45.30'E; WD 4200-5150 m; recovered many manganese nodules - dredge approx. 3/4 full; lost weights

Saturday 15th June
[moderate to rough sea; moderate swell; cloudy with rain squalls]
0030 - commenced transit to Albany
1140 - arrived Albany; collected bearings from Pilot Launch; and departed immediately on long transit to seismic area
1430 - streamed magnetometer

Sunday 16th June
[moderate sea; moderate swell; fine and clear]
0600 - ship stopped because of fuel line leak; magnetometer recovered
0742 - ship underway
0800 - magnetometer deployed

Monday 17th June
[moderate sea; moderate swell; cloudy, fine and clear]
0810 - magnetometer recovered
0815 - commenced deploying streamer
2000 - streamer deployed; bad channels still present

Tuesday 18th June
[slight sea; low swell; partly cloudy, fine and clear]
0200 - retrieved watergun array
0500 - deployed single airgun; crashes continued

1312 - retrieved airgun; commenced retrieval of streamer
1500 - streamer on board and underway to 102GC01 site
2049 - cored 102GC01; 3.85 m recovery; 34°09.99'S 128°01.47'E; 3615 m WD
2340 - cored 102GC02; 4.30 m recovery; 34°04.99'S 128°01.50'E; 3114 m WD

Wednesday 19th June
[slight to moderate sea; low swell; cloudy, fine and clear]
0245 - cored 102GC03; 2.63 m recovery; 34°00.00'S 128°01.48'E; 2755 m WD
0522 - cored 102GC04; 2.24 m recovery; 33°55.01'S 128°01.51'E; 2282 m WD
0748 - cored 102GC05; 2.44 m recovery; 33°49.98'S 128°01.55'E; 1787 m WD
0958 - cored 102GC06; 4.57 m recovery; 33°44.99'S 128°01.52'E; 1427 m WD
1148 - cored 102GC07; 3.00 m recovery; 33°40.02'S 128°01.45'E; 1178 m WD
1359 - cored 102GC08; 4.90 m recovery; 33°35.01'S 128°01.52'E; 913 m WD
1539 - cored 102GC09; 4.80 m recovery; 33°30.00'S 128°01.51'E; 769 m WD
1728 - cored 102GC10; 0.01 m recovery; 33°24.99'S 128°01.55'E; 527 m WD
1806 - cored 102GC11; 0.22 m recovery; 33°25.01'S 128°01.51'E; 529 m WD
2042 - cored 102VC01; 0.00 m recovery; 33°19.57'S 128°01.49'E; 277 m WD
2210 - grab 102GR01; 1.0 kg recovery; 33°16.49'S 128°01.53'E; 184 m WD
2225 - cored 102VC02; 0.30 m recovery; 33°16.49'S 128°01.53'E; 184 m WD
2311 - cored 102VC03; 0.40 m recovery; 33°16.48'S 128°01.53'E; 184 m WD

Thursday 20th June
[moderate to slight sea; moderate to low swell; partly cloudy, fine and clear]
0014 - grab 102GR02; 1.0 kg recovery; 33°15.03'S 128°01.50'E; 152 m WD
0029 - cored 102VC04; 1.37 m recovery; 33°15.03'S 128°01.50'E; 152 m WD
0248 - grab 102GR03; 2.0 kg recovery; 33°04.94'S 128°01.51'E; 112 m WD
0259 - cored 102VC05; 1.04 m recovery; 33°04.98'S 128°01.52'E; 113 m WD
0508 - grab 102GR04; 0.06 kg recovery; 32°55.00'S 128°01.53'E; 80 m WD
0515 - cored 102VC06; 0.00 m recovery; 32°55.00'S 128°01.53'E; 80 m WD
0532 - cored 102VC06A; 0.01 m recovery; 32°55.00'S 128°01.53'E; 80 m WD
0729 - grab 102GR05; 4.0 kg recovery; 32°45.00'S 128°01.53'E; 67 m WD
0740 - cored 102VC07; 1.30 m recovery; 32°45.00'S 128°01.53'E; 67 m WD
0924 - grab 102GR06; 4.0 kg recovery; 32°34.99'S 128°01.52'E; 70 m WD
0932 - cored 102VC08; 0.75 m recovery; 32°35.00'S 128°01.52'E; 69 m WD
1110 - grab 102GR07; 1.0 kg recovery; 32°25.00'S 128°01.51'E; 58 m WD
1115 - cored 102VC09; 0.00 m recovery; 32°25.00'S 128°01.51'E; 58 m WD
1128 - cored 102VC09A; 0.00 m recovery; 32°24.99'S 128°01.51'E; 58 m WD
1318 - grab 102GR08; 1.0 kg recovery; 32°15.01'S 128°01.54'E; 31 m WD
1329 - cored 102VC10; 0.00 m recovery; 32°15.02'S 128°01.54'E; 31 m WD
1347 - cored 102VC10A; 0.01 m recovery; 32°15.02'S 128°01.54'E; 31 m WD
1516 - grab 102GR09; 1.0 kg recovery; 32°09.98'S 128°01.52'E; 22 m WD
1546 - cored 102VC11; 0.76 m recovery; 32°09.97'S 128°01.53'E; 22 m WD
1615 to 1625 - photographs 102CM01; 32°09.97'S 128°01.53'E; 22 m WD
1724 to 1739 - photographs 102CM02; 32°15.00'S 128°01.53'E; 31 m WD
1918 to 1933 - photographs 102CM03; 32°25.02'S 128°01.55'E; 39 m WD
2052 to 2107 - photographs 102CM04; 32°35.00'S 128°01.52'E; 45 m WD
2128 to 2143 - photographs 102CM05; 32°45.05'S 128°01.52'E; 49 m WD

Friday 21st June
[slight to moderate sea; moderate to heavy swell; partly cloudy, fine and clear]
0002 to 0017 - photographs 102CM06; 32°55.00'S 128°01.51'E; 59 m WD
0154 to 0212 - photographs 102CM07; 33°04.99'S 128°01.51'E; 91 m WD
0230 - recommenced attempts at seismic acquisition on Eucla Shelf/Eyre Terrace transect;
0900 - completed deployment of waterguns and streamer

0930 - approx 200 shots recorded before computer crashed; remainder of day spent attempting to cure fault
1500 - recovered waterguns; deployed single airgun; removed extra 2 stretch sections from streamer; streamer now has full 96 channels
1800 - abandoned seismic; recovered gun and streamer
2047 to 0045 - dredge 102DR02; 33°19.10'S 128°01.51'E to 33°55.59'S 128°01.49'E; WD 260-180 m; chain bag and grid pipe dredges empty, closed pipe dredge full of medium to coarse sand

Saturday 22nd June
[moderate sea; heavy swell; cloudy, fine and clear]
0100 - commenced transit to site 102GC12
1636 - cored 102GC12; 0.00 m recovery; 31°31.43'S 131°00.51'E; 498 m WD
2022 - cored 102GC13; 5.20 m recovery; 33°49.46'S 130°48.21'E; 1008 m WD

Sunday 23nd June
[moderate sea; moderate to heavy swell; cloudy, fine and clear]
0138 - cored 102GC14; 3.26 m recovery; 34°22.49'S 130°25.07'E; 1502 m WD
0430 - cored 102GC15; 3.10 m recovery; 34°35.23'S 130°15.65'E; 2003 m WD
0709 - cored 102GC16; 2.36 m recovery; 34°45.17'S 130°08.46'E; 2495 m WD
0944 - cored 102GC17; 2.58 m recovery; 34°53.45'S 130°03.33'E; 3001 m WD
1200 - cored 102GC18; 2.13 m recovery; 34°57.32'S 130°00.43'E; 3504 m WD
1406 - commenced EPC bathymetric survey of Ceduna Terrace 1 site
1620 - cored 102GC19; 0.50 m recovery; 34°55.45'S 129°47.20'E; 3901 m WD
1852 - cored 102GC20; 0.00 m recovery; 34°55.44'S 129°47.20'E; 3902 m WD
1852 - cored 102GC21; 1.40 m recovery; 34°55.44'S 129°47.17'E; 3900 m WD
2204 - commenced transit to Ceduna Terrace 2 site

Monday 24th June
[moderate to rough sea; moderate to heavy swell; cloudy to overcast, fine and clear]
0340 - commenced EPC survey of Ceduna Terrace 2 site
0621 - cored 102GC22; 1.00 m recovery; 34°02.15'S 129°53.35'E; 1458 m WD
0645 - commenced extra EPC survey of Ceduna Terrace 2 site
0830 - cored 102GC23; 0.00 m recovery; 34°02.14'S 129°53.39'E; 1465 m WD
0915 - cored 102GC24; 0.01 m recovery; 34°02.21'S 129°53.36'E; 1404 m WD
1031 - cored 102GC25; 0.02 m recovery; 34°02.19'S 129°53.33'E; 1453 m WD
1057 - commenced transit to Ceduna Terrace 3 site
1955 - commenced EPC bathymetric survey of Ceduna Terrace 3 (un-named canyon) site

Tuesday 25th June
[rough to very rough sea; heavy to very heavy swell; cloudy to overcast with rain squalls]
0015 to 0600 - dredge 102DR03; 35°16.76'S 130°45.10'E; WD 4180 m; approx. 4 kg of mudstone in chain bag and grid pipe dredges, mud and small mudstone fragments in closed pipe dredge
0828 - cored 102GC26; 0.53 m recovery; 35°22.56'S 130°44.43'E; 4568 m WD
1005 - commenced transit to Ceduna Terrace 4 site
1447 - commenced EPC bathymetric survey of Ceduna Terrace 4 (steep slope) site
1818 - cored 102GC27; 0.80 m recovery; 35°45.22'S 131°30.05'E; 4536 m WD
2032 to 0400 - dredge 102DR04; 35°45.00'S 131°30.00'E; WD 4680 m; dredge, weights, and 800 m wire lost, despite there being only a single pull of 95 kN

Wednesday 26th June
[rough to moderate sea; very heavy to heavy swell; cloudy to overcast and clear]
0405 - commenced transit to Ceduna Terrace 5 (Fowlers Canyon south) site
1436 - commenced EPC bathymetric survey of site
1705 - cored 102GC28; 0.00 m recovery; 36°13.67'S 133°17.43'E; 4960 m WD; wire out readings on

winch recorders now a long way out, and the continuing rough to very rough conditions make determination of impact and pull out from the winch tension meter difficult
2005 - cored 102GC29; 0.40 m recovery; 36°13.67'S 133°17.37'E; 4930 m WD
2125 - commenced transit to Ceduna Terrace 6 (Fowlers Canyon north) site
2230 - commenced EPC bathymetric survey of Ceduna Terrace 6 site

Thursday 27th June
[moderate to rough sea; heavy swell; overcast with rain squalls]
0009 - cored 102GC30; 2.63 m recovery; 36°04.59'S 133°24.18'E; 3804 m WD
0356 - cored 102GC31; 0.00 m recovery; 36°05.88'S 133°22.15'E; 3994 m WD
0600 - cored 102GC32; 1.53 m recovery; 36°05.80'S 133°22.24'E; 4014 m WD
0852 - cored 102GC33; 0.00 m recovery; 36°06.84'S 133°20.77'E; 4630 m WD
1057 - cored 102GC34; 0.98 m recovery; 36°06.87'S 133°20.78'E; 4378 m WD
1209 - commenced transit to Ceduna Terrace 7 (Pearson Canyon) site
1700 - commenced EPC bathymetric survey of Ceduna Terrace 7 site
1822 to 2315 - dredge 102DR05; 36°16.73'S 134°12.71'E to 36°16.22'S 134°14.90'E; WD 5206-4370 m; approx 20 kg mud and 20 kg rock recovered

Friday 28th June
[rough sea; heavy to very heavy swell; cloudy with occasional showers]
0159 - cored 102GC35; 0.35 m recovery; 36°16.58'S 134°11.09'E; 5219 m WD
0320 - commenced transit to Ceduna Terrace 8 (Whidbey Canyon) site
0623 - commenced EPC bathymetric survey of Ceduna Terrace 8 site
0732 to 1125 - dredge 102DR06; 36°08.98'S 134°44.23'E to 36°09.04'S 134°46.13'E; WD 3815-3694 m; approx 50 g mud recovered; suspect that weather conditions, with seas and wind behind, made effective dredging impossible
1130 - commenced transit to Ceduna Terrace 10 (Topgallant Canyon) site (Ceduna Terrace 9 site deferred because of weather)
1237 - commenced EPC bathymetric survey of Ceduna Terrace 10 site
1338 to 1849 - dredge 102DR07; 36°08.98'S 134°44.23'E to 36°09.04'S 134°46.13'E; WD 4550-3560 m; approx 50 g mud and 250 kg rocks recovered; 1 weight and the grid pipe dredge lost; highly effective dredge - probably because the ship was much more controllable into the weather
1858 - commenced transit to Ceduna Terrace 11 (Topgallant Canyon) site
2015 - commenced EPC bathymetric survey of Ceduna Terrace 11 site
2314 to 0501 - dredge 102DR08; 36°13.30'S 134°58.10'E to 36°13.30'S 135°02.50'E; WD 4550-3700 m; nil recovery; once again, weather made effective dredging impossible

Saturday 29th June
[rough to moderate sea; heavy swell; cloudy with occasional showers]
0505 - commenced transit to Ceduna Terrace 9 (Whidbey Canyon) site
0859 - cored 102GC36; 2.29 m recovery; 36°05.14'S 134°47.96'E; 3320 m WD
1047 - cored 102GC37; 0.00 m recovery (core catcher failure); 36°05.15'S 134°46.70'E; 3792 m WD
1145 - commenced transit to Abyssal Plain site 2
1711 - deployed magnetometer (seas calmed sufficiently for the ship to be slowed and the magnetometer cable run through the sheave on the boom)

Sunday 30th June
[moderate sea; moderate swell; cloudywith occasional showers]
0820 - retrieved magnetometer
0805 - commenced EPC bathymetric survey
0920 to 1912 - dredge 102DR09; 37°46.87'S 132°19.98'E to 37°48.78'S 132°18.00'E; WD 5550-4940 m; 20 kg mud and 250 kg rock recovered
1920 - commenced transit to Abyssal Plain site 3
1935 - deployed magnetometer

Monday 1st July
[slight sea; low to moderate swell; partly cloudy, fine and clear]
0935 - commenced EPC bathymetric survey
0955 - retrieved magnetometer
0959 to 1910 - dredge 102DR10; 39°55.28'S 131°59.59'E to 39°55.12'S 131°58.97'E; WD 5550-5241 m; 5 kg mud and 200 kg rock recovered
1922 - commenced transit to start of ORMS bathymetric Line 1
1926 - deployed magnetometer

Tuesday 2nd July
[rough to very rough sea; heavy swell; cloudy to overcast with frequent showers]
1709 - commenced ORMS bathymetric traverse Line 1

Wednesday 3rd July
[rough to very rough sea; moderate to heavy swell; overcast with squalls]
0018 - completed ORMS Line 1; commenced ORMS Line 2
1144 - completed ORMS Line 2; commenced ORMS Line 3
1801 - completed ORMS Line 3; commenced ORMS Line 4
2341 - completed ORMS Line 4; commenced ORMS Line 5

Thursday 4th July
[rough to very rough sea; moderate to heavy swell; cloudy with showers]
0349 - completed ORMS Line 5; commenced ORMS Line 6
0902 - completed ORMS Line 6; commenced ORMS Line 7

Friday 5th July
[rough sea; heavy swell; cloudy with showers]
0546 - completed ORMS Line 7; commenced transit to Abyssal Plain Site 4
2145 - commenced EPC bathymetric survey of Abyssal Plain Site 4
2230 - recovered magnetometer
2310 to 0614 - dredge 102DR11; 39°45.92'S 119°46.02'E to 39°46.75'S 119°44.70'E; WD 5240-5050 m; approx 50 g mud and 60 kg rocks recovered

Saturday 6th July
[rough sea; heavy swell; cloudy with squalls]
0620 - commenced transit to Abyssal Plain Site 5 (Diamantina Fracture Zone)
0633 - deployed magnetometer
2025 - recovered magnetometer
2030 - commenced EPC bathymetric curvey of Abyssal Plain Site 5
2125 to 0650 - dredge 102DR12; 37°28.80'S 119°40.00'E to 37°35.89'S 119°39.19'E; WD 5300-3961 m; approx 25 kg Mn nodules recovered

Sunday 7th July
[moderate sea; heavy to moderate swell; cloudy to overcast, fine and clear]
0650 - commenced transit to Abyssal Plain Site 6
0650 - deployed magnetometer
1634 - commenced EPC bathymetric curvey of Abyssal Plain Site 6
1648 - recovered magnetometer
1856 to 0158 - dredge 102DR13; 37°14.62'S 118°09.35'E to 37°10.00'S 118°09.35'E; WD 4480-3950 m; approx 5 kg mud and 150 kg rocks recovered

Monday 8th July
[slight to moderate sea; low to moderate swell; cloudy, fine and clear]

0215 - commenced transit to 102GC38 site
0419 - cored 102GC38; 3.62 m recovery; 37°15.89'S 118°21.13'E; 5339 m WD
0430 - commenced oiling wire rope on retrieval of corer
0727 - corer recovered; commenced transit to Fremantle
0730 - deployed magnetometer

Tuesday 9th July
[moderate to slight sea; low to moderate swell; overcast, fine and clear]
1400 - post-cruise Safety Meeting held
1600 - recovered magnetometer

Wednesday 10th July
[slight sea; low swell; partly cloudy, fine and clear]
0745 - pilot onboard
0915 - docked at ASI Yard
1200 - completed unloading of materials into containers

APPENDIX 5 - Scientific and Technical Personnel and Ship's Crew

Scientific and Technical Personnel

D. Feary	Chief Scientist
S. Shafik	Micropaleontologist
E. Chudyk	Systems Scientist
P. Petkovic	Systems Scientist
G. Birch [1]	Visiting Scientist
T. Boreen [2]	Visiting Scientist
R. Lanyon [3]	Visiting Scientist
C. Buchanan	Marine Technician
P. Butler	Marine Technician
L. Hatch	Marine Technician
G. Sparksman	Marine Technician
J. Stratton	Marine Technician
P. Vujovic	Marine Technician
C. Saroch	Electronics Technician
U. Reike	Electronics Technician
V. Wierzbicki	Electronics Technician
C. Dyke	Mechanical Technician
J. Roberts	Mechanical Technician
D. Sewter	Mechanical Technician
S. Wiggins	Mechanical Technician
R. Lockhart	RACAL Consultant

[1] - Department of Geology and Geophysics, University of Sydney
[2] - Department of Geological Sciences, Queen's University, Ontario, Canada
[3] - Geology Department, University of Tasmania

Ships Crew

R. Hardinge	Master
L. Gillies	Chief Officer
M. Gusterson	Second Officer
R. Thomas	Chief Engineer
T. Ireland	Second Engineer
W. Hanson	Electrician
P. Morecombe	E.A./Seaman
A. Dale	A.B.
D. Kane	A.B.
G. Pretsel	A.B.
H. Dekker	Chief Steward/Cook
W. Leary	Cook
S. Staveley	Steward
S. O'Rourke	Steward/Seaman